Universitetet i Stavanger

Faculty of Science and Technology

MASTER'S THESIS

Study program /Specialization: **Petroleum Technology/Drilling**	Vår.................semester, 2015.... Open / Konfidensiell
Writer: **Mohammed Ahmed Iqbal**	………………………………………… (Writer's signature)
Faculty Supervisor: **Kjell Kåre Fjelde** External Supervisor(s):	
Thesis title: **Use of AUSMV scheme for simulation of particle transport** English title: **Use of AUSMV scheme for simulation of particle transport**	
Credits (ECTS): **30**	
Key words: **AUSMV Scheme** **Bottomhole Pressure (BHP)** **Cuttings concentration** **Drift flux model**	Pages: ……………**77**…… + enclosure: …**26**……… Stavanger, ………**15.06.2015**……….. date/year

ABSTRACT

It is quite a challenge to perform a detailed analysis on the dynamics of particles flow in well operations. In this thesis the dynamics of the cuttings transport in a well are described. Simulations have been performed when we have studied the effect of ROP on bottomhole pressure development considering transport of cuttings. The effects of numerical diffusion and discretization errors have also been demonstrated.

An existing computer model code was used in the Matlab software. The model was a drift flux model and made use of the AUSMV scheme to simulate the transient/ dynamic transport of particles (cuttings).

In chapter 6, different graphs were obtained with the help of Matlab to show the behavior of cuttings concentration α_c and BHP (Bottomhole Pressure) for different time steps. A no slip model was used which meant that the cuttings were transported with same velocity as the liquid.

Finally calculations were made to find the theoretical α_c and BHP (Bottomhole Pressure) and comparison was made with the simulation results. It was shown that by increasing the number of boxes from 25 to 100 in the well the values obtained for BHP (Bottomhole Pressure) and α_c was closer to the theoretical value as compared to values obtained for the case with 25 boxes. This effect was related to discretization errors associated with the numerical scheme. It was observed that by refining the grid, the effects were reduced. Another issue is numerical diffusion. The interface between different zones, liquid vs liquid/cuttings are in reality sharp. Numerical diffusion tends to smear out this interface and this has impact on how we can predict when cutting arrive at surface. However, by increasing number of boxes, the effect of numerical diffusion is reduced.

Increases in the value of ROP (Rate of Penetration) lead to an increase in the value of cuttings concentration α_c and BHP (Bottomhole Pressure). Also finally the time it took for cuttings to be transported from the bottom of the well to the top was calculated. It was observed that cuttings reached the surface of the well more sharply when the number of boxes was increased from 25 to 100. This was due to reduced numerical diffusion. As the cuttings flowrate was increased from 2kg/s to 4kg/s and finally to 6kg/s, it was seen that the maximum BHP (Bottomhole Pressure) value and the concentration of the cuttings α_c increased.

AUSMV scheme made it easy to perform a detailed analysis in the form of graphical representation and mathematical calculations of parameters involved in cuttings transport mechanism in a well. The simulations gave very precise and

accurate results and it became easy to understand the dynamics of cutting particles transport in a well. However, it must be emphasized that the effect of numerical diffusion and discretization error must be taken into account. Precise simulations can be obtained by refining the grid.

TABLE OF CONTENT

ACKNOWLEDGEMENT

I would like to thank my supervisor Kjell Kåre Fjelde for helping and guiding me immensely throughout my whole thesis. Without his help and support it would not have been possible to accomplish my thesis.

At the end I would like to thank my family who has been a great support throughout my years of study.

Stavanger, June 2015

_____

Mohammed Ahmed Iqbal

LIST OF FIGURES

NOMENCLATURE

TUDRP	Tulsa University Drilling Research Projects
BHA	Bottomhole Assembly
BHP	Bottomhole Pressure
CT	Coiled Tubing
CCT	Concentric Coiled Tubing
MNSL	Mobil North Sea Ltd
MMH	Mixed Metal Hydroxide
ECD	Equivalent Circulation Density
CTFD	Critical Transport Fluid Velocity
SCFF	Subcritical Fluid Flow
ROP	Rate of Penetration
RIH	Run in Hole
FDS	Flux Difference Splitting
SSS	Succession of Steady States
AUSMV	Advection Upstream Splitting Method

1. INTRODUCTION

In this thesis, the parameters that affect the transport of cuttings in a well are described. The AUSMV scheme is used to simulate different cases.

In chapter 2, the issues related to hole cleaning are discussed and how important it is to monitor the hole cleaning process properly. The consequences related to hole cleaning process are also described. The role CT (Coiled Tubing) plays in sand clean out process is also explained. The problems related to removal of swarf in P&A operations are also discussed.

In chapter 3, the CTFV (Critical Transport Fluid Velocity) is described and other general considerations made on cuttings and liquid flow in a well is illustrated. In this chapter, the effect of ROP (Rate of Penetration), importance of appropriate flowrate for transport of cuttings and the effect of density of transport medium on cuttings is accounted for along with the effect of liquid velocity on the concentration of particles. Further, the difference between steady state and transient flow condition are discussed.

In chapter 4, The AUSMV scheme is defined along with the three fundamental conservation laws that apply to the flow in a well and pipe. Closure laws, liquid density model and gas density model are also defined along with friction model. Mathematical properties of the existing drift flux model, discretization process of the well, application of the numerical AUSMV scheme is interpreted. The specification of the numerical fluxes at the inlet and outlet boundaries of the well is also discussed.

In chapter 5, the changes and the adjustments that were made to the existing drift flux model and the AUSMV scheme used in the thesis for simulation of cuttings transport in the well are shown.

Finally in chapter 6, the simulation results are shown and discussed for the cuttings transport and liquid flow in well. Graphs were plotted and the changing trends of cuttings concentration α_c against well depth and BHP (Bottomhole Pressure) against time were analyzed for different ROP (Rate of Penetration), liquid massrate and cuttings massrate values. Further the effect of numerical diffusion by changing the number of boxes in the well from 25 to 100 is represented. Finally comparison between theoretical and simulation results are made by calculating α_c values and BHP (Bottomhole Pressure) values. The time it takes for the cuttings to reach the surface of the well from the bottom of the well is also calculated. Finally a conclusion is made in chapter 7 of the results obtained from the simulation and the impact of results for different cases are concluded.

2. WELL OPERATIONS AND PARTICLE/LIQUID FLOW

(Much of the literature in this chapter is taken from reference [1]) [1] As the use of the directional and horizontal drilling is increasing with time, the issue of hole cleaning has become a significant problem both technically and economically. It has been a great matter of concern in cases where we have to drill larger and longer wellbores. In the past twenty years the problem of cutting transport have been taking into consideration through carrying out numerous field observations and laboratory studies. Several models have been investigated and approved for the field engineer to figure out the hydraulic requirements for the hole cleaning process. [1]

[1] Improper cleaning of hole can lead to many costly problems while drilling horizontal wells. Some of these problems are poor drilling rate (slow), high torque, premature bit wear and situations such as formation fracture and stuck pipe. If the hole cleaning problem is not handled properly, it can lead to sidetracking or loss of well. However, many studies have shown that cutting transport in highly inclined wells is a complicated problem and cleaning of hole is problem that occurs quite often. [1]

[1] The Tulsa University Drilling Research Projects (TUDRP) carried out large scale transport cutting studies in inclined wellbores about two decades ago [1]. A flow loop was constructed consisting of a 40-ft length of 5-in. transparent annular test section and it had the ability to alter and control (1) angles of inclination between vertical and horizontal, (2) flowrate of mud pumping, (3) drilling rate and (4) eccentricity and rotation of drill-pipe. Results in the past have shown significant difference between cutting transport in inclined wellbores and vertical wellbores. [1]

[1] A cuttings bed forms at inclination angles greater than 35° from vertical and this bed can slide back down for angles around 50°. Mud velocities in the range between 3 to 4 ft/s are required for high angles with no rotation of pipe. For vertical drilling mud velocities from 1 to 2 ft/s are required. Eccentricity formed by drill pipe lying on the lower side of annulus makes the situation worse. Annular fluid analysis has shown that eccentricity redirects most of the mud flow away from the low side of the annulus. This leads to cuttings settling to the more open area above the drill pipe. [1]

[1] Studies done by Okrajni and Azar confirmed the effect of mud rheology on hole cleaning. Their study stated that when cuttings bed is removed with a high viscosity mud, it provides a solution for hole cleaning problem in vertical wells but it may be detrimental in wellbores with high angles (assuming a zero to low

drill-pipe rotation). Use of a low viscosity mud could promote turbulence and is helpful. Previous findings, observations and studies have proved that hole cleaning depends on factors such as mud rheological properties, angle of inclination, drill-pipe eccentricity, hydraulics and rate of penetration. During mid -1980's a general qualitative understanding of the hole cleaning problem in highly inclined was developed. But this subject was complex and further analysis was required. As more and more directional and horizontal wells were drilled, there was an increase in the level of difficulties faced in hole cleaning. Numerous field problems were reported due to lack of required drilling equipment, inadequate field experience, lack of good quality predictive models and inefficient transfer of research results to the field. [1]

[1] Considering solving hole cleaning problems, the oil industry urged for more research and development in cuttings transport. The increase in need for experimental data created demand for additional flow loops. In collaboration with Chevron, Conoco, Elf Aquitaine and Philips, TUDRP created new and bigger flow loop, with 100-ft long test section of 8-in. annulus [1]. Near late 1980's a few flow loops were built which had different sizes and capability levels [1]. Flow loops had an annular transparent test section through which cuttings transport mechanism was observed. These flow loops provided the tools that were required to collect the experimental data that was needed. [1]

[1] Experimental data was collected on the basis of effects that different parameters had on cuttings transport under varying conditions. After several observations and analysis the data which was collected lead toward formulation of correlations/models. Larsen conducted detailed studies on cuttings transport and over 700 tests were carried out with TUDRP's 5-in. flow loop [1]. Under critical and subcritical flow conditions tests were performed for vertical and horizontal angles. Critical flow corresponds to the minimum annular average fluid velocity that prevents cuttings bed's stationary accumulation. Subcritical flow is when stationary cuttings bed has started to form. However, analysis of experimental data has shown that a cutting bed is created when the fluid velocity is below the critical value and it will increase in thickness until the fluid velocity above the bed reaches the critical velocity value. The range of critical velocity has been reported to be between 3 to 4 ft/s depending on parameter values such as mud rheology, drilling rate, pipe eccentricity and rotational speed. [1]

[1] At high angles the performance of cuttings flow in muds in the turbulent regime is better than that in laminar regime. This was confirmed by Larsen's data. There are other several new findings which are significant. (1) Under subcritical flow conditions a medium rheology mud with plastic viscosity (PV) = 14, yield point (YP) = 14 lead to slightly smaller cutting beds as compared to those obtained with the low rheology (PV = 7, YP=7) or high rheology (PV =

21, YP =21) muds [1]. The flow regime for this mud was in the transition between laminar and turbulent flow. (2) The small cuttings size (0.1 inch) which was used was more difficult to clean as compared to large cuttings size (0.275 inch) and medium cuttings size (0.175 inch). A more packed and smooth bed was formed by small cuttings. (3) For angles between 55 º and 90º there was no change in the height of the cuttings bed, but a slight increase was noticed for angles ranging from 65º to 70º. (4) For angles between 35º to 55º the cuttings bed backslided significantly. Based on this, Larsen, Pilehvari and Azar [1] developed a model for wellbores which were inclined from 50º to 90º. The model predicted the critical velocity and the thickness of the cuttings bed when the flowrate was below the critical flowrate. The Larsen's data [1] was collected through tests performed with the water based mud. It was showed by Hemphill and Larsen [1] that oil base muds with comparable rheological properties gave about the same result. [1]

2.1 CUTTINGS TRANSPORT IN DRILLING

(Much of the literature in this chapter is taken from reference [1]) Ford et al. [1] published a model which predicted minimum transport velocity for two modes: (1) cuttings suspension and (2) cuttings rolling. A comparison of the predictions was done with laboratory data. Rasi [1] developed a 'hole cleaning tool' for wellbores which were large and had high angles. It was noticed that the presence of cuttings bed did not cause a very high overpull as long as the open area above the cuttings bed was greater than the cross-sectional area of the bit. A lower overpull was seen when stabilizers with smaller cross-sectional areas, bottom hole assembly (BHA) elements with smaller outside diameters and larger drill pipes were used. [1]

[1] A cuttings transport model based on fluid mechanics relationships was presented by Clark and Bickham [1] in which three cutting transport modes were assumed: (1) settling (2) lifting and (3) rolling. The presence of each was dependent on the wellbore angle. A comparison between critical and subcritical flow data which was collected with the TUDRP's 5 and 8 inch flow loops was done to test the predictions of the model. The model was also utilized to examine several situations where poor cuttings transport lead to drilling problems. [1]

[1] Campos et al. [1] developed a mechanistic model to predict the critical velocity and the height of the cuttings bed for subcritical flow conditions. The work done by them was based on earlier work done by Oroskar and Whitmore [1] for transport of slurry in pipes. The predictions made by the model were good for muds which were thin, but the model needed to be further refined in order to account for muds which were thick and when considering pipe rotation.

[1] Kenny, Sunde and Hemphill [1] defined a lift factor which was used by them to indicate performance of cuttings transport. The lift factor was a combination of the fluid velocity in the lower part of the annulus and the mud settling velocity which was found by using Chien's [1] correlation. The effect that drill pipe rotation had on cuttings transport in inclined wellbores was done by Bassal [1]. Use of TUDRP's 8 inch wellbore simulator, 10-ft long [1], with a 4-inch drill pipe was applied for the study [1]. Drill pipe rotary speed, hole inclination, mud rheology, cuttings size and mud flowrate were the variables considered in the study. Results showed that the drill pipe rotation had a significant effect on hole cleaning in directional well drilling. The manner in which the drill string behaves dynamically in combination with mud flowrate, cuttings size and mud rheology gives the level of enhancement with respect to removal of cuttings as a result of rotary speed. Normally the cuttings which are smaller in size are more difficult to transport [1]. With high rotary speed and high viscosity mud the

smaller cuttings become easier to transport. The cleaning of the hole is better with low viscosity mud as compared to if done with high viscosity mud when there is no rotation of the drill-pipe. [1]

[1] Laboratory studies have verified that for proper hole cleaning we need a critical flow condition and velocities of the fluid that range from 4 to 6 ft/s, but it was shown by field experiences that large holes did not require very high velocities and were easily cleaned at lower velocities ranging from 2 to 3 ft/s. the reson for this is the effect of rotation. Cuttings usually fall quickly to the low side of the annulus if the pipe rotation is low or if there is no pipe rotation at all. It becomes easier to pick up the cuttings and they can be rolled by a thin mud. Therefore cuttings can be transported easily by a thin mud at a lower fluid velocity. On the other hand, high pipe rotation draws the cuttings from the low side of the annulus by the dynamics of the drill pipe and the cuttings are settled more slowly in thicker mud than in thinner mud. When deciding which mud is better thin or thick we have to take rotation of pipe in consideration. [1]

Guild and Hill [1] presented another example of application of hole cleaning research which was practiced into the field. After their one well was lost due to poor hole cleaning, they reported trouble free drilling in two extended reach wells. The program was designed to maximize the footage which was drilled between wiper trips and to avoid hole cleaning backreaming trips before casing point was reached. They avoided the accumulations of cuttings by monitoring the pick-up weight, rotating weight and slack-off weight carefully as drilling was taking place. It was observed that the cuttings accumulation in the hole lead to an increase in the difference between pick-up weight and slack off-weight. The reason for this is there it will be more difficult to pull cuttings which are putting weight on BHA (Bottomhole Assembly). By using these observation parameters they were better able to monitor the hole conditions in the well. [1]

[1] Though hole cleaning is not a very big problem today compared to as it was 10 or 20 years ago [1]. [1]The percentage for stuck pipes and lost wells incidents has become quite low in recent times but the way it is being handled today is still very costly. [1] [12] However, we must be aware that the way we try to avoid cuttings accumulation in wells takes time and it is very costly. Large part of the operational time is used on extra circulation, wiper trips and backreaming procedures. If we can reduce this by having a better understanding of what is necessary, rig time can be saved. Here there is still need for more research on hole cleaning and development of better predictive models. An example of recent developed model is given in the reference list. [12]

[1] Fluid flow modeling of drilling fluids under in-situ conditions is the basic information that is needed to understand cuttings transport. To predict any fluid

flow model, i.e., annular velocity and viscosity profiles it is important to keep in mind what kind of fluid model that is assumed. Hemphil, Pilehvari and Campos [1] showed that the representation of drilling muds was far better represented by yield-power law model in contrast to power law and Bingham plastic models. Hacjislamoglu and Langlinais [1] performed model simulations laminar flow of yield-power law fluids in eccentric annuli. A similar study was conducted by Azouz et al. [1]. However, to model non-Newtonian fluids was much more complex and there is also a need to extend it to include drill pipe rotation and dynamics. [1]

[1] A major shortcoming of the laboratory data, correlations and models lead to inadequate drill pipe role representation. The study made by Bassal [1] and field data reflected the significant role high speed rotation had. More laboratory data and field studies are required to understand the effect of drill pipe rotation. The present cuttings transport correlations and models have empirical coefficients that were determined based on laboratory and field data. But still there is a need for the development of comprehensive cuttings transport mechanistic models that could be verified with experimental data. Ideally how a particle and liquid interacts in a flow process should be studied by transient fluid flow model. The challenge there will be to describe properly the interaction between particles and liquid, for instance the formation and removal of beds. [1]

[12] Since the cuttings transport model is quite complex and depends on many variables, it can be a bit dangerous to rely too much on model predictions. The models will have errors. Hence, we need to take into account downhole well data. For instance, the relation between pick up and slack off weights of the drill string can be a good indicator of emerging cuttings accumulations problems. Use of measurement of downhole pressures can also be useful since increasing pressures can be an indication of cuttings bed accumulation and possible emerging stuck pipe scenarios. By using real time data in combination with models and possible real time calibration, one can obtain tools that can warn about deteriorating downhole conditions. [12]

For efficient hole cleaning, the following guidelines are recommended. (Taken from reference [1])
  1. Designing the well path in such a way that it avoids possible critical angles.
  2. Making use of top drive rigs if possible in order to allow the pipe rotation while tripping.
  3. Maximizing the fluid velocity while avoiding hole erosion. This can be done by increasing pumping power and by making use of drill pipes and drill collars that have large diameters.

4. The mud rheology should be designed such that it enhances turbulence in inclined/horizontal sections while the sufficient suspension properties in the vertical section are maintained.
5. Using muds with high suspension properties and muds that give high meter dial readings at low shear rates in horizontal wellbores with large diameters and where turbulent flow is not possible.
6. Selecting bits, stabilizers and BHAs (Bottom Hole Assembly) with minimum cross section areas in order to reduce plowing of cuttings while tripping.
7. Performing wiper trips as dictated by hole condition.
8. Using different monitoring techniques that include a drilled cuttings retrieval rate, drilled cuttings physical appearance, pressure while drilling and a comparison between pick-up weight, slack off weight and rotating weight. [1]

2.2 Sand Clean out and Coiled Tubing

(Much of the literature in this chapter is taken from reference **[3]** and **[4]**) **[4]** Efforts have been made for eliminating sand production in a producing well, but sometimes sand fill can become an unavoidable by-product because of well conditions and demands for a cleanout intervention. Removal of sand fill from well by making use of CT is one of the earliest applications for CT and it has continuously been providing important services to the industry till date. CT cleanouts make use of costly fluids, reverse circulation and high circulation rates for solids removal. Excess hydrostatic pressure is exerted on the formation in many of these conventional sand cleanout methods and this as a result leads to lost circulation in low formation pressure reservoirs. Large liner geometries are combined with smaller completion restrictions increases the task at hand as a significant reduction in annular velocities is observed despite using higher CT circulation rates. **[4]**

[4] To increase the efficiency of solids removal operation to as good as near 100 %, a specially developed cleanout tool and a computer simulator is used to optimize the operation. This would result in the removal of all fluidized solids. Simplified operational procedures make it easier to take a qualitative decision about the cleanout efficiency. The transport of the solids along the wellbore is simulated by using a computational approach. This computational approach uses control volumes. Some empirical formulas are applied in order to predict significant parameters such as solids transport, fluid velocities and pressure. The division of wellpath is made and the wellpath is divided into particular control volumes. These wellpaths provide us information on horizontal, build and vertical sections of a well. The control volume shows homogenous properties. The rates at which the solids are removed are predicted by parameters such as flowrates of the fluid and properties of the fluid. Then the concentration of the solid for each control volume used is integrated with fluid properties and flowrates. A clean out job is a process which consists of four phases. These phases include analysis of the distribution of the solids after the CT has reached to the TD (Total Depth). How solids are initially distributed needs to be estimated, this is also an important phase. Other two important phases include the transport of the solids during the process of the wiper trips and transport of solids with stationary circulation at TD. **[4][3]** Cleaning of the fill from the wellbores is a problem which is solved by using CT (Coiled Tubing). The process depends on numerous variables which include fluid properties, wellbore geometry and deviation, properties of particles, speed of wiper trip, fill penetration rate. **[3]**

[3] A number of clean out methods have been developed in the past, which incorporated high circulation rates, wiper trips, reverse circulation for removal

of solids and special fluids. Many of these conventional sand clean out methods often exert extra frictional pressure on the formation, which leads to lost circulation in pressure depleted reservoirs. To overcome excess frictional pressure on the formation, the conventional solution has been to inject nitrogen in order to reduce density of the fluid and lower the hydrostatic head. However, an alternative technique that has been used for relocating fill without the placement of a hydrostatic head load on the reservoir is sand vacuuming technology which makes use of a CCT (Concentric Coiled Tubing). In the past years, use of wiper trip method to clean sand has become the preferred technique. In order to achieve proper cleaning, return flowrate needs to be maintained for carrying the sands to the surface. To maintain proper return flowrate an adequate pump rate and reservoir pressure is required. For reservoirs which are pressure depleted and completed with horizontal wells, use of sand vacuuming system is made for effective removal of the debris without circulation of nitrogen and high pump rates. Fluids with high solid trips suspension capability in combination with wiper trips are used to remove a fill that is not possible to be removed from large diameter deviated wellbores which use conventional low cost clean out fluids. In fact fluids with high solids suspension capability combined with wiper trips can be a more economical option. [3]

[3] The main reason to apply reverse circulation technique is to clean the sand accumulated from large diameter wellbores when it is difficult to achieve required pump rates for conventional "forward" circulation. A venture junk bailer is often used for retrieving larger or heavier material which is not possible to be circulated out by using traditional methods. For a wellbore which contains large or heavy junk, a venturi basket is deployed for cleaning of the wellbore. [3]

[3] When we have to select a suitable sand cleanout method it is necessary to take technical as well as logistical issues into consideration. Numbers of factors play an important role in various sand cleanout methods some of them are cost of the equipment, weight of the reel for example string weight and diameter and some other issues such as cost of nitrogen and its availability. Some other technical issues which are a matter of concern and should pay attention to size and type of debris, the extent to which pressure zone has depleted, the potential damage that the formation has went through and small completion tubular. [3]

[3] CT fill cleanouts have existed since four decades almost and today 30% of the services are performed with CT. The use of CT and conventional jointed pipe both offer two circulation modes for removing solids: the mode was either forward or reverse circulation mode. Making use of conventional water-based fluids, conventional sand cleanout method can apply excess hydrostatic pressure on the formation causing loss of circulation to a sub-hydrostatic reservoir. If the

losses are too high then it would make removal of sand impossible. Hydrostatics can be reduced by injection in the well. But this demands a specific job design and execution. Wellbores which have large diameters in horizontal wells especially need large amounts of nitrogen which leads to economical and logistical consequences. [3]

[3] Sand vacuuming technology was developed to reduce the risk of challenges associating with large nitrogen requirements. CCT (Concentric Coiled Tubing) string connected with specialized downhole jet pump constitutes the vacuuming system. Three operation modes of the tool were: well vacuuming, sand vacuuming and high pressure jetting. The tool provided a localized drawdown wherever it was positioned in the wellbore and effectively removed sand in the sand vacuuming mode and removal of mud damage was performed in the well vacuuming mode. [3]

[3] The use of coiled tubing was made for conveying circulation fluids and tools for removing material such as formation fines, drill cuttings, scale and milling debris, frac proppant and so on out of the wellbore is a normal routine industry practice. For a typical sand cleanout process the two different modes in which a fluid can be circulated are: forward circulation and reverse circulation. In the forward circulation mode, the wash tool pumps down the carrying fluid through CT and through completion annulus/ CT they are flown back to surface. High energy jets or drill bits running on motors is the mechanism in forward circulation that can help breaking up and dispersing any compacted fill in the wellbore. However, for reverse circulation the mechanism is that the CT/ completion annulus pumps down the fluids with returns back up the coil. There are limited options for breaking up compacted fill when reversing. [3]

[3] Customized nozzles are available for delivering high energy jetting in the forward circulation mode but they allow reverse circulation without any drop in pressure. Emptying solids inside the CT string is necessary first when reversing a compacted sand "bridge" and then forward jetting mode needs to be switched for breaking up the "bridge" and then succeeding switching back to reverse mode. Certain limitations exist when reversing up the coiled tubing due to safety reasons. [3]

Figure 1: A picture of Coiled Tubing [Taken directly from [5]]

2.3 P&A (PLUGGING AND ABANDONMENT) AND SWARF

(Much of the literature in this chapter is taken from reference [8] and [9]) [8] The problems that are associated with the removal of swarf during milling operations is the same as those problems which occur while transporting drilled cuttings. The phenomena of swarf transport is quite similar in nature as the one experienced when transporting cuttings during drilling. In both cases we operate with the same well geometry and Non Newtonian fluid for transporting the debris. The major difference is that the swarf has much larger density (7.85sg versus 2.5 sg) than cuttings and the swarf can have very different irregular shapes compared to what is seen for cuttings. [8]

[8] Swarf is generated in the hole when a casing milling operation is performed. The use of milling fluids are important for carrying swarfs and these milling fluids are important elements when deciding the total cost of the milling operations. Both technical and financial aspects are considered significantly when the selection of the milling fluid is made. Three common and generic types of milling fluids that were used by Mobil North Sea Ltd (MNSL) were used in experiments that were conducted at Heriot-Watt University. The milling fluids studied were Bentonite/Bicarbonate Mud, Xanthan Gum/sea water Mud and Bentonite/MMH (Mixed Metal Hydroxide) Mud. The purpose of the investigation was to study the impact of fluid rheology on the capability to transport swarf out of the hole. [8]

[8] The shape of the swarf affects the settling velocity of the swarf present in static fluids. But problems like bird nesting of the swarf can occur in the annulus. Another important parameter that significantly affects the settling velocity of the swarf is surface area to weight ratio. It is an advantage to produce swarfs which are small in size and thin in shape and possess a plate like structure. This is achieved with help of milling tools. The swarfs will then have large surface area to weight ratio and possess low weight which again is an advantage. We have to measure the strength of the gel because it has important impact on the transport of the swarf. The gel strength also gives an indication on how good suspension properties the milling fluid has. [8]

[8] It is important to keep the effective viscosity of the fluid as high as possible because the swarf transport has a significant link with the viscous and pressure drag forces that normally act on the swarf by the circulating fluids. However, experiments were carried out with a steel ball. The purpose here was to indicate that the yield or gel strength of fluid was not accurately found by using conventional techniques like i.e, coaxial viscometer. It has been observed that there is an increase in the transport velocity of the steel ball if the size of the

steel ball decreases. There is a correlation that exists between the effective viscosity of the fluid and the transport velocity of the steel ball. But a precise determination of the gel strength is obtained when a constant rheometer is used. Steel balls are used because they are regular in shape and by using them we can avoid the effect irregular shape of the swarf has on the settling velocity of the fluids. Use of steel balls makes it easier to calibrate the fluid with respect to their transport capability and suspension. **[8]**

[8] It has been verified with the help of experiments that gel strength and effective viscosity of the fluid and the shape, surface area and settlement orientation of the swarf does affect the settling rates of swarf in static fluids. Bentonite/MMH mud system exhibits the best combination of suspension and transport characteristics as a fluid. **[8]**

[9] Mixed Metal Hydroxide (MMH) mud increases the efficiency of swarf removal and is more effective as compared to other fluids. In addition to that, it minimizes normally occurring wellbore problems such as excessive reaming, packing off, difficulty in obtaining hole logs and stuck pipe. The most common contaminants found in drilling fluids are solids. MMH system is quite tolerant to these solids that exist in the drilling fluid. A contaminant that exists in drilling fluids is carbonates and MMH is a very good tolerant to carbonate contaminants. MMH mud also has a low solubility in water and helps dispersion phenomena in the fluid. It is also useful in situations where stabilization of the borehole wall is needed and this is achieved by minimizing the erosion caused by the viscous drag of the dynamic fluids. The loss of the fluid should be reduced in order to achieve effective transport of cuttings to the surface. Because if there is a loss in the fluid then cuttings will accumulate in the bottom and deposits will store in possum bellies which are irregularities that exist on the borehole wall due drag forces that have acted on the borehole wall. As a result we will face problems like hole instability. However, MMH mud has been acting as a remedy in solving much of the hole problems by exhibiting good rheological properties and this is achieved because the MMH mud system has a unique rheology which is different from the conventional muds. **[9]**

[8] MMH mud has also proved to be very cost effective and cheap as compared to other available fluids. **[8]**

3. Some General Considerations on Particle/Liquid Flow in Well Operations

[10] As described earlier in this thesis, hole cleaning (cuttings transport) is a matter of concern and challenge when inclined wells are drilled. Insufficient hole cleaning can lead to critical problems which can be expensive such as increased ECD (Equivalent Circulation Density), excessive torque and drag, pack-off, cementing problems, stuck pipe, etc. [10]

[10] However, the physics of particles cuttings flow is very complex and it is impossible to make accurate predictions. Complicating factors are that the cutting particles can vary in size, shape and density. In addition, when considering Non Newtonian fluids multiple flow regimes can occur. [10]

[10] In order to ensure that stationary cuttings bed does not form, a minimum fluid flow velocity is required in the flow geometry considered (pipe or annular). This minimum velocity is called Critical Transport Fluid Velocity (CTFV). [10]

[2] More properly defined CTFV is the minimum fluid velocity required for maintaining a continuous upward movement of cuttings. No accumulation of the cuttings will take place on the low side of the wellbore for fluid flow velocities at CTFV and higher. In a situation where the annular fluid velocity is less than CTFV, the accumulation of the cuttings will begin. If we have an annular flow velocity that is lower than CTFV, we say that we have Subcritical Fluid Flow (SCFF). [2]

[10] The accumulation of cuttings is very challenging to model in a pure theoretical way. Larsen (1990) [10] made large number of measurements and built simplified correlations based on experiments while approaching the problem. [10]

Larson [10] acquired an approach for determining CTFV, which corresponds to minimum fluid flow velocity needed for transportation of cuttings in a given situation. The CTFV is defined as the sum of the slip velocity, V_s and the cuttings travelling velocity, V_c:

$$CTFV = V_c + V_s$$

[10, 2] Cuttings travelling velocity, V_c is only related to the volume of cuttings drilled out: This depends on ROP (Rate of Penetration), annular geometry and cuttings concentration. The volume drilled out depends on hole size and ROP. The velocity is found by taking the volume rate drilled out and dividing it by

annular cross sectional area and cuttings concentration. V_c is not the same or have a link to the fluid velocity itself. [2, 10] This corresponds to the volume produced due to drilling. The flow velocity of the cuttings relative to the pipe wall refers to cuttings slip velocity subtracted from fluid velocity $= V_{fluid} - V_s$. In order to ensure proper cuttings and no buildup of beds, one needs to ensure that the V_{Cpipe} is greater than CFTV. This means $V_{Cpipe} \geq V_c$. [10]

[10, 2]The cuttings concentration C_{conc} was defined by Larsen [2] as the concentration of cuttings in the annular geometry when having flow velocities equal to CTFV. For higher concentrations of cutting, cuttings bed build up would start to take place. He carried out experiments and measured C_{conc} for various angles of inclination in the range as 55° to 90° from the vertical. [10] He also measured C_{conc} that was present just before the beds started to build up. He also probably varied the cuttings injection rate. By using linear regression on the data he found a relation between C_{conc} and $(ROP) \left(\frac{ft}{hr}\right)$:

$C_{conc} = 0.0001778 \times ROP + 0.00050.$ [10, 2]

[10, 2] Larsen made the assumption that the cuttings slip velocity, $V_s = V_\mu \times C_{ang} \times C_{size} \times C_{mwt}$

The first term V_μ is defined as the slip velocity term which depends on viscosity. C_{ang} is described as the relative change caused by different pipe angle (from 55° to 90° angle). The relative change caused by the particle size of the cuttings is called as C_{size} and C_{mwt} represents the relative change caused by the fluid density. [10, 2]

In our simplified cuttings transport model considered here, we have only assumed a simple relation $V_c = KV_{mix} - S$ where $V_{mix} = V_c \alpha_c + V_l \alpha_l$. Here we don't consider the critical velocity when beds start to form etc. and we have not incorporated all effect that should be included (ROP, mud weight, inclination, cutting size). Here S represents that cutting will slip relative to the liquid. For a stagnant liquid, S would be the falling velocity of cuttings in a vertical well. The main objective in this thesis is to just test if we are able to incorporate cuttings in the AUSMV scheme. Future work should include more realistic slip relations taking into account all effects as well as the transition to bed build up.

3.1 PARAMETERS THAT AFFECT PARTICLE FLOW IN LIQUID IN GENERAL

[11] As discussed earlier in the thesis there are certain factors that affect the transport of solids particles during the hole cleaning process. We will discuss how these parameters affect the transport of the solids transport in this section. [11]

[11] There are two phases in which we can transport solids which are gas phase and liquid phase. Both the phases have different carrying capacities. The density and the viscosity of both the phases is different. Due to this difference we get a two phase flow effect on particle transport. The circulation part which is in the liquid phase has a significant impact on the transport of the solids. However, the change in the flowrate of the liquid has a greater effect on the transport of solid particles while circulation as compared to change in the flowrate of the gas has. The important thing to be noted is when the liquid volume fraction is less than 50 % for a combined total flowrate of gas and liquid, then solids transport reduces quite a lot. So it can be stated that generally it is the liquid velocity that controls the concentration of the solids present in the annulus in the wellbore. [11]

[11] Now we would discuss the impact deviation angle of the wellbores and ROP (Rate of Penetration) of the solids have on their transport mechanism. There is a difference between transport mechanism of solids present in vertical wellbores and those present in highly deviated wellbores. If the pump rate is low then the concentration of sand increases significantly with an increase in (RIH) Run-in-Hole speed in horizontal wellbore. If the ROP is increased further then the concentration of cuttings begins to become constant. This happens because the velocity profile on the low side of the annular section of the wellbore becomes low. Shear stress which acts at the bed interface plays an important role in solids transport because most solids are transported through a thin moving layer which exists between the stationary bed and the flow stream. This movement of the layer that takes place is called as 'saltation'. Now if the ROP is increased further then the flow channel will be reduced. As a result of this the in-situ liquid velocity will be increased and reaches a critical value at which there will be no increase shown in bed height of the solids with a further increase in the ROP. When the pump rate is high enough then what happens is that there is no stationary bed that is created and all the solids are transported in suspension. [11]

[11] In a near vertical wellbore, the solids exist in suspension and hence there is no stationary solids bed which is present. Two other factors that have a critical impact on solids transport are the drag force and the weight that a particle

possesses. Another important thing to take into consideration is in a deviated wellbore with an angle which lies between 30° to 55°, most solids are found to be present near the low side of the wellbore. The solids bed that is formed is unstable and it is possible that it slides back and gets re-trained in the flow stream which is lower down in the well. This would depend on the flowrate of the solids. Therefore it is important to maintain an appropriate minimum flowrate to prevent this from happening. For each deviation angle there is minimum in-situ liquid velocity which is required to transport solids and at this velocity the carrying capacity of the sand approaches towards zero. A change is shown in the values of minimum in-situ velocities required for different deviation angles. At an angle of 60° the minimum critical velocity has the highest value because hole cleaning for this build-up section around 60° is quite challenging. **[11]**

3.2 THE DIFFERENCE BETWEEN STEADY STATE AND TRANSIENT FLOW CONDITIONS

[14] In a steady state situation, the mass flowrate is the same at every point along the linear section of the pipeline. If this doesn't happen then the flow situation is not a steady state one. [14]

[14] However, in a transient flow there are variations shown in the flow along the pipeline. The changes that occur in the boundary conditions, the statuses of the equipment used create transients and surges that travel across the pipeline. In steady state solutions, no such transients are present. [14]

[14] Normally a pipeline flow is a transient process. This can be stated because the inlet and outlet flow change. In addition to that, there is a change in the temperature with change in ambient conditions, variation in control setpoints. Hence, it is an advantage to have a transient flow model that can describe the dynamics taking place. [14]

[14] The main difference between the steady state and transient state models is that in transient equations of motion there is a rate of change shown in the dynamic variables such as pressure, velocity, density and temperature with respect to time. When all time dependent terms in the transient model are removed, we will end up with the steady state equations. There is one common thing in the results that are produced by making use of the two approaches. This thing is the spatial arrays that the dynamic variables produce at successive points in time. An important thing that should be noted is that the values that are used in these produced arrays are normally not same for both models. As mentioned earlier in this section the transient model causes changes in the dynamic variables and as a result we get transient values. However, in case of steady state, the values do not depend on previous values. The arrays of values that are obtained from SSS (Succession of steady states) process are persistent with regard to current boundary conditions and steady state assumption. Each successive steady-state solution is independent of the previous one. But it is important to note that pipeline model is not independent of previous steps in both SSS (Succession of steady states) and transient models. [14]

[14] It is easy to implement models that are based on SSS (Succession of steady states) approximation as compared to fully transient models because the steady-state solutions are not exposed to numerical instabilities unlike transient models. However, this doesn't mean that transient models are very unstable but it's just that they are more difficult to apply robustly. The issue to be concerned is mostly the changes in time when implementing the models. It is very important

to take into consideration the accuracy in the magnitudes of the changes occurring in the model. Such issues are more essential in transient state solution conditions. What happens here is that we achieve rate of change of the dynamic variables and this happens when the current values of these variables are put back into the equations of motion. As a result of this, these equations of motions represent the rates of change. Now the rates of change that we get form SSS (Succession of steady states) results are also quite straightforward but the difference here is that the rates of change from SSS (Succession of steady states) results are estimated by taking the difference between current values and the previous values and dividing the difference by the time interval. The problem in this case is the accuracy of these estimates. [14]

[14] Now we would discuss the importance of accuracy for implementation of the models. We get inaccuracies in both the models because the results that we achieve form SSS (Succession of steady states) and transient models are actually approximations to the actual conditions in the pipeline that result because we don't have perfect knowledge of the boundary conditions, properties of the fluids, equipment properties and surrounding conditions. These accuracies also result because of the limitations of the numerical solution techniques that are used for both models. These inaccuracies from numerical techniques exist because the calculation of the dynamic variables is made at discrete points in time and space. The changes in the values between these points are linear for all the numerical models. Numerical techniques are different in the way they solve the physical equations. The physical equations that most pipelines use are not exposed to analytical solution; the differences that occur are used in the form of approximation. We will get different results by making different approximations. But generally these results converge to same solution in the limit for short time steps and hence short distance steps. [14]

[14] Other issues that lead to inaccuracies include the viscosity property of the fluids does not change during the time step. This property depends on density and temperature in a complicated way. Other parameters that cause inaccuracies include ground thermal properties such as effective conductivity and undisturbed ground temperature. The turbulent state of the fluid and the transition zone between the laminar and turbulent flow also leads to inaccuracies. The accuracy of the model is also reduced by measurement errors that are made in real time models. [14]

4. DRIFT FLUX MODEL AND AUSMV SCHEME

[15] In this section, we will describe the importance of transient flow models in planning and follow up of advanced well operations such as managed pressure drilling and underbalanced operations. Flow models and in combination with controlled engineering algorithms with different settings are used to control flow parameters. To achieve this we need robust flow models and need to understand the uncertainties that exist in the modeling process. [15]

[15] A robust model that handles dynamic flow systems very well is called the AUSMV (Advection Upstream Splitting Method) scheme. The purpose of this model is to make it easier to investigate different flow scenarios and pressure control problems that take place normally in automation drilling, underbalanced drilling, well control procedures and managed pressure drilling. [15]

[15] Hybrid flux-splitting schemes are used to solve compressible Euler and Navier-stokes equations. These schemes are developed by combining the accuracy of flux-difference splitting (FDS) schemes (Evje and Fjelde 2013) and the efficiency of flux-vector splitting (FVS) schemes. Advection Upstream Splitting Method (AUSM) (Liou and Steffen, 1993) is an example of such a scheme and so is its extension called $AUSM^+$ (Liou 1996). The AUSM scheme is more accurate, efficient and robust compared to other upwind schemes. However, $AUSM^+$ was proved to be very effective in producing exact resolution of shock discontinuities and also discontinuities caused by contact. It was also useful in solving and simplifying hyperbolic systems. [15]

[15] Then based on AUSM, Fjelde and Evje (2003) came up with a hybrid schme called 'AUSMV' which solved a hyperbolic system of conservation laws. This was followed by a scheme which was put forward by Evje and Fjelde (2002). The AUSMV scheme is one dimensional and is used for solving the two phase drift flux model. In this model we take the average of the flow component which is perpendicular to the pipe or tube axis. The model has the universal form stated below:

$$\partial_t W + \partial_x F(x, W) = G(x, W)$$

[15] Here W represents conservative variables and F is flux and the source term is represented by G. T is the time and the direction along which flow is occurring is represented by x. When AUSM and FVS schemes are combined in an appropriate way we get the AUSMV scheme. When this approach is used it reduces the numerical computational time and gives accurate resolution of contact discontinuities such as mass fronts and non-oscillatory approximations

of acoustic waves (Evje and Fjelde 2003). One will also avoid the numerical computation of the Jacobian of the flux equation by using AUSMV scheme. [15]

[16] There are three fundamental conservation laws that apply to flow that occur in pipe and well. These are the following:

- Conservation of mass
- Conservation of energy
- Conservation of momentum

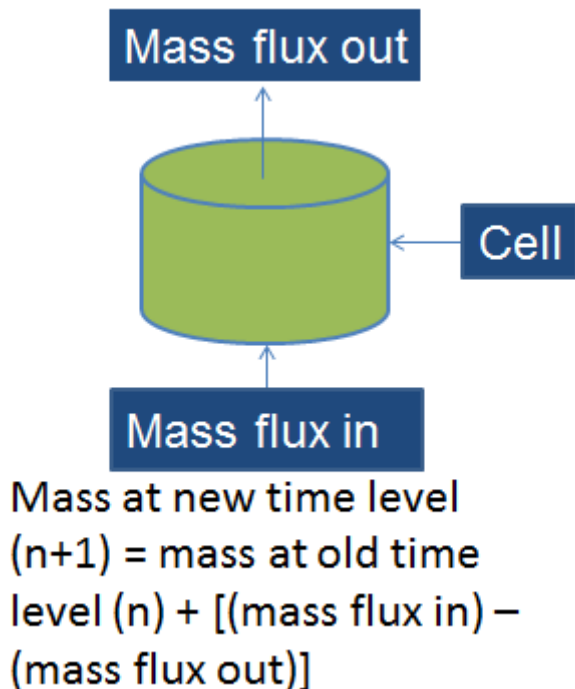Let us consider the conservation of mass by looking at the segment of the pipe given below in the figure. [16]

Mass at new time level (n+1) = mass at old time level (n) + [(mass flux in) − (mass flux out)]

Figure 2: Conservation of Mass (Taken directly from [15])

[16] The drift flux model which is used for well and pipe flow can describe one or two phase flow in pipes and is completely transient in nature. This means that it is used for describing well conditions that change with respect to time. An example of this is when we reduce the bottomhole pressure in a situation where nitrogen is injected into a dead well to kick it off for production. [16]

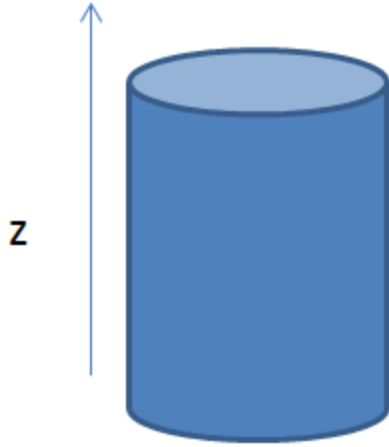Now let us consider a well segment shown in the figure below:

Z

Figure 3: A well segment (Taken directly from [16])

[16] Given below are partial differential equations that represent the conservation of mass and momentum across the segment given in figure 3. Here the conservation of energy equations are neglected because the assumption that is made here is that the temperature is a constant variable. [16]

[16] Conservation of liquid mass:

$$\frac{\partial(A\rho_l\alpha_l)}{\partial t} + \frac{\partial(A\rho_l\alpha_l v_l)}{\partial z} = s_1$$

[16] Conservation of gas mass:

$$\frac{\partial(A\rho_g\alpha_g)}{\partial t} + \frac{\partial(A\rho_g\alpha_g v_g)}{\partial z} = s_2$$

[16] Conservation of mixture momentum:

$$\frac{\partial A\left((\rho_l\alpha_l v_l + \rho_g\alpha_g v_g)\right)}{\partial t} + \frac{\partial(A(\rho_l\alpha_l v_l^2 + \rho_g\alpha_g v_g^2))}{\partial z} + A\frac{\partial}{\partial z}p$$
$$= -A\left(\rho_{mix} + \frac{\Delta p_{fric}}{\Delta z}\right)$$

[16] Definition of variables

A- (m^2)

ρ_i- Phase densities (kg/m^3), liquid -> $i = 1$, gas -> $i = g$

v_i- Phase velocities (m/s)

p- Pressure (pa)

s_i- Source or sink terms (inflow, leakage, and phase transfer between phases)

g- Gravity constant 9.81 m/s^2

α_l- Phase volume fractions taking values between 0 and 1. $\alpha_i + \alpha_g = 1$.

μ_l- Phase viscosities, (pas)

$\mu_{mix} = \alpha_i \mu_l + \alpha_g \mu_g$- Mixture viscosity

d_{out}- Outer diameter in annulus (m)

d_{in}- Inner diameter in annulus (m), corresponds to the outer diameter of drill string. [16]

[16] Now we would look at some closure laws which are needed and which are important to consider when solving the drift flux model. Here one needs to make sure that the number of equations have the same number as the independent unknowns. [16]

[16] **Closure laws:**

$$v_g = K v_{mix} + S \ (K = 1.2, S = 0.55)$$

[16] **Liquid Density Model (simple)**

$\rho_l(p) = \rho_{l0} + \frac{(p - p_0)}{\alpha_L{}^2}$, Assume water so we get: $\rho_{l0} = 1000$ kg/m^3,

$p_0 = 100000Pa$, $\alpha_L = 1500$ m/s

[16] **Gas Density Model (simple)**

$\rho_g(p) = \frac{p}{\alpha_g{}^2}$, Ideal gas: $\alpha_g = 316$ m/s.

[16] **Friction Model**

[16] The friction model presented here is taken from [18]. The general expression showing the frictional pressure loss gradient term is stated as follows:

$$\frac{\Delta p_{fric}}{\Delta z} = \frac{2 f \rho_{mix} v_{mix} abs(v_{mix})}{(d_{out} - d_{in})} (pa/m)$$

The frictional pressure gradient is directly proportional to v_{mix}^2. This means that the friction is increased by a factor of 4 when the velocity is doubled. The friction will increase as the area of flow decreases. Friction always acts against the flow direction and an 'absolute value' is used to make sure that friction changes sign if the direction of the flow is reversed. When we have two phase flow, mixture values are used in the expressions. The friction factor changes and depends on different factors such as flow pattern, pipe roughness etc. The friction factor can be calibrated. [16]

[16] Mathematical Properties of the Drift flux Model

[16] The drift flux model is classified as a system of nonlinear partial differential equations which are of hyperbolic type. This model describes the behavior of wave propagation where transitions and sharp fronts occur. By introducing conservative variables, the conservation laws can be written in the following form:

$$\frac{\partial}{\partial t} U + A(U)\frac{\partial}{\partial z} U = S$$ Where $A(U)$ would be a 3×3 matrix.

When the following eigenvalue problem is solved: $\det(A(U) - \lambda I) = 0$ we get the following real eigenvalues:

$$\lambda_1 = v_l - w, \ \lambda_2 = v_g, \ \lambda_3 = v_l + w$$ Here w represents sound velocity.

These eigenvalues provide us with information about the speed of the waves that are propagating in the system. The first and the latter eigenvalues are related to the sound waves that propagate upstream and downstream in the well. The pump rate changes and changes in the openings of the valve in the flowpath create small pressure disturbances. These pressure disturbances propagates rapidly. The mass transport wave is defined by the second eigenvalue, for example a situation where gas bubble migrates upwards in with liquid. However, this model is quite similar to the Euler equations that are used to describe flow of air. The Euler Equations are normally used in simulators which are used for constructing an airplane. [16]

Discretization Process & Application of a Numerical Scheme

[16] It is necessary to divide the well into a certain number of segments and this is done for applying the conservation laws and closure laws that are described above in this section of the thesis. This division process is denoted as the discretization of the well. For each segment the equations are solved and the

flow variables for each segment are assumed to be constant. The accuracy of the solution depends on number of boxes chosen in the discretization. If the grid is refined, one also has to reduce the time step and the simulations will become more time consuming. Normally a typical discretization consists of segments ranging from 50 to 100. By doing this it is assured that the local variations such as pressure and temperature variations are reflected in the calculations made for finding the density. Finally we can find the hydrostatic pressure in the well. [16]

Explicit AUSMV Scheme

Flow path / computational domain

$$U_j^{n+1} = U_j^n - \frac{\Delta t}{\Delta x}\left(F_{j+\frac{1}{2}}^n - F_{j-\frac{1}{2}}^n\right)$$

- Simple updating of conservative variables in time
- Fluxes are calculated based on old/ known values
- The equations are solved componentwise (no need for matrix solver like in OLGA)
- The flux formulas are simple (require only knowledge of sonic velocity)

Application Areas
Master thesis and Ph.D. work covering topics within
- Well control
- Managed pressure drilling
- Dual gradient
- Underbalanced drilling
- Control Engineering

JOHN EMEKA UDEGBUNAM, KJELL KÅRE FJELDE, AND STEINAR EVJE

Formation influx

Schematic of Underbalanced Drilling System

Annular returns to choke and separator

Time development

Figure 4: Diagram showing a discretized well and use of AUSMV Numerical Scheme (Taken directly from [17])

[16] As seen above in the diagram what happens here is that calculation begins at an initial stage where all flow variables are known in the well. The formulas shown in the diagram are used to update each cell in time. Variables of mass and momentum are updated in each cell and these variables depend on the mass fluxes (in and out) and momentum fluxes at boundaries of the cell. All the cells

get updated when they reach a new time level and then we can see a display of the situation of the well at this new time level. Generally all simulators perform numerical discretization and update the conservative variables present in different well segments by using numerical fluxes. [16]

Numerical Discretization

[15] The well is divided into N number of cells as shown in figure 5. When the AUSMV fluxes are found at the interfaces of the cell, the calculation of the conservative variables are made at a new time level $(n + 1)$ by making use of the old time level (n). The equation stated below is made use of for computing the values of w_1, w_2 and w_3 at new time level. [15]

$$w_{i,j}^{n+1} = w_{i,j}^{n+1} - \frac{\Delta t}{\Delta z}\left(F_{j+\frac{1}{2}}^{AUSMV} - F_{j-\frac{1}{2}}^{AUSMV}\right) - \Delta t q_i^n$$

[15] In this equation, i and j denotes conservative variables and their respective cells. The fluxes are treated explicitly in time and due to this the length of the time step is limited by the CFL condition. The CFL is a number between 0 and 1. [15]

[15] The following equation represents the CFL condition:

$$\Delta t = CFL \frac{\Delta z}{\max(|\lambda_1|, |\lambda_2|, |\lambda_3|)}$$
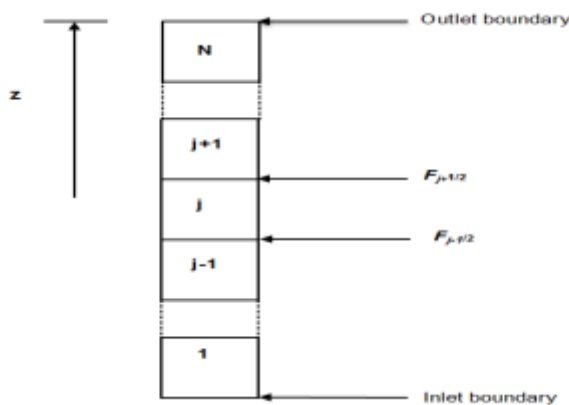
Figure 5: A discretized wellbore where the conservative variables are updated explicitly in time. [15].

Boundary Conditions

[15] It is important to specify numerical fluxes at the inlet and outlet boundaries of the well. This is done by AUSMV scheme which implements extrapolation method for pressure fluxes. [15]

[15] The mass flowrates of liquid and gas are known at the inlet boundary and transmitting fluxes are provided directly. Extrapolation is done with pressures in the first two adjacent cells and like this we are able to find pressure flux, P_{inlet}. This extrapolation includes the effect of gravity and friction. [15]

$$P_{inlet} = p(1) + 0.5(p(1) - p(2))$$

[15] We have two conditions and those are open and closed condition which can be specified at the outlet boundary. [15]

[15] The important thing to note for open conditions is that the fluxes which are convective are based on extrapolation of the primitive variables such as phase densities, volume fractions and velocities in the last cell. [15]

[15] At the outlet, for an open end the pressure is set equal to atmospheric pressure. [15]:

 [15] When the fluid is flowing through the tubes a change in the flow area is observed quite often. Unsteady one dimensional flow in an enclosed passage of varying cross sectional areas was considered by Corbean and Gascon (1995) to address the issue. But because it was difficult to discretize the source terms, AUSMV scheme makes use of another approach that helps in solving the flow area changes to achieve correct results. The main purpose here is to locate the flow area discontinuity at the center of a cell and then bring the mass balance requirements into operation. [15]

$$(A\alpha_l\rho_l v_l)_L = (A\alpha_l\rho_l v_l)_R,$$

$$(A\alpha_g\rho_g v_g)_L = (A\alpha_g\rho_g v_g)_R,$$

[15] Here the subscript L and R represent the left and right hand boundaries of a numerical cell. Average is taken of the volume fraction while an assumption is made of the pressure and corresponding density of each phase. The numerical scheme will then take the following form [15]:

$$w_{i,j}^{n+1} = w_{i,j}^n - \frac{\Delta t}{\Delta z}(H^c + H^p) - \Delta t q_i^n,$$

Where $H^c = A_R(F_{l,g}^c)_{j+\frac{1}{2}} - A_L(F_{l,g}^c)_{j-\frac{1}{2}},$

$$H^p = A_{avg}\left(F^p_{j+\frac{1}{2}} - F^p_{j-\frac{1}{2}}\right),$$ The parameter, A here is de the flow cross sectional area where $A = \frac{\pi}{4}\left(d_o^2 - d_i^2\right)$, $A_{avg} = \frac{1}{2}(A_L + A_R)$ [15]

[15] The pressure and phase volume fractions for each cell are found from the variables $w_{1,j}$ and $w_{2,j}$ after each time interval. What happens next is that the mass conservative variables are divided by A_{avg} and multiplied by the same parameter after the parameters p, α_l and α_g have been investigated.

Then finally the phase velocities are calculated with the momentum conservative variable, $w_{3,j}$. For no slip conditions we normally have following conditions:

$(K = 1, \ S = 0, \ v_l = v_g)$ and the liquid velocity a the left and right hand side of the discontinuity is given as [15] :

$$v_{l,L}\frac{w_{3,j}}{A_L(\alpha_l\rho_l + \alpha_g\rho_{g)}},$$

$$v_{l,R}\frac{w_{3,j}}{A_R(\alpha_l\rho_l + \alpha_g\rho_g)},$$

5. ADJUSTMENT OF THE DRIFT FLUX MODEL OF AUSMV SCHEME TO SIMULATE PARTICLE/LIQUID FLOW

In this section an attempt will be made to study cuttings and liquid flow using a transient flow model. This is based on the drift flux model and the conservation laws that are solved using the numerical scheme AUSMV. The starting point was an existing code that consider liquid and gas flow. In the following we will describe the model and the numerical scheme and what adjustments had to be made to be able to simulate particle/liquid flow. All the variables representing the gas phase were used to represent cuttings.

Following are the adjustments that were made in order to alter the model:

Density Model for Cuttings.

The replacement of gas density model was made by a model for cuttings density. The cuttings density was assumed fixed to be 2500 kg/m^3.

New transition between physical and conservative variables.

In the AUSMV scheme, the calculation of conservative variables is made at new time level based on old values and the fluxes existing between the numerical cells. For a two phase flow system consisting of gas and liquid, the following conservative variables w_1 and w_2 indicate liquid and gas mass to be calculated:

$w_1 = \rho_l(p) \cdot (1 - \alpha_g)$ Known value

$w_2 = \rho_g(p) \cdot \alpha_g$ Known value

The variable p represents pressure and ρ_l, ρ_g are the liquid and gas density variables which depend on pressure. The gas volume fraction is stated by α_g. The two equations are required to be solved to find the stated physical variables which we are concerned with. If a system with solids instead of gas is assumed the last equation will become as follows:
$w_2 = \rho_c \cdot \alpha_c$. The point to be noted here is that the cuttings density ρ_c remains constant. By combining these two equations, the following equation is obtained and this equation is used for finding pressure:

$$\rho_l(p)(1 - \frac{w_2}{\rho_c}) - w_1 = 0 \text{ Or}$$

$$(\rho_{l0} + \frac{(p - p_0)}{a_l^2})(1 - \frac{w_2}{\rho_c}) - w_1 = 0$$

Here the density of particle liquid flow and pressure at standard conditions is denoted by ρ_{l0}, p_0 and the speed of sound in the liquid is represented by

Here $c = 1 - \frac{w_2}{\rho_c}$ defined as a constant. The equation above can be simplified and written as: $\left(\rho_{l0} + \frac{(p - p_0)}{a_l^2} \right) . c - w_1 = 0$

Finally, we are able to find the pressure by the following expression:

$$\frac{(p - p_0)}{a_l^2} = \frac{w_1}{c} - \rho_{l0}$$

The pressure can then be found by the following expression finally:

$$p = p_0 + (\frac{w_1}{c} - \rho_{l0}) \cdot a_l^2$$

Now the cuttings concentration can be found from:

$$\alpha_c = \frac{w_2}{\rho_c}$$

And the liquid density is found by the given formula quite easily:

$$\rho_l = \rho_{l0} + \frac{(p - p_0)}{a_l^2})$$

Slip model

The same model is used for liquid/gas flow and gas/cuttings flow in the form as given below:

$$v_c = K((1 - \alpha_c)v_l + \alpha_c v_c) + S$$

No slip conditions apply when $K = 1.0$ and $S = 0$. This means that the cuttings and the liquid will be transported with the same velocity. In this thesis, we have only performed simulations with no slip conditions. If we want to incorporate

that the cuttings fall downwards in the well, relative to the liquid, a negative value for S must be chosen. For a system which consists of liquid and gas, the value of S has to be positive. This is because gas tends to travel faster upwards as compared to liquid.

Sound Velocity

The numerical fluxes between the cells depend on the sound velocity of the mixture which is denoted by $\alpha_l = 1500 m/s$. We have neglected any contribution from the cuttings particles on the sound velocity.

How the model is run

The massrates of the liquid and cuttings are changed at the bottom of the well in order to simulate the different transient scenarios and the results, effects and observations are described further in the thesis. It was assumed that there is atmospheric pressure at the outlet of the well.

6. Simulation Results and Discussion

In this section, the main code given in appendix A was used to see how cuttings affected bottom-hole pressure and how BHP (Bottomhole Pressure) varied with changes in time and how changing rate of penetration affects the BHP (Bottomhole Pressure) versus time. The model here is a transient one as time is varying.

Let us start with describing the geometry of the well which is the same for different cases. Everything is given in appendix A. The depth of the well was H = 2000m and the well was discretized into 25 boxes initially then into 100 boxes and the effect of changing the number of boxes was observed later for different massrates of cuttings which is shown later in the calculation part. The end time for simulations and the changes were shown in the plots. The flow-rate of the mud was 22kg/s which was converted to l/m (liter/minute) by multiplying it with 60 seconds so we got 1320 l/m and the density of the cuttings mud is assumed to be = 2500kg/m^3. The density of the liquid used was assumed to be = 1000kg/m^3. So by using this information we can find the time cuttings used to circulate from bottom to top in the well. Time for circulation:

Flowrate = 22 kg/s; also 1kg corresponds to 1 liter
Flowrate of liquid (Water) = 22 l/s $\rightarrow$ $(22 \times 60 = 1320 \, l/m)$, where $m = 1$ minute = 60 seconds
$T = V_{well}/V_{rate}$ = 47.8 m^3/ 0.022 m^3/s = 2172 seconds
$V_{well} = A_0 L = 0.0239 m^2 \times$ 2000m = 47.8 m^3

Where area of the cross section of the well is found by using the following formula: A= area= $\pi/4(D_o^2 - D_i^2) = \pi/4(0.2159^2 - 0.127^2) = 0.0239$ m^2 where outer diameter of the cross section of the well is 8.5" and inner diameter of the cross section of the well is 5.0". Both of these diameters are multiplied by 0.0254 in order to convert them from inches to meter length units. Below figures were plotted using the main Matlab code given in appendix A. First case is a no slip model where the changes in the cuttings concentration are observed for different time intervals and finally a bottomhole pressure time plot is shown for end time= 4100 seconds and the massrate of the pumped cuttings used in this case is 2kg/s. The well is initially filled with pure liquid and we start pumping with 22kg/s of liquid and 2kg/s of cuttings at the bottom of the well. Let us now see and discuss the observations shown in the graphs below.

Case 1: K= 1, S=0 Massrate= 2kg/s no slip model
The following changes were made to the code in appendix made for case 1:
if (time < 150)

   inletliqmassrate=0.0;
   inletgasmassrate=0.0;

elseif ((time>=150) & (time < 160))
  inletliqmassrate = 22*(time-150)/10;
  inletgasmassrate = 2.0*(time-150)/10;

elseif ((time>=160)&(time<4000))
   inletliqmassrate = 22;
   inletgasmassrate = 2.0;
elseif((time>4000)&(time<4010))
   inletliqmassrate = 22-22*(time-4000)/10;
   inletgasmassrate = 2.0-2.0*(time-4000)/10;
elseif((time>4010))
   inletliqmassrate=0;
   inletgasmassrate=0;
end

However, the end time was changed accordingly for different times in case 1. For example for 500 seconds the Matlab code in appendix A was changed to the following:
endtime = 500; % Time for end of simulation
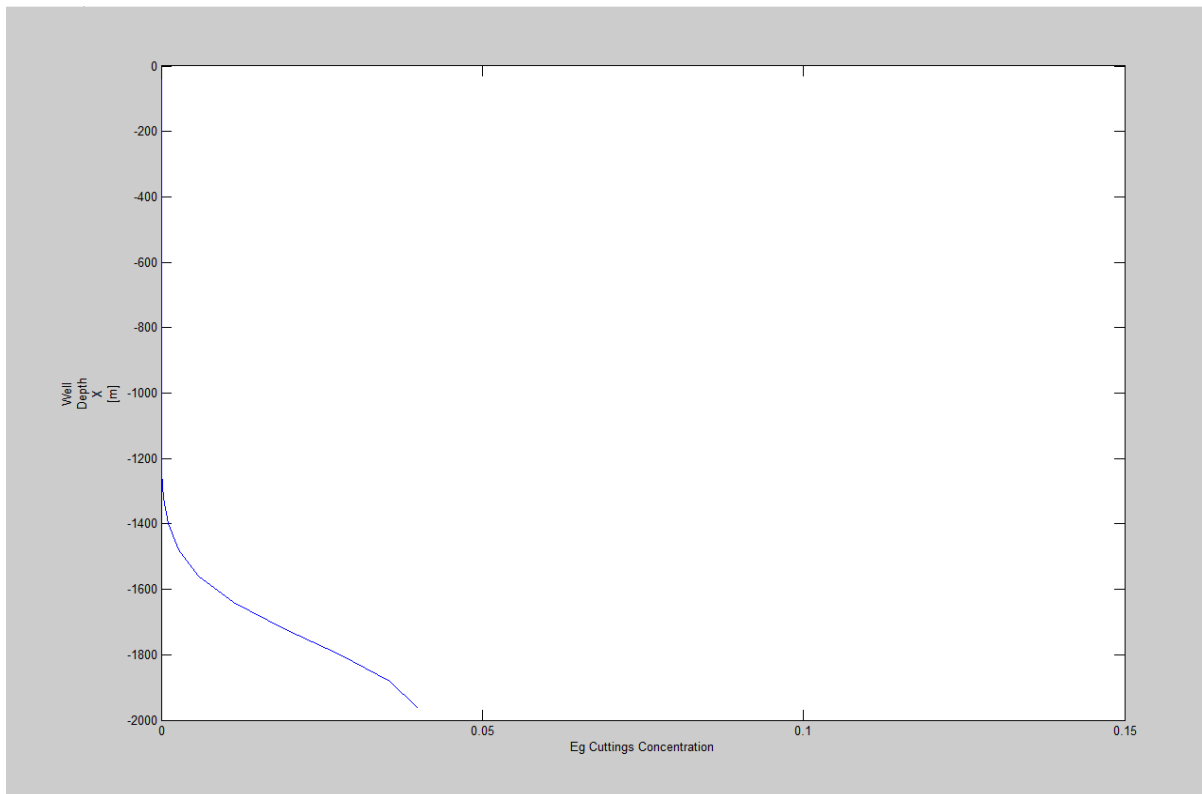
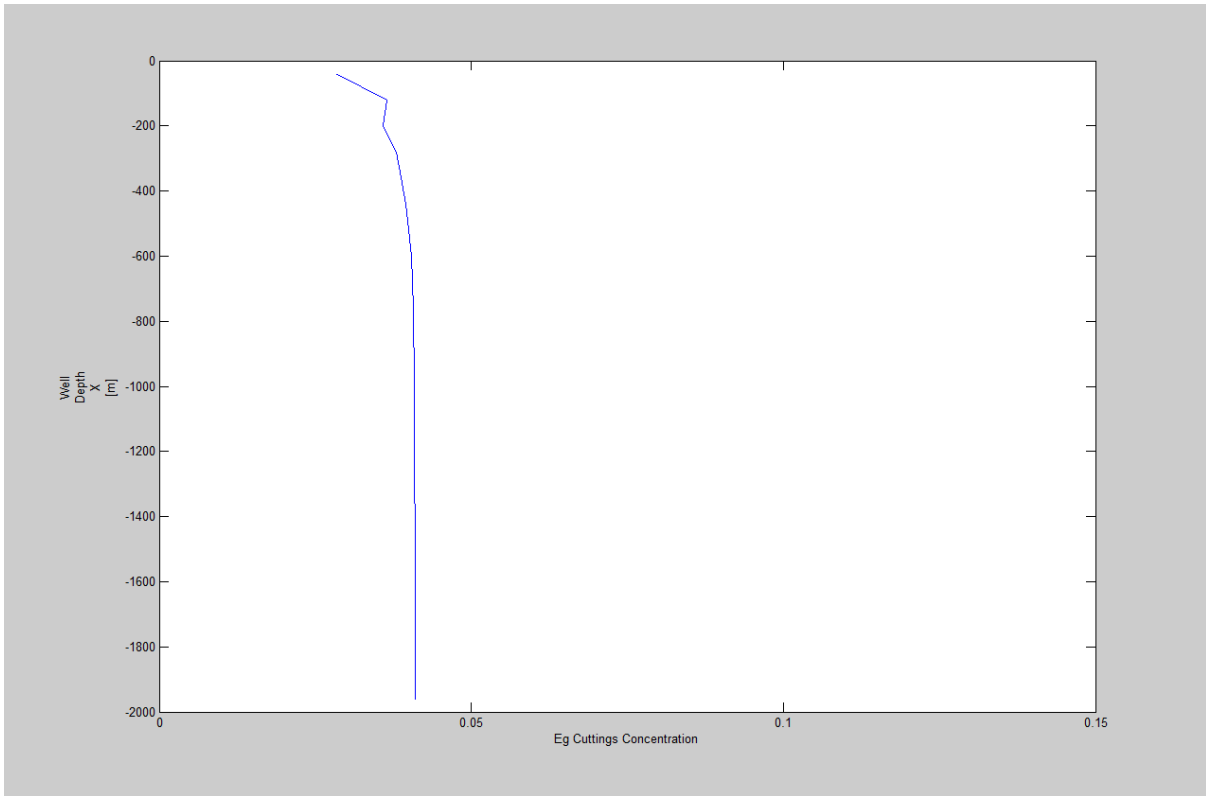**Figure 6: 2kg/s, 25 Box, t= 500sec, well depth against cuttings concentration plot.**

In Figure 6 it can be seen that at 500 seconds the lower parts of the well contains cuttings. Therefore the cuttings will need to be transported out of the well. However, the trend shown here is that the cuttings concentration is zero to almost 1250m and then it starts to increase steadily reaching a value close to 0.04.
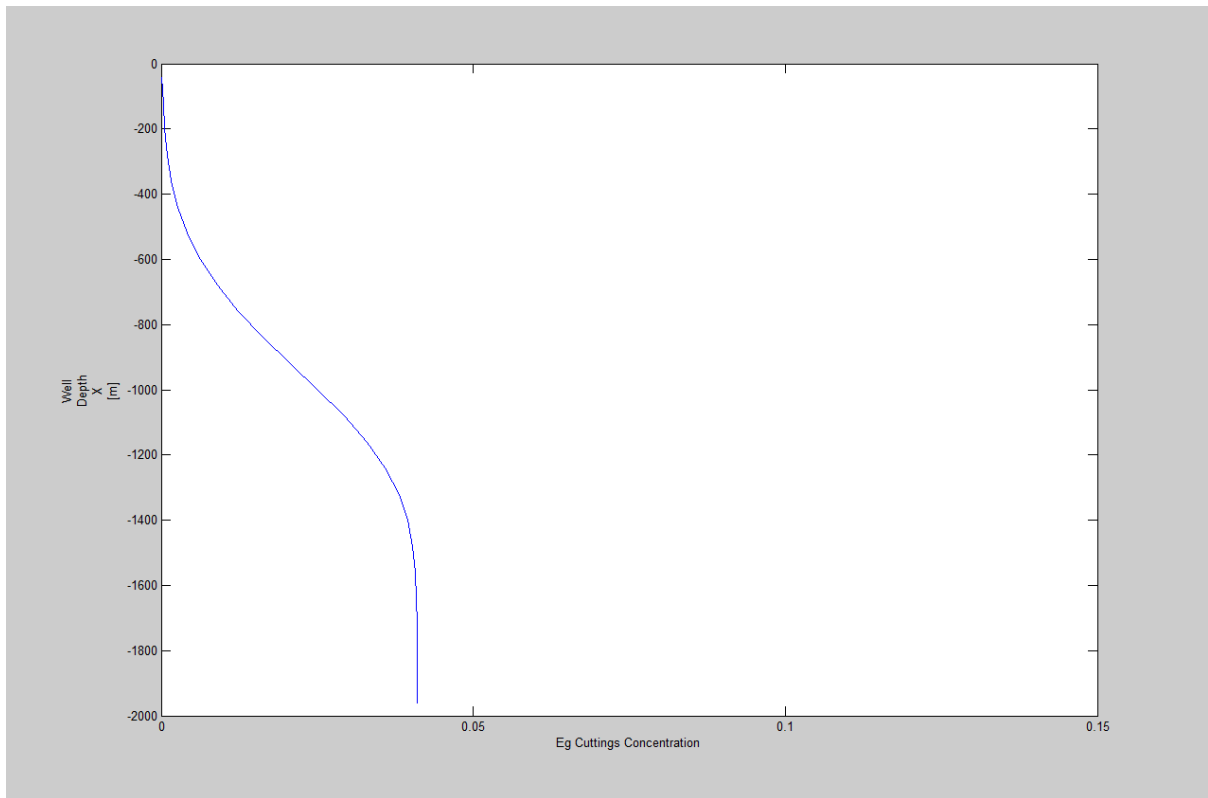
In Figure 7 it is shown that when the time is 1500 seconds, the cuttings have moved further up in the well. We observe constant concentration values from 1400m to 200m.
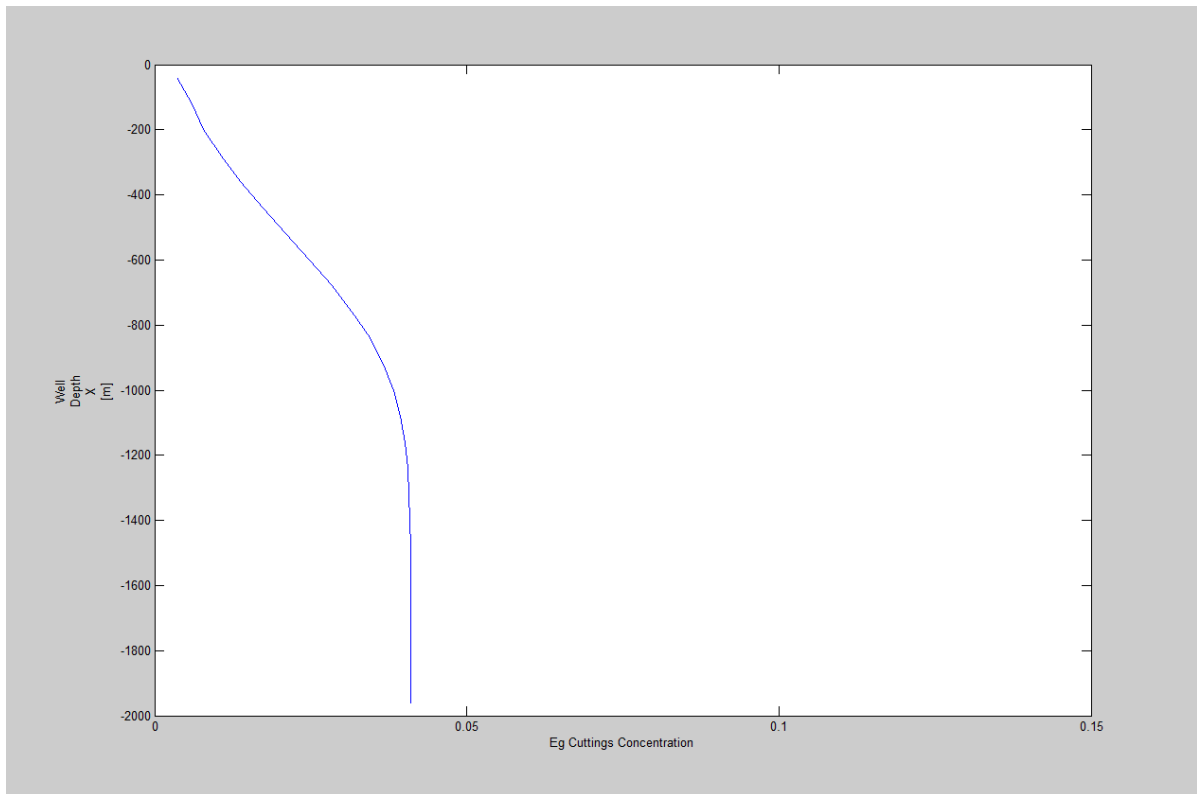
Figure 8: 2kg/s, 25 Box, t= 2000sec, well depth against cuttings concentration plot.

As the end time was increased to 2000 seconds, it can be seen in the Figure 8 that the steady state of the cuttings concentration was reached at a shorter well depth as compared to in Figure 7 and 6. From 1150m onwards, we observe constant cuttings concentration values.

Figure 9: 2kg/s, 25 Box, t= 3000sec, well depth against cuttings concentration plot.

In Figure 9 we can see that after 3000 seconds, we are approaching a steady state situation, where we almost have the same cuttings concentration in the whole well.
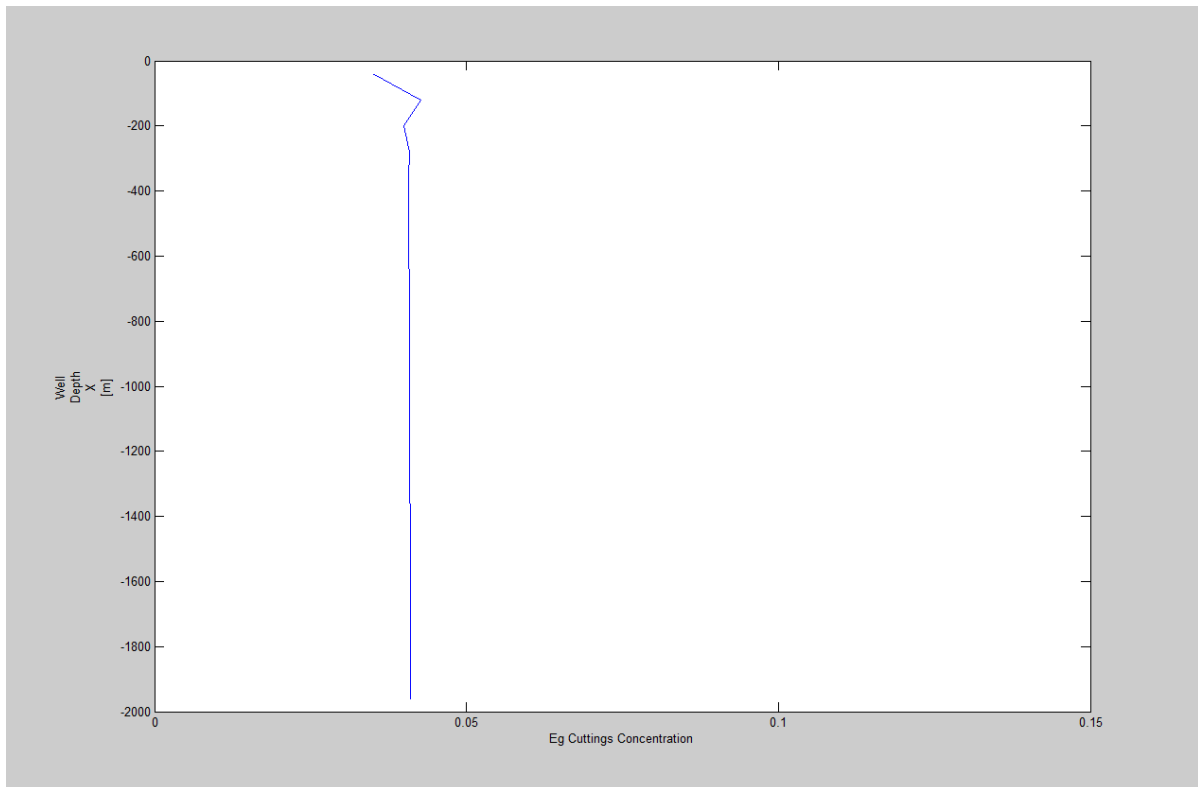
Figure 10: 2kg/s, 25 Box, t= 4000sec, well depth against cuttings concentration plot.

In Figure 10 it is shown that when the time is 4000 seconds, we have reached final steady state conditions. The cuttings concentration is 0.04. This means the cuttings have distributed through the whole well.
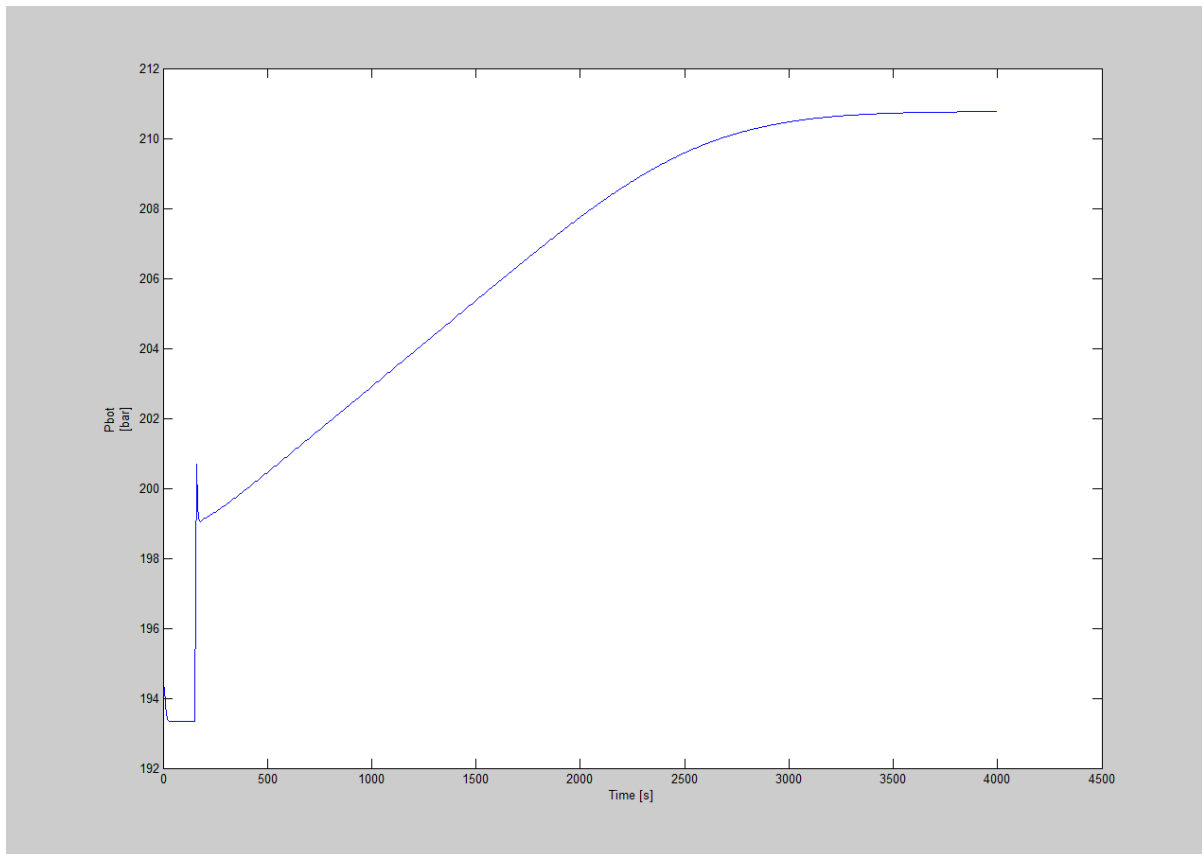
Figure 11: 2kg/s, 25 Box, t= 4000sec, bottomhole pressure against time plot.

Let us now see the changes shown in the bottomhole pressure versus time plot in the well and the effect the cuttings rate has on the BHP (Bottomhole Pressure). We start by pumping cuttings in the well. After 200 seconds there is an increase in BHP. This is due to well friction which comes into play when flowrates are turned on. The reason that the Bottomhole Pressure increases steadily, is due to that more and more of the well is filled with cuttings.

Case 2: K= 1, S=0 Massrate= 4kg/s no slip model

Now in this case the massrate of the cuttings was changed to 4kg/s and the changes in the concentration of the cuttings was observed for different end times. Number of boxes was kept at 25 and all other variables were the same as in case 1. Let us see at the plots obtained from Matlab simulations in appendix A given below and comment on the changes observed in the figures given below.
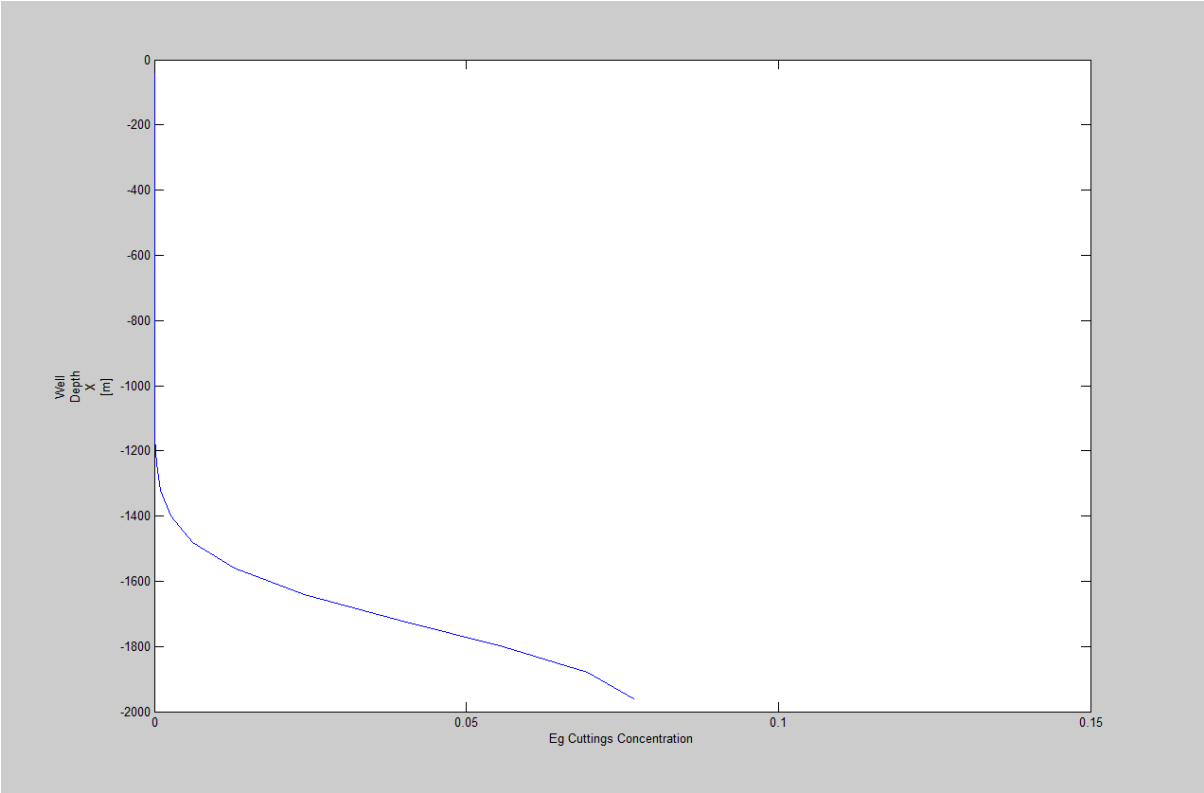

Figure 12: 4kg/s, 25 Box, t= 500sec, well depth against cuttings concentration plot.

In figure 12 at 500 seconds, we observe that the cuttings have reached 1250m. At the bottom, we observe that the cuttings concentration is 0.077 almost. It is higher in this case as compared to previous case, since a larger cuttings rate is used.

42
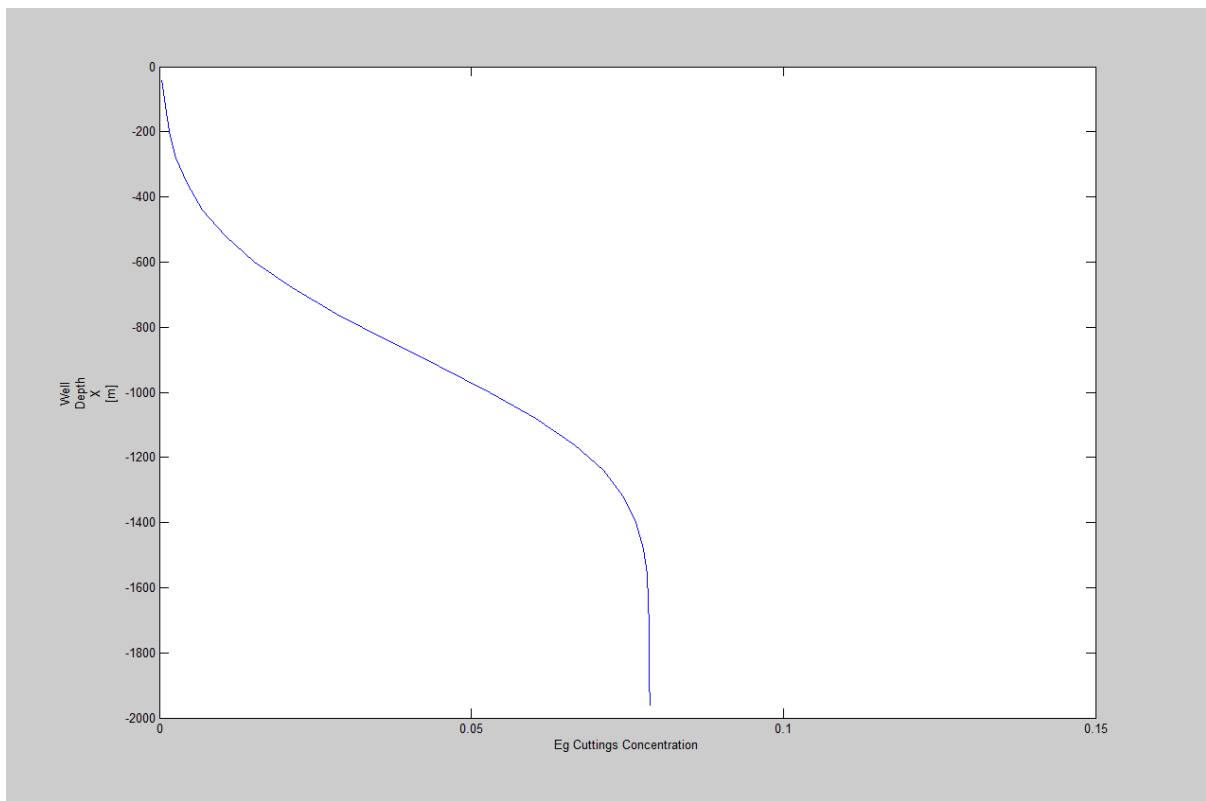
Figure 13: 4kg/s, 25 Box, t= 1500sec, well depth against cuttings concentration plot.

In Figure 13 it can be seen that from 400m to 1400m the concentration of the cuttings increases gradually and then reaches a steady state with a concentration corresponding to 0.077 which means that the cuttings have spread out and distributed evenly in the lower part of the well. The end time here was 1500s.
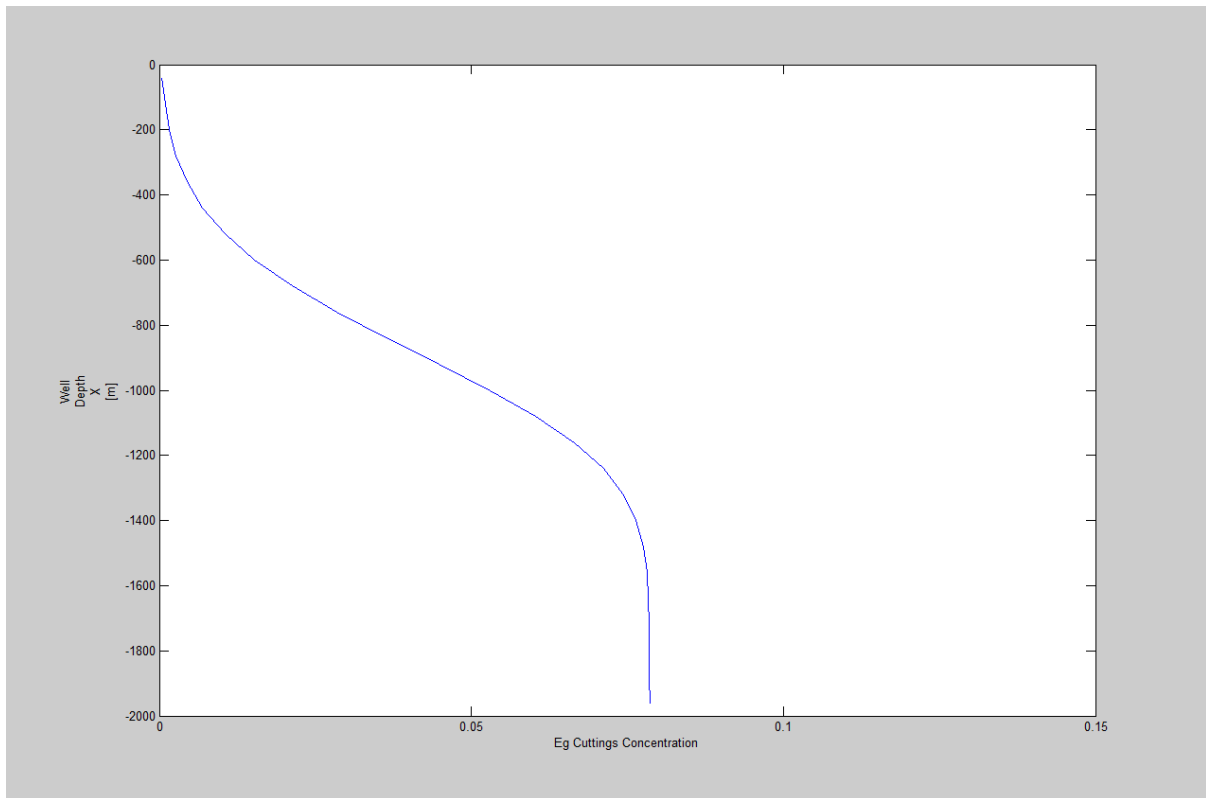
42

Figure 14: 4kg/s, 25 Box, t= 2000sec, well depth against cuttings concentration plot.

As the end time was increased to 2000 seconds it can be seen in figure 14 that the steady state of the cuttings concentration was reached at a shorter well depth as compared to in figure 13 and 12. The steady state is reached around 1150m.
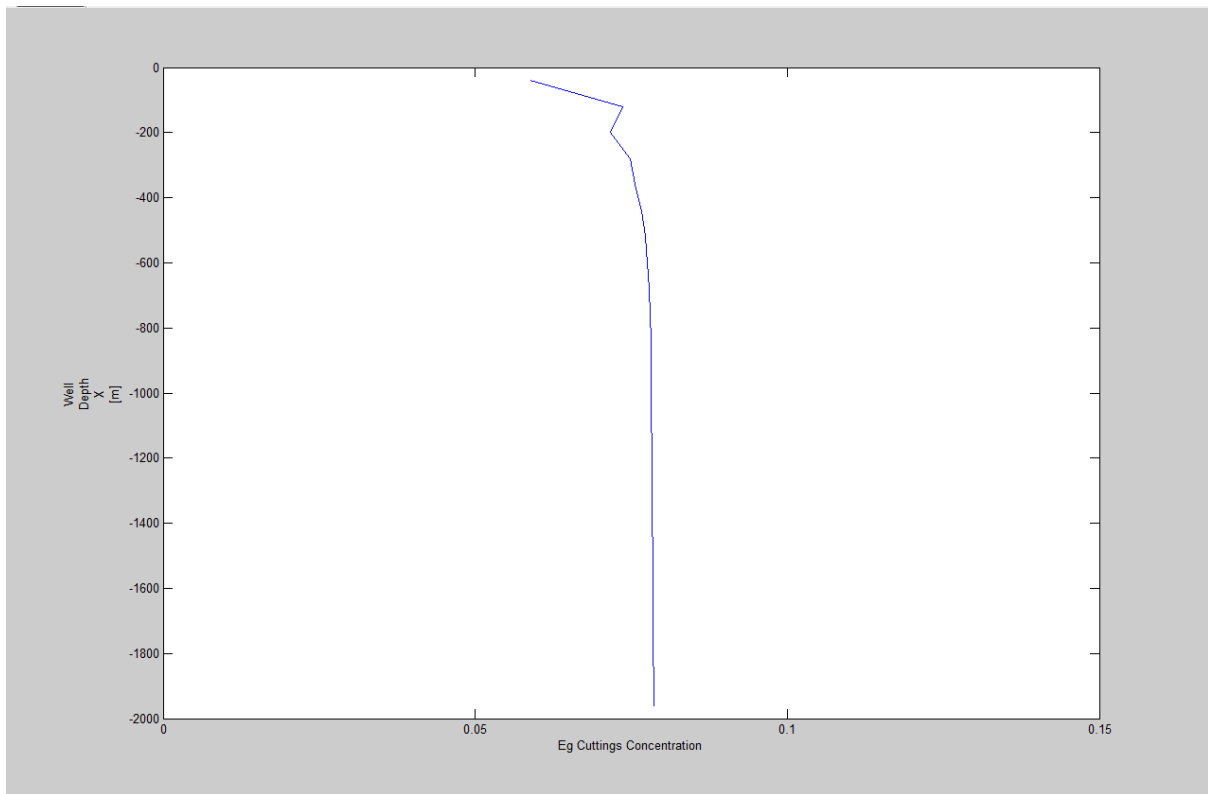
Figure 15: 4kg/s, 25 Box, t= 3000sec, well depth against cuttings concentration plot.

In figure 15 we observe that the cuttings have soon distributed in the whole well. From 250m to almost 2000m, we observe a constant cuttings concentration value.
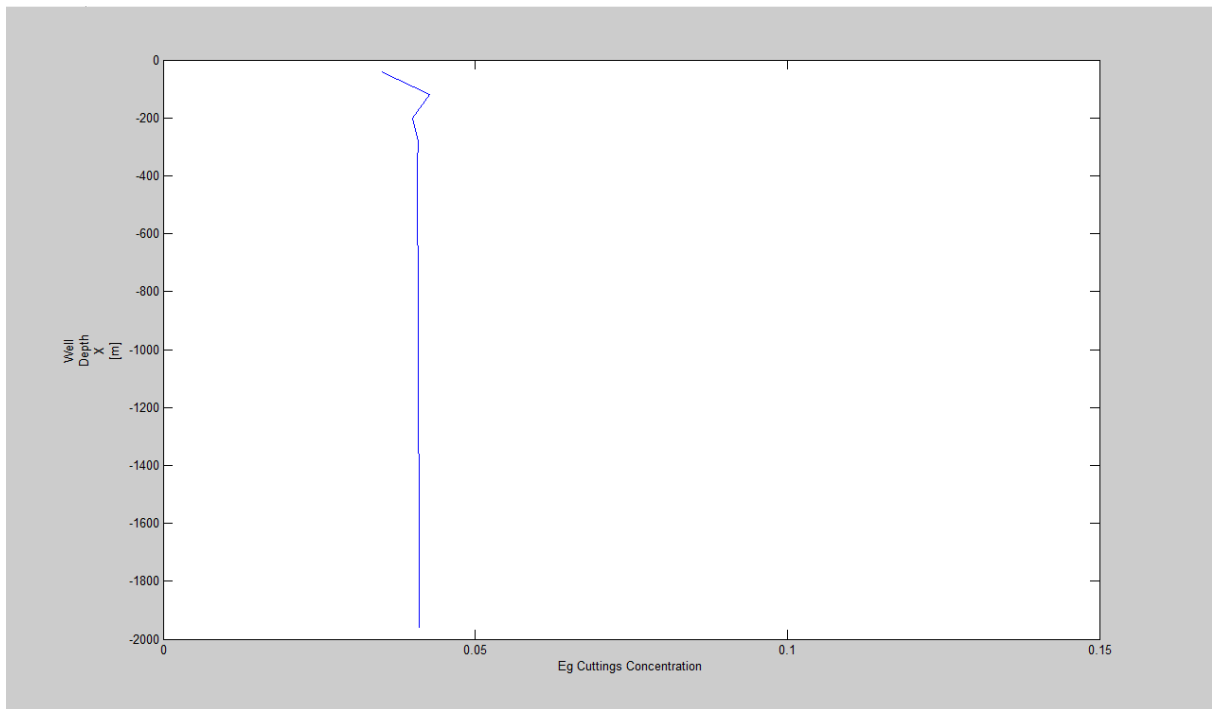
Figure 16: 4kg/s, 25 Box, t= 4000sec, well depth against cuttings concentration plot.

At 4000 seconds in figure 16, we observe that we have reached the final steady state conditions with a constant cuttings concentration value of 0.077 in the whole well.
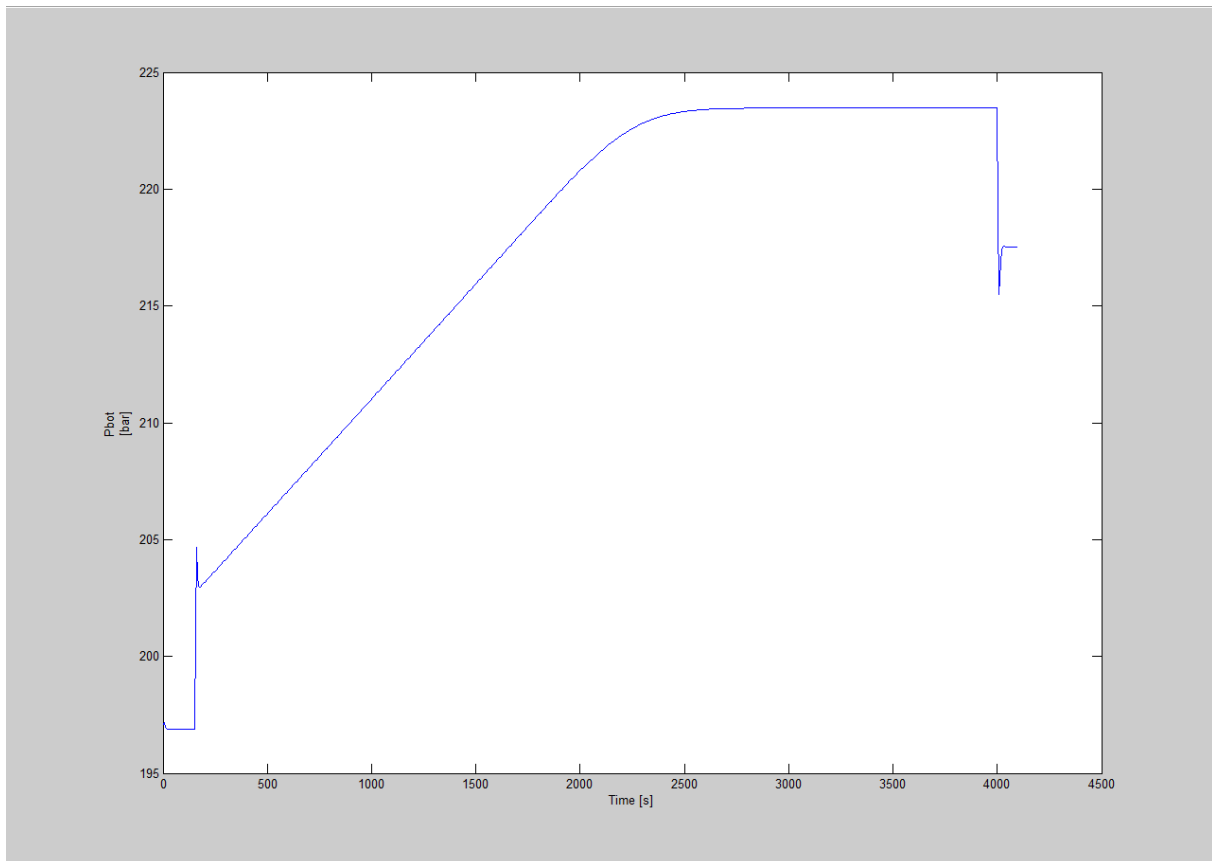
Figure 17: 4kg/s, 25 Box, t= 4100sec, bottomhole pressure against time plot.

Let us now see the changes shown in the bottomhole pressure versus time plot in the well and the effect the cuttings rate has on the BHP (Bottomhole Pressure). The first increase in BHP at 200 seconds is due to friction when starting to pump liquid and cuttings. Then when cuttings start to move upwards in the well, the bottomhole pressure will gradually increase due to increase in hydrostatic pressure. Steady state is reached after 3500 seconds. At 4000 seconds, the injection rates are set to zero and the well friction disappears. The pressure we then have is just the hydrostatic pressure. The difference between this value and the one we had in the beginning of the simulation is due to the content of cuttings in the well. We also observe that the steady state pressure we obtain during circulation before we shut down the pumps are larger in this case compared to the previous simulation. This is because we use a higher cuttings rate and thereby obtain a higher cuttings concentration.

46

Case 3: K= 1, S=0 Massrate= 6kg/s no slip model

In this case we will simulate with 6kg/s. The following changes were made into the code in appendix made for case 1:

```
if (time < 150)

    inletliqmassrate=0.0;
    inletgasmassrate=0.0;

elseif ((time>=150) & (time < 160))
    inletliqmassrate = 22*(time-150)/10;
    inletgasmassrate = 6.0*(time-150)/10;

elseif ((time>=160)&(time<4000))
    inletliqmassrate = 22;
    inletgasmassrate = 6.0;
elseif((time>4000)&(time<4010))
    inletliqmassrate = 22-22*(time-4000)/10;
    inletgasmassrate = 6.0-6.0*(time-4000)/10;
elseif((time>4010))
    inletliqmassrate=0;
    inletgasmassrate=0;
end
```

However, the end time was changed accordingly for different times in case 3. For example for 3000 seconds the Matlab code in appendix A was changed to the following:

```
End time = 3000; % Time for end of simulation
```
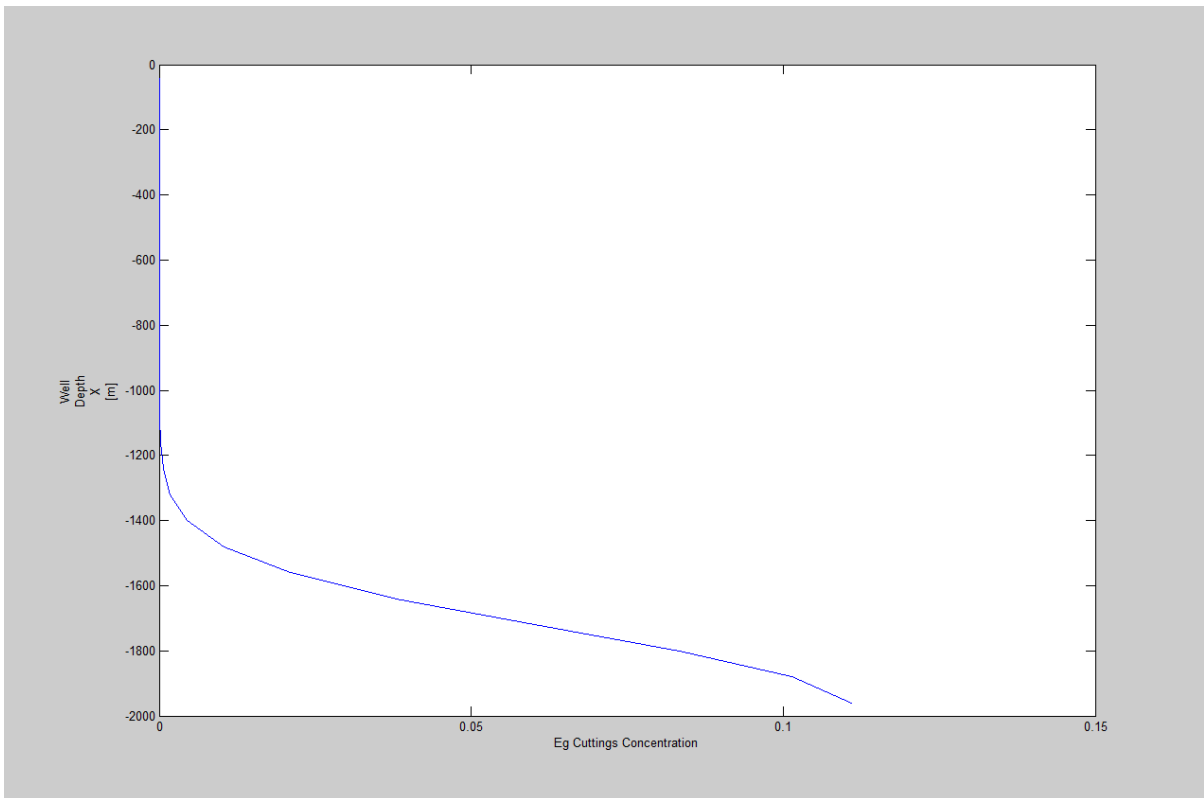
Figure 18: 6kg/s, 25 Box, t= 500sec, well depth against cuttings concentration plot.

In figure 18 at 500 seconds, we observe that the cuttings have reached 1250m. At the bottom, it was observed that the cuttings concentration is 0.115 almost. It is higher in this case as compared to previous case, since a larger cuttings rate is used.
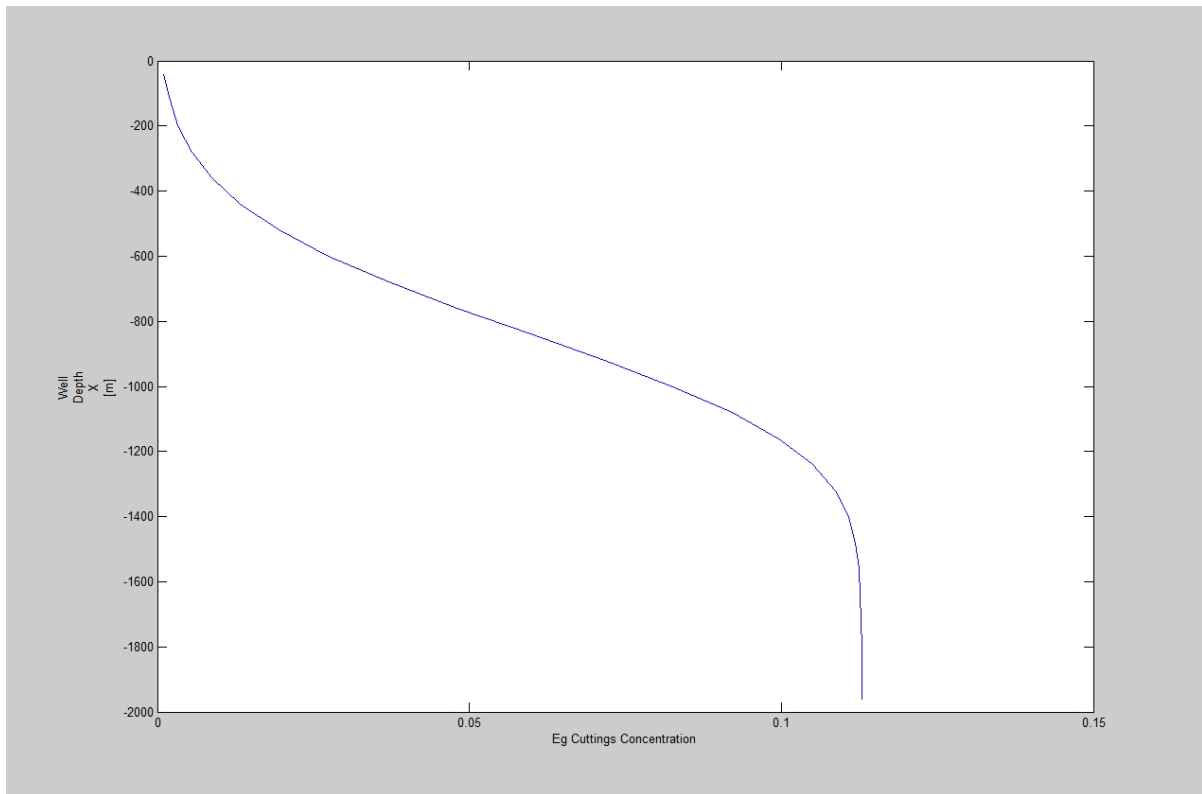
Figure 19: 6kg/s, 25 Box, t= 1500sec, well depth against cuttings concentration plot.

In Figure 19 it can be seen that from 400m to 1400m the concentration of the cuttings increases uniformly and then reaches a steady state with a concentration corresponding to 0.115 which means that the cuttings have spread out and distributed evenly in the well. The end time here was 1500s.
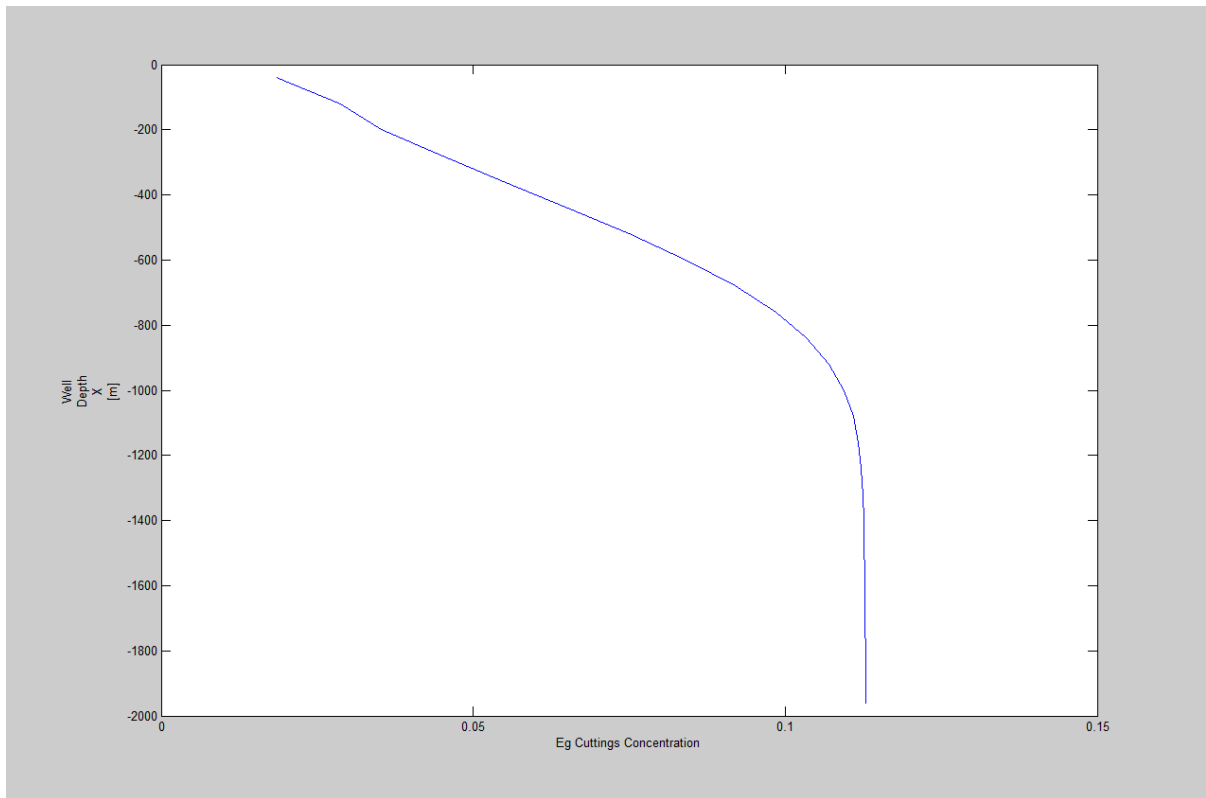
Figure 20: 6kg/s, 25 Box, t= 2000sec, well depth against cuttings concentration plot.

As the end time was increased to 2000 seconds it can be seen in the Figure 19 that the steady state of the cuttings concentration was reached at a shorter well depth as compared to in Figure 18 and 19. The steady state is reached around 1150m.
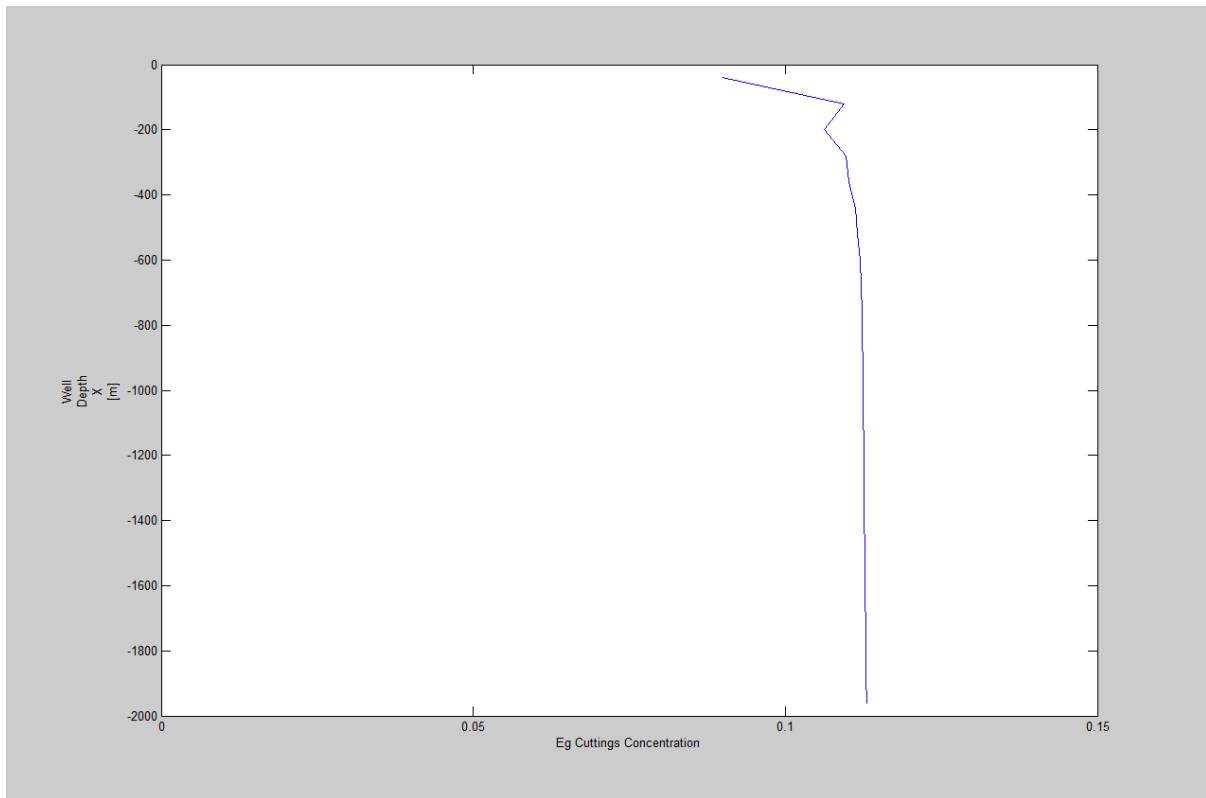
Figure 21: 6kg/s, 25 Box, t= 3000sec, well depth against cuttings concentration plot.

In Figure 21, we observe that at 3000s, the cuttings have almost distributed in the whole well. From 250m till almost 2000m, we observe a constant cuttings concentration value.
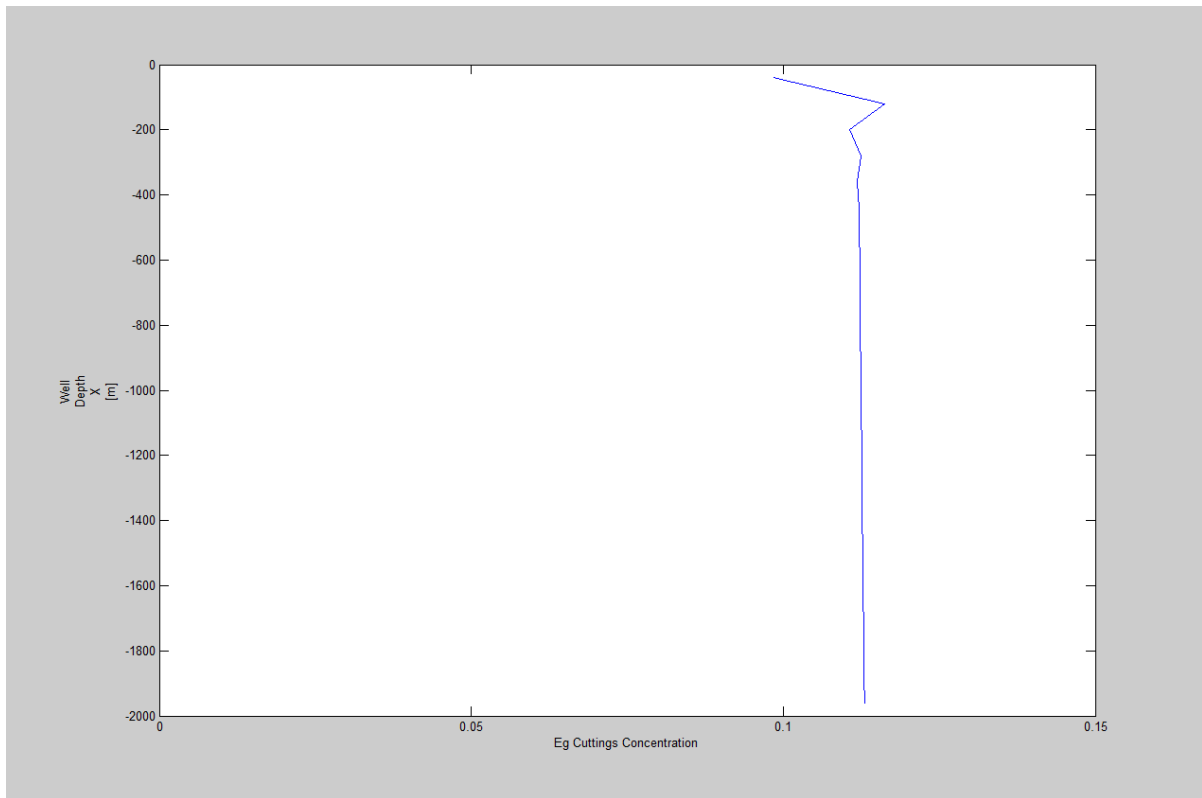
Figure 22: 6kg/s, 25 Box, t= 4000sec, well depth against cuttings concentration plot.

In Figure 22, we observe that after 4000s, the final steady state conditions are reached and the cuttings concentration is the same in the whole well. In this case the cuttings concentration increase as the cuttings massrate was increased from 2, 4 until 6kg/s.
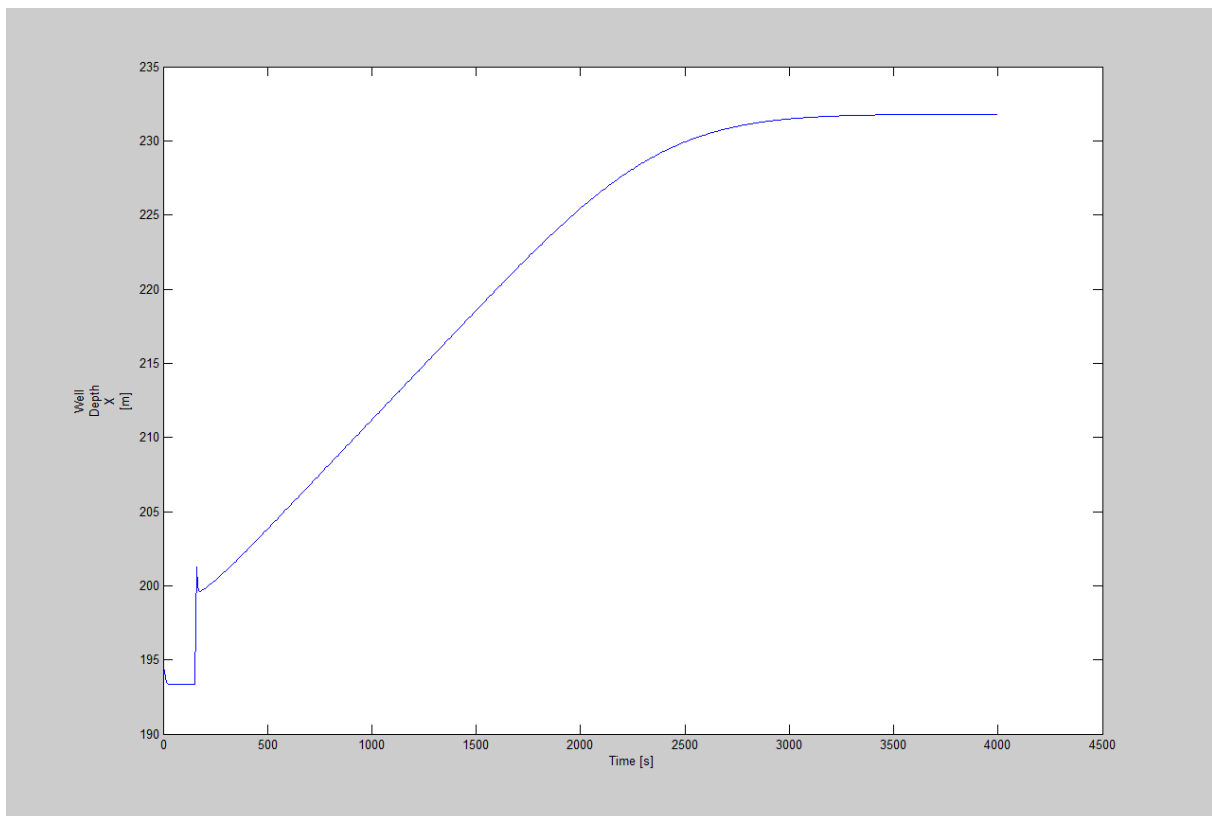
Figure 23: 6kg/s, 25 Box, t= 4000sec, bottomhole pressure against time plot.

The first increase in BHP at 200 seconds is due to friction when starting to pump liquid and cuttings. Then when cuttings start to move upwards in the well, the bottomhole pressure will gradually increase due to increase in hydrostatic pressure. Steady state is reached after 3500 seconds. At 4000 seconds, the injection rates are set to zero and the well friction disappears. The pressure we then have is just the hydrostatic pressure. We get a higher pressure in this case as compared to previous case. This is because we have used a larger cuttingsrate in this case, which has led to a larger cuttings concentration. It can be clearly observed that the higher the cuttings rate the higher the pressure becomes. This is because we get more hydrostatic pressure as the cuttings rate is increased. The cuttings concentration also increased from 0.04 to 0.115.

Case 4: Let us look at more realistic cuttings rates in case 4. In this case we will investigate the effect of different ROP (Rate of Penetration) values on BHP (Bottomhole Pressure). Here we have chosen the following rates: 10m/h and 30m/h as examples. But first it is important to convert the ROP values to cutting rates in kg/s. This is done below and the calculations are shown.

53

Calculations:

ROP= Rate of Penetration = **10m/h**,

V = Volumrate = $A \times ROP$ (m³/s)

M= massrate, ρ = 2500 kg/m³

A= area= $\pi/4(D_o^2 - D_i^2)$ = $\pi/4(0.2159^2 - 0.127^2)$ = 0.0239 m²

$M = \rho \times V$ = 2500 × V where $V = A \times ROP$ = $\pi/4(0.2159^2 - 0.127^2) \times$ 10m/3600s

= 6.639 × 10⁻⁵ m³/s

M = 2500 kg/m³ × 6.639 × 10⁻⁵ m³/s = **0.166 kg/s**

ROP= Rate of Penetration = **30m/h**,

V = Volumrate = $A \times ROP$ (m³/s)

M = massrate, ρ = 2500 kg/m³

A = area= $\pi/4(D_o^2 - D_i^2)$ = $\pi/4(0.2159^2 - 0.127^2)$ = 0.0239 m²

$M = \rho \times V$ = 2500 × V where $V = A \times ROP$ = $\pi/4(0.2159^2 - 0.127^2) \times$ 30m/3600s

= 1.992 × 10⁻⁴ m³/s

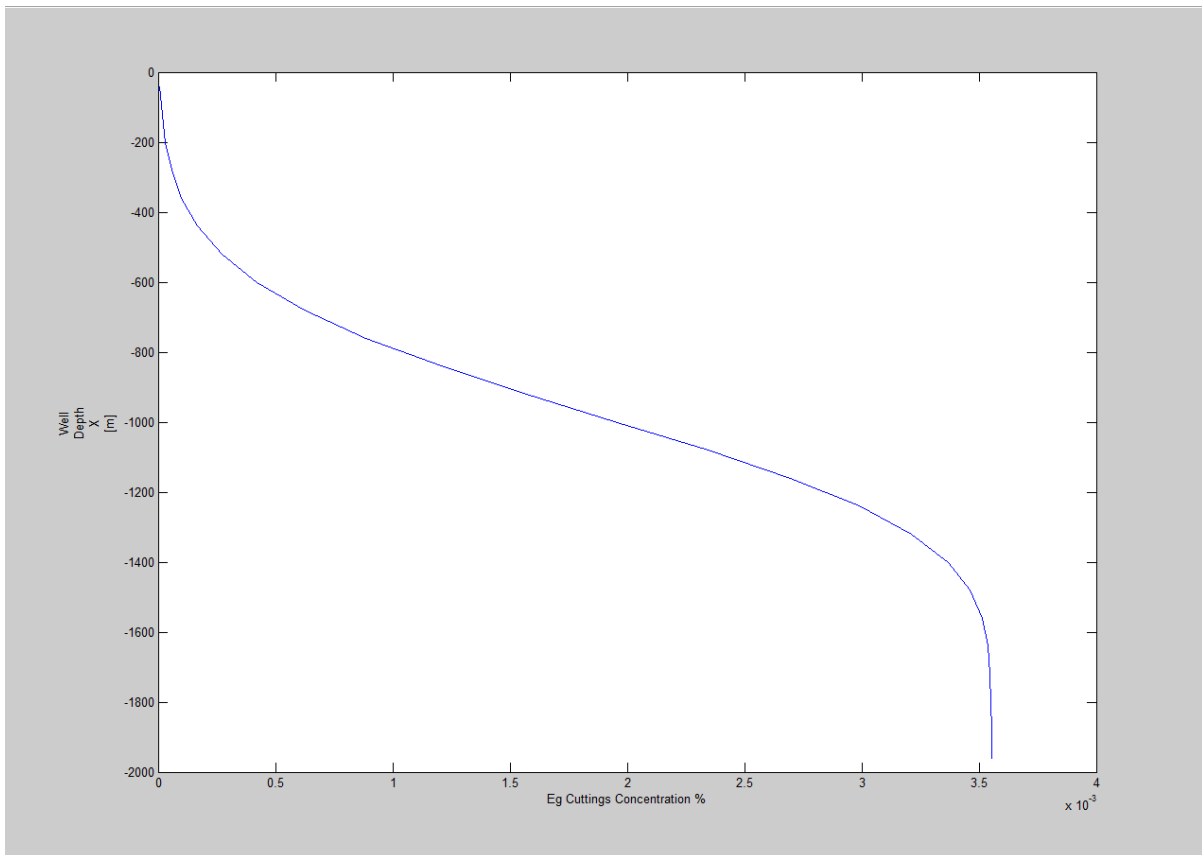M = 2500 kg/m³ × 1.992 × 10⁻⁴ m³/s = **0.498 kg/s**

Figure 24: 0.166kg/s, 25 box, t=1500sec, well depth against cuttings concentration plot.

54

According to figure 24, the cuttings concentration is increasing before reaching a constant value of cuttings concentration near $3.55 \times \mathbf{10^{-3}}$. We observe that the cuttings front has smeared out. This is due to numerical diffusion **[19]**.
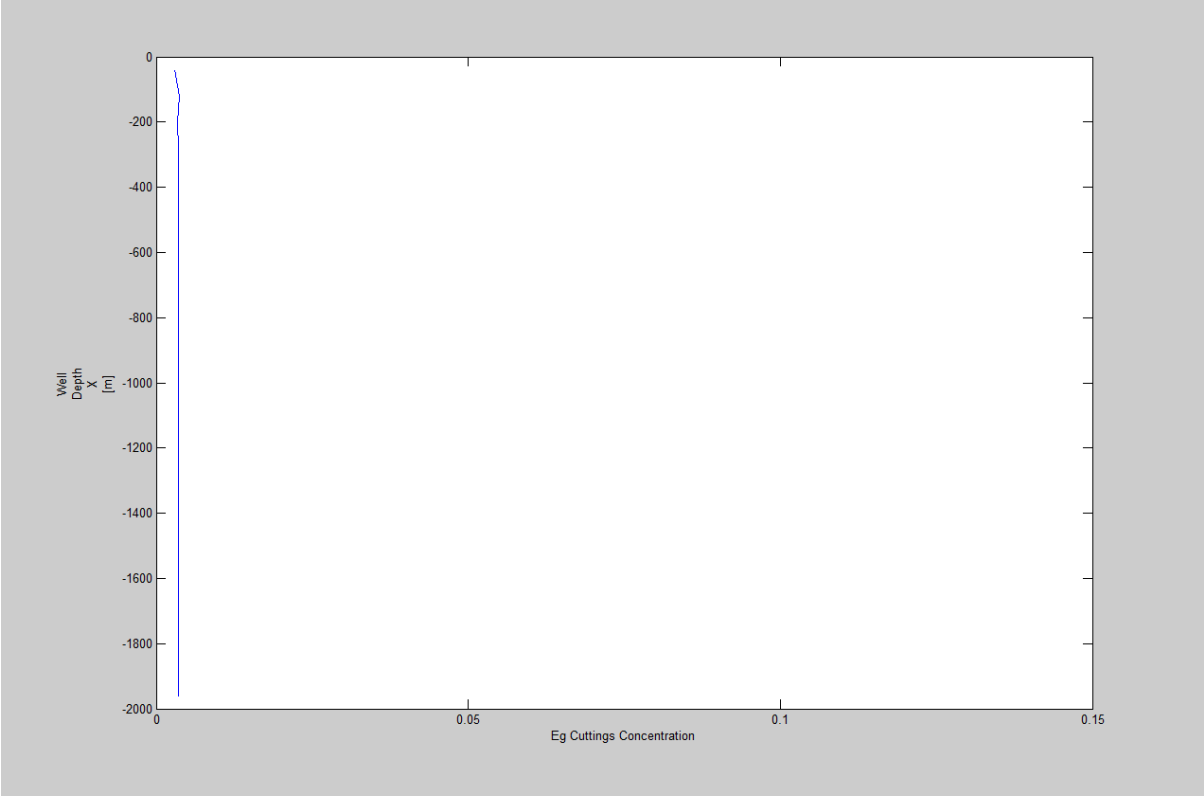
Figure 25: 0.166kg/s, 25 box, t=4000sec, well depth against cuttings concentration plot.

As we can see in figure 25 for time = 4000 seconds the cuttings concentration remains constant at a value almost near 0.00355.
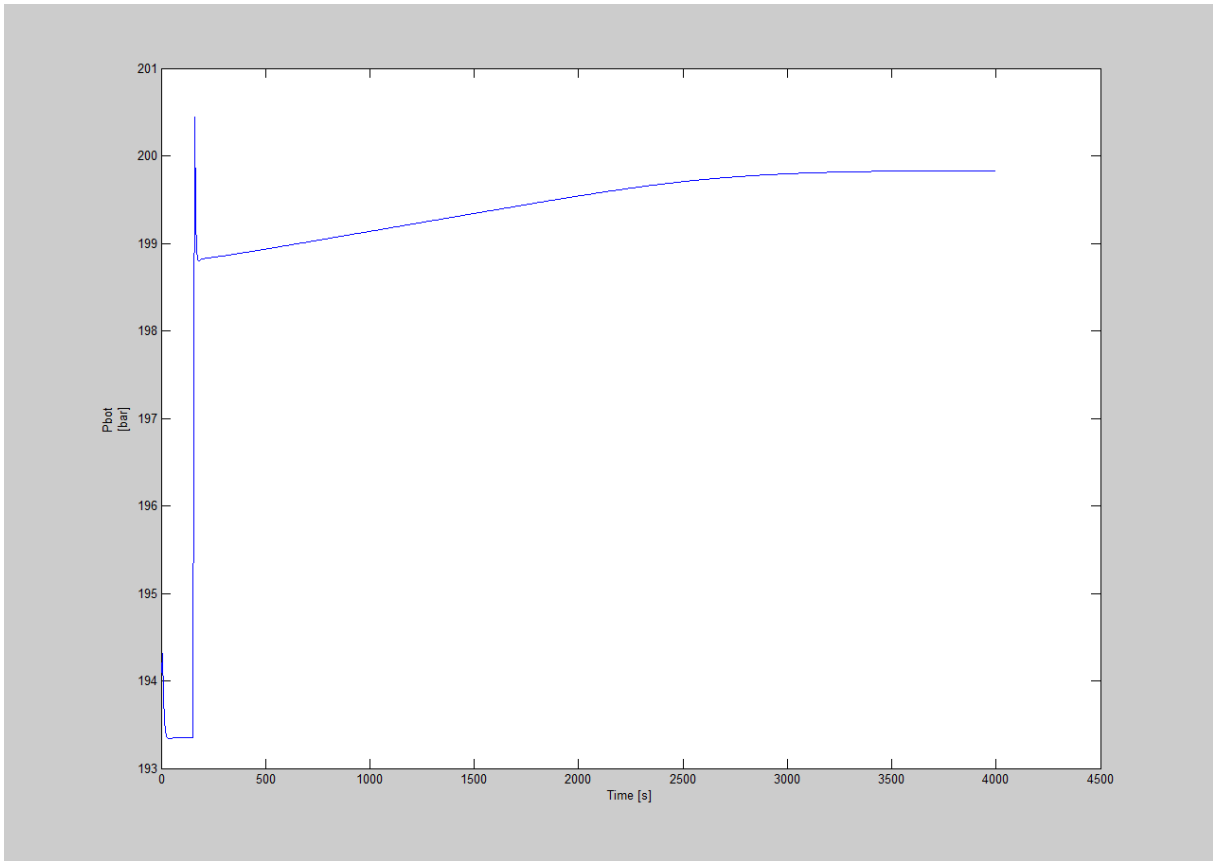
Figure 26: 0.166kg/s, 25 box, t=4000sec, bottomhole pressure against time plot.

In the beginning, the well is static. Then at 200 seconds, flowrates are turned as well pressure increases due to friction. Then the pressure increases gradually. However in this case the buildup is much lower since the cuttings rate is much lower.
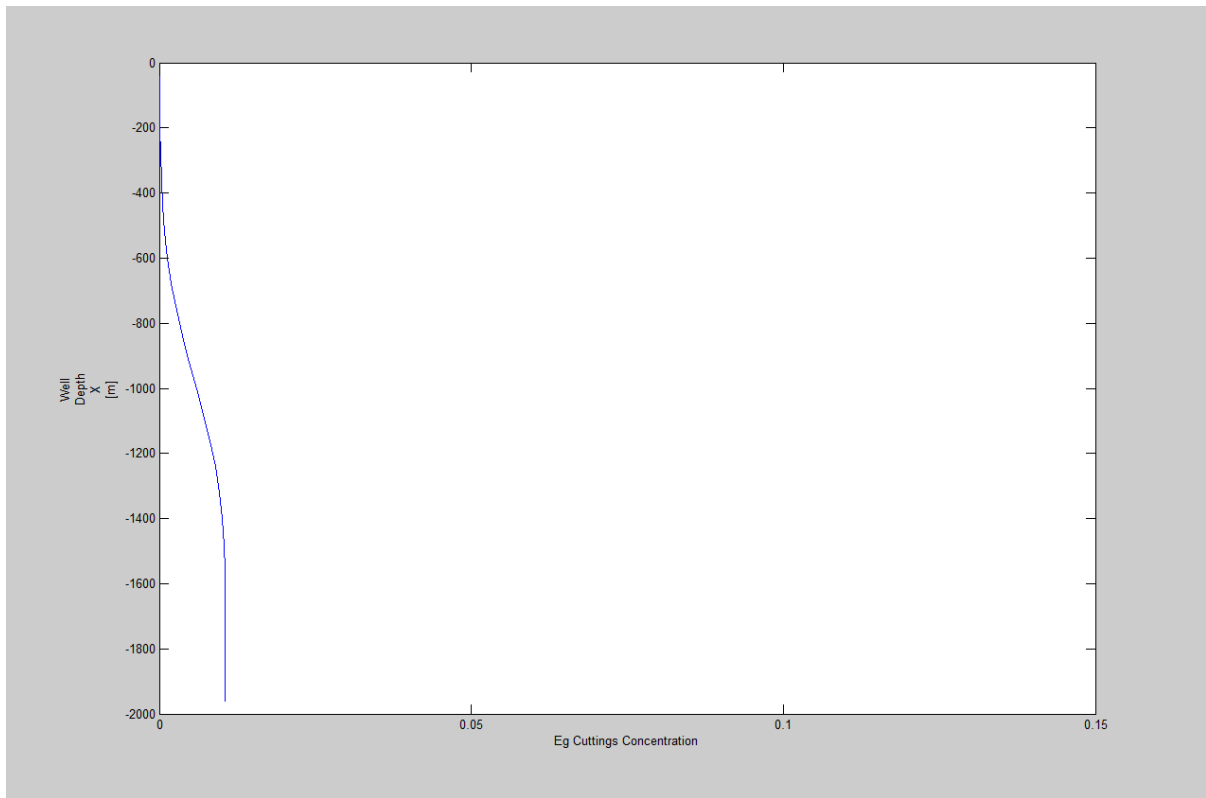
Figure 27: 0.498kg/s, 25 box, t=1500sec, well depth against cuttings concentration plot.

In this simulation, we use a ROP of 30m/h. After 1500 seconds, we can observe cuttings in the lower part of the well. The concentration is larger for this massrate corresponding to ROP (Rate of Penetration) of 30m/h.

Figure 28: 0.498kg/s, 25 box, t=4000sec, well depth against cuttings concentration plot.

Now as we can see in figure 28 a constant value 0.01 of cuttings concentration is achieved which is around 3 times larger than the cuttings concentration value of 0.00355 obtained in figure 25. This clearly indicates that as the ROP (Rate of Penetration) is increased the cuttings concentration is increased.
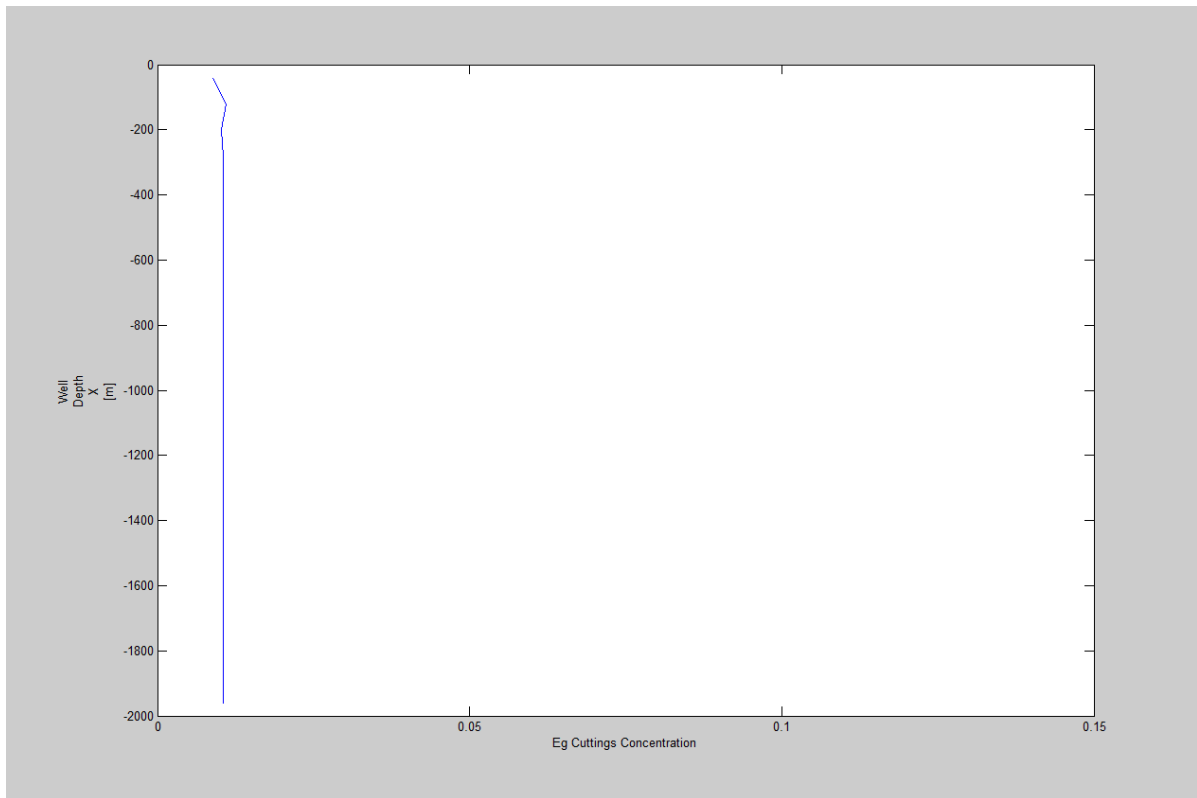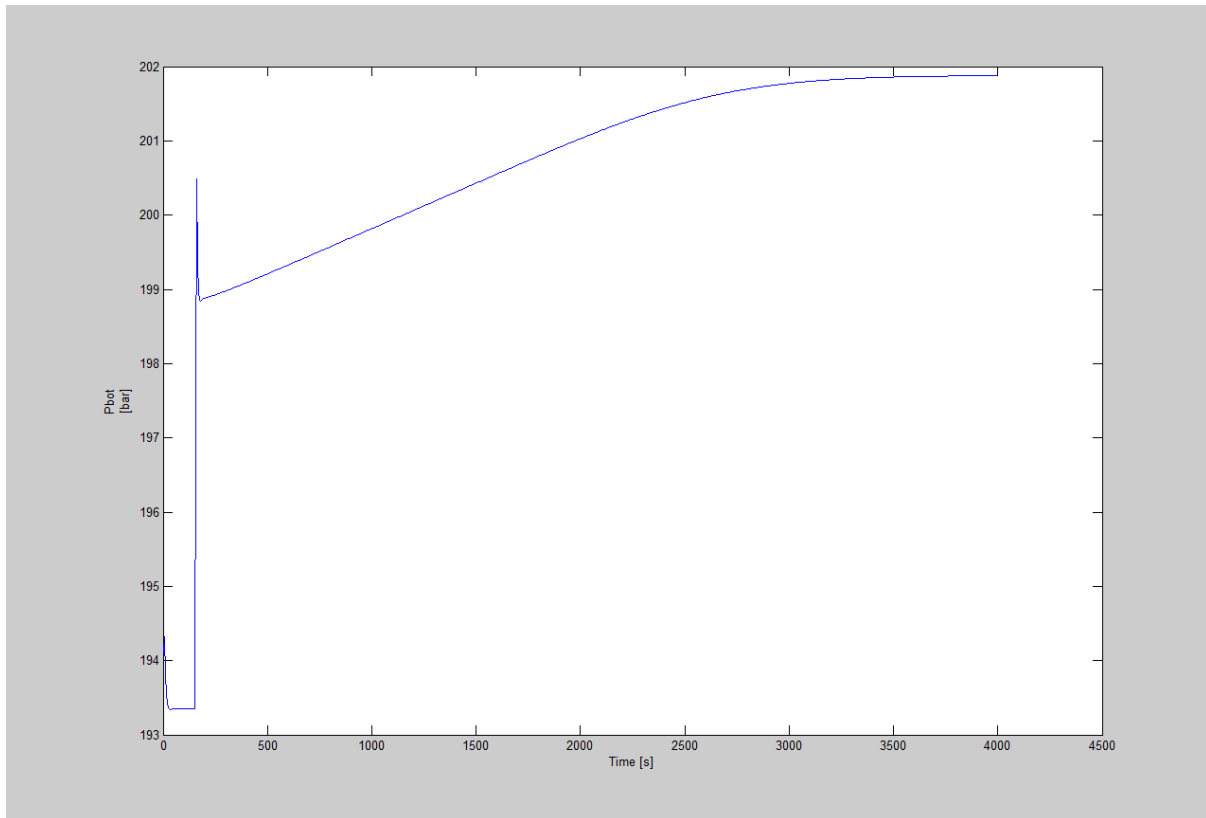
Figure 29: 0.498kg/s, 25 box, t=4000sec, bottomhole pressure against time plot.

Here we obtain a final steady state of 201.9 bar compared to 199.8 bar in the previous simulation. This is caused by increased cuttings concentration. We also seen the difference in BHP at 2000 seconds vs 4000 seconds. This is 201.9 − 198.8 = 2.1 bar and this the hydrostatic contribution of the cuttings. The peak seen at 2000 seconds can be caused by pressure pulses but further investigations must be performed. An increase in the maximum BHP value is shown. The difference is 201.9 − 198.8 = 2.1 bar. So it can be concluded that the BHP also increases with an increase in the ROP (Rate of Penetration).

Case 5: In this case the effect of changing the number of boxes the well is discretized into will be observed for 4kg/s massrate of cuttings. The purpose here is to reduce numerical diffusion [19] by increasing number of boxes from 25 to 100. Let us start by looking at figure 30.
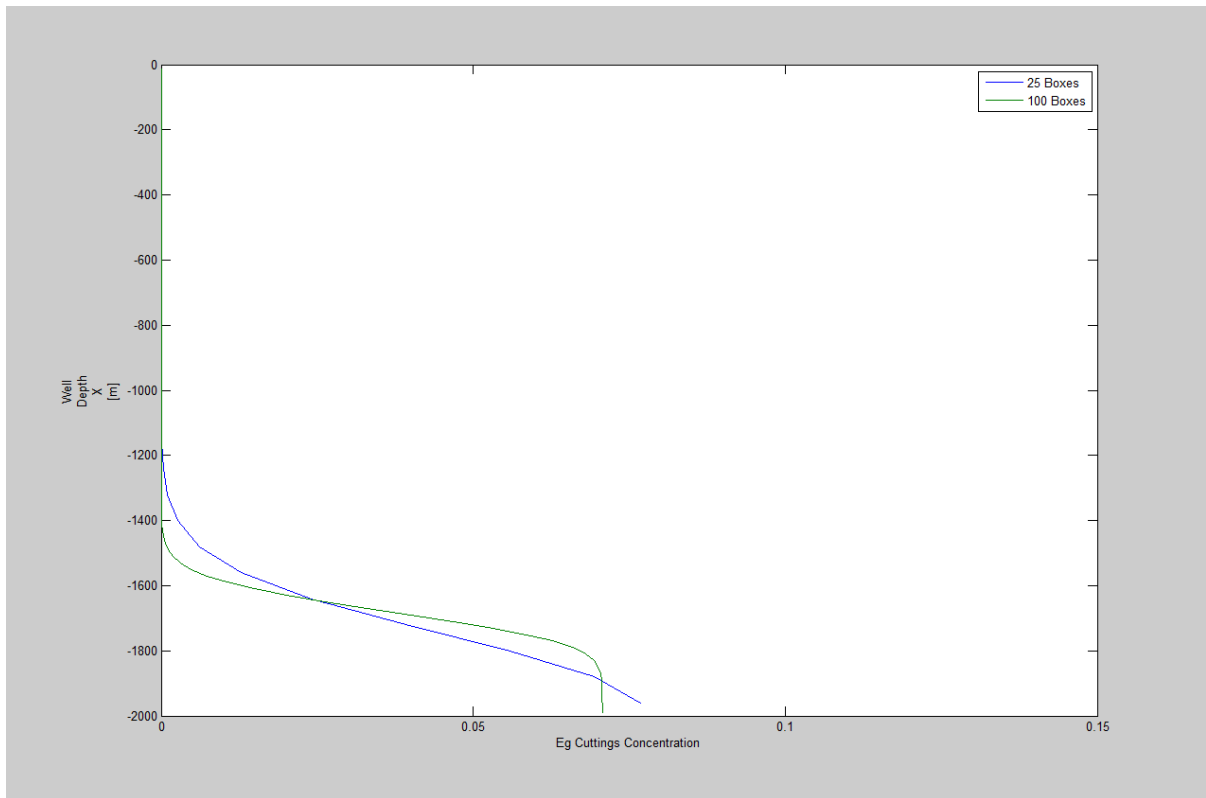
Figure 30: 4kg/s, 25 box, 100box, t=500sec, well depth against cuttings concentration plot.

In the following, we have studied the effect of increasing number of boxes from 25 (blue curve) to 100 (green curve). Ideally, the transition zone between pure liquid and liquid/cuttings should be a sharp front. We observe that by increasing number of boxes, the transition zone will become sharper but we also observe that the steady state cuttings concentration value becomes lower to a more refined grid (0.07 vs 0.077). As shown later, the true value is 0.0678. Hence, by refining the grid we approach the true value.
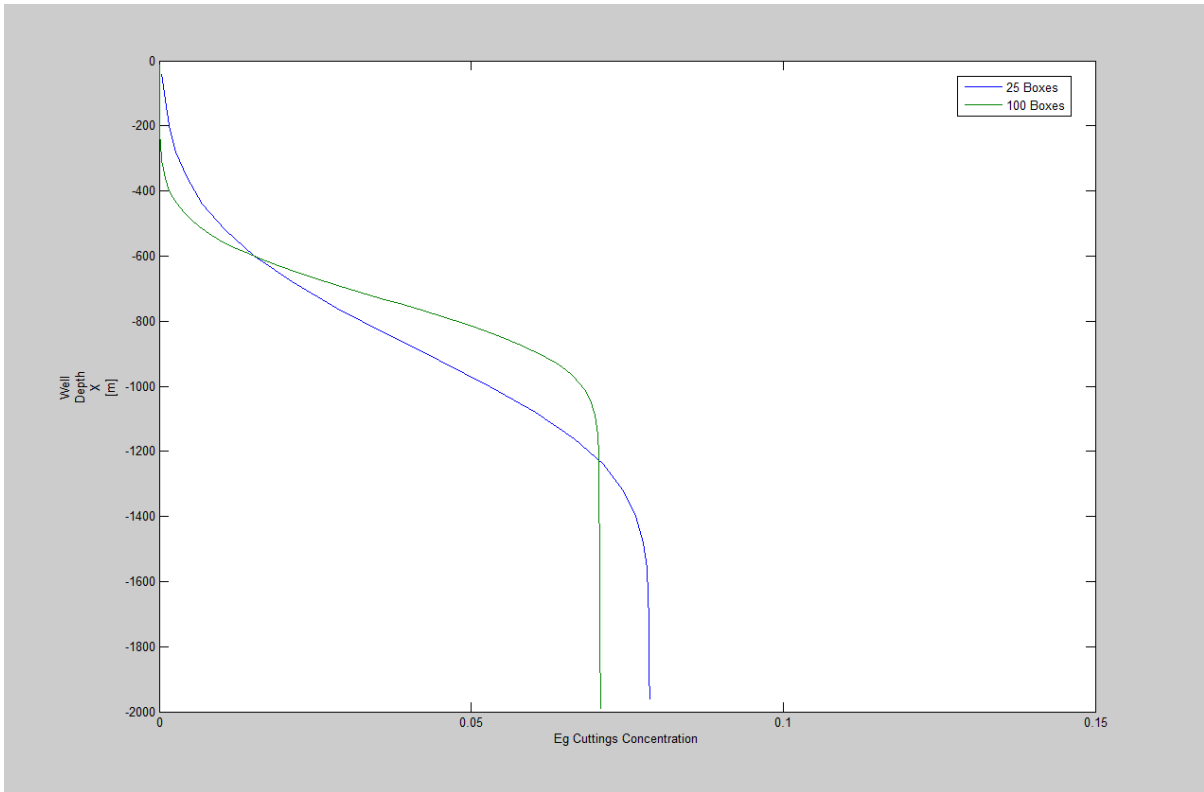
Figure 32: 4kg/s, 25 box, 100box, t=1500sec, well depth against cuttings concentration plot.

Figure 31, shows the cuttings concentration at 1500 seconds. We see that the simulation using 100 boxes gives a less smeared front.
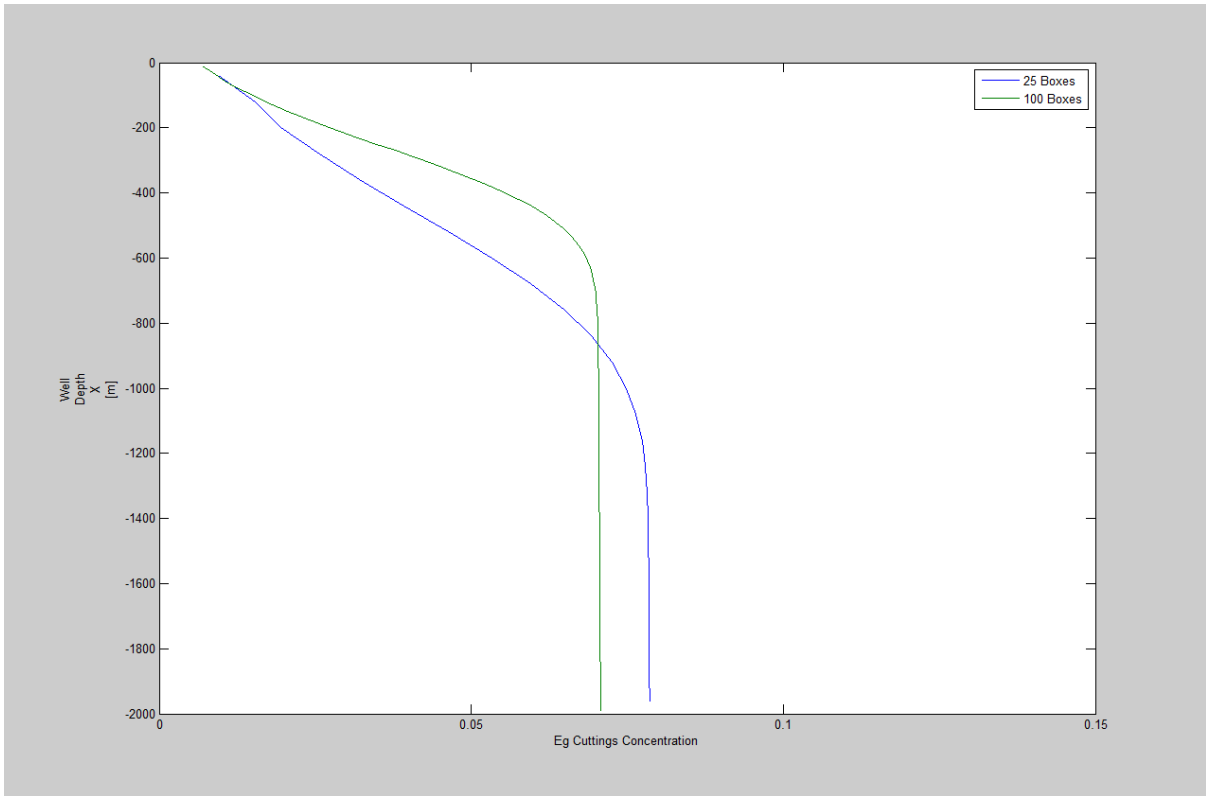
Figure 32: 4kg/s, 25 box, 100box, t=2000sec, well depth against cuttings concentration plot.

This shows cuttings concentration at 2000 seconds and 100 boxes here give less smeared front. We end up with different steady state concentration values.
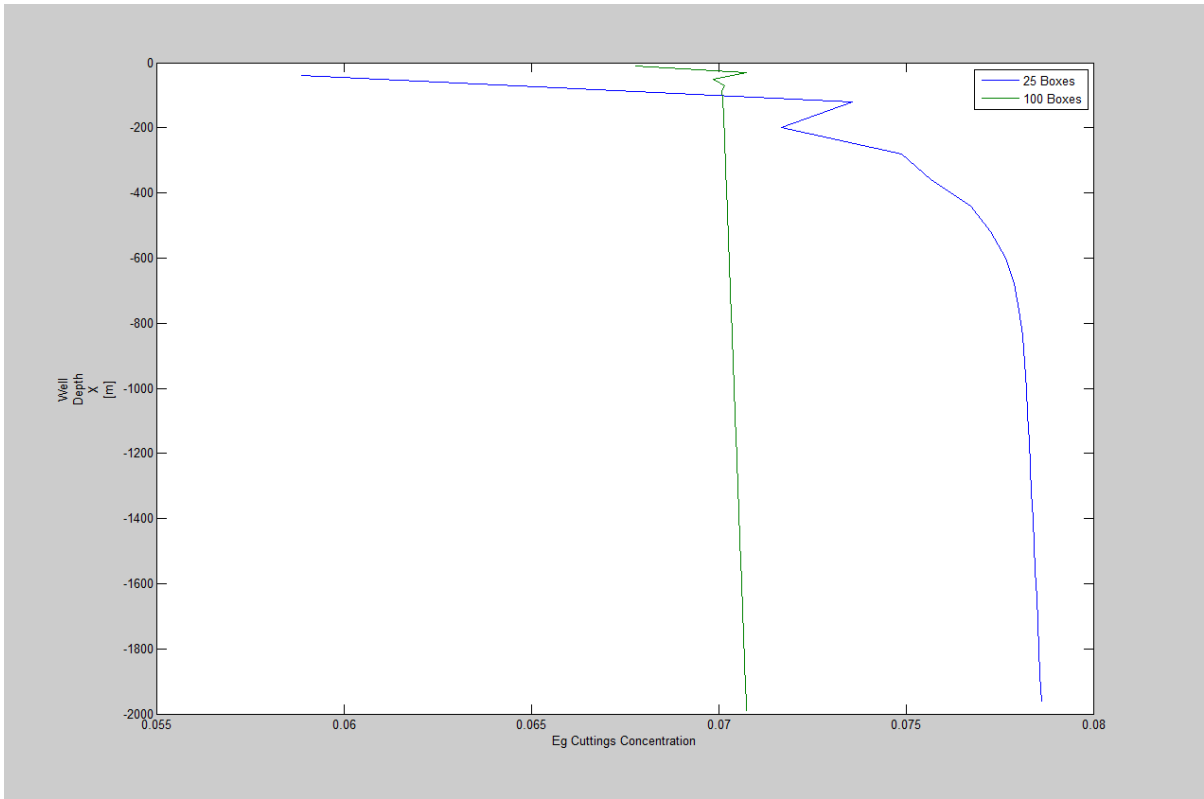
Figure 33: 4kg/s, 25 box, 100box, t=3000sec, well depth against cuttings concentration plot.

After 3000s, we have achieved a steady state condition.

63
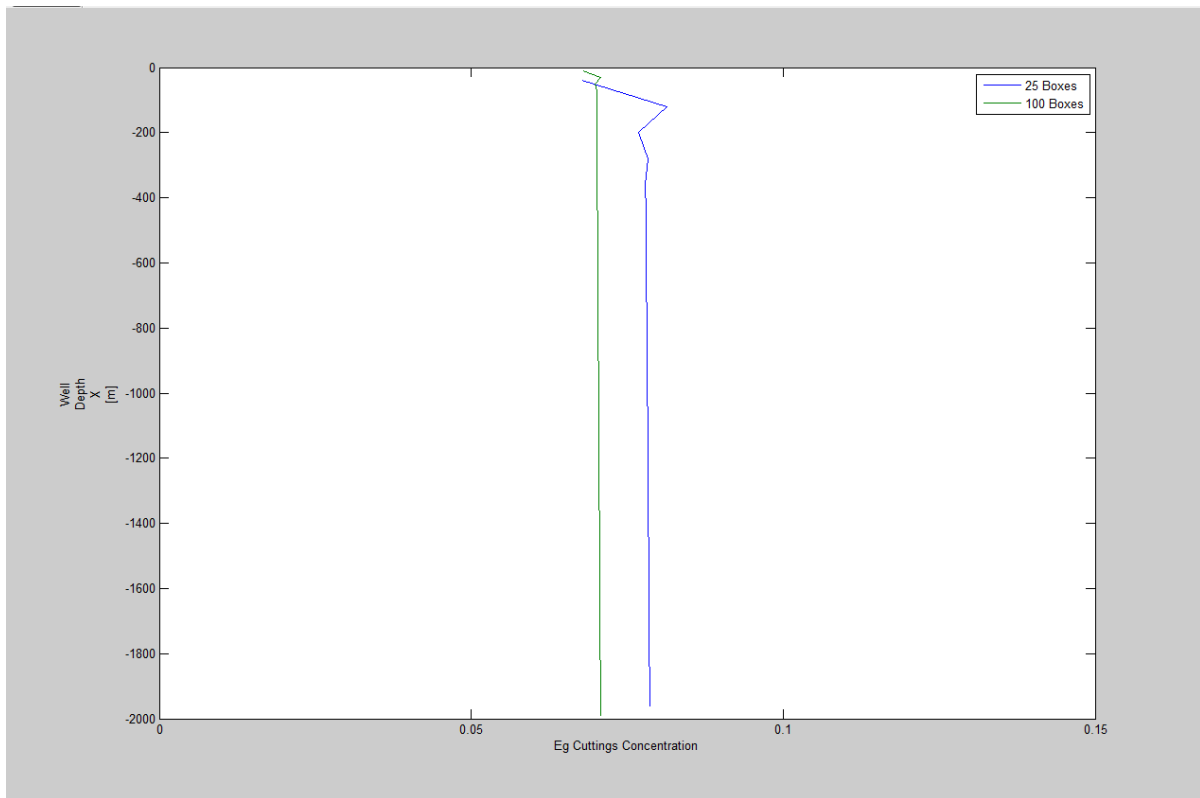
Figure 34: 4kg/s, 25 box, 100box, t=4000sec, well depth against cuttings concentration plot.

In Figure 34, a steady state is achieved but the cuttings concentration values are different.
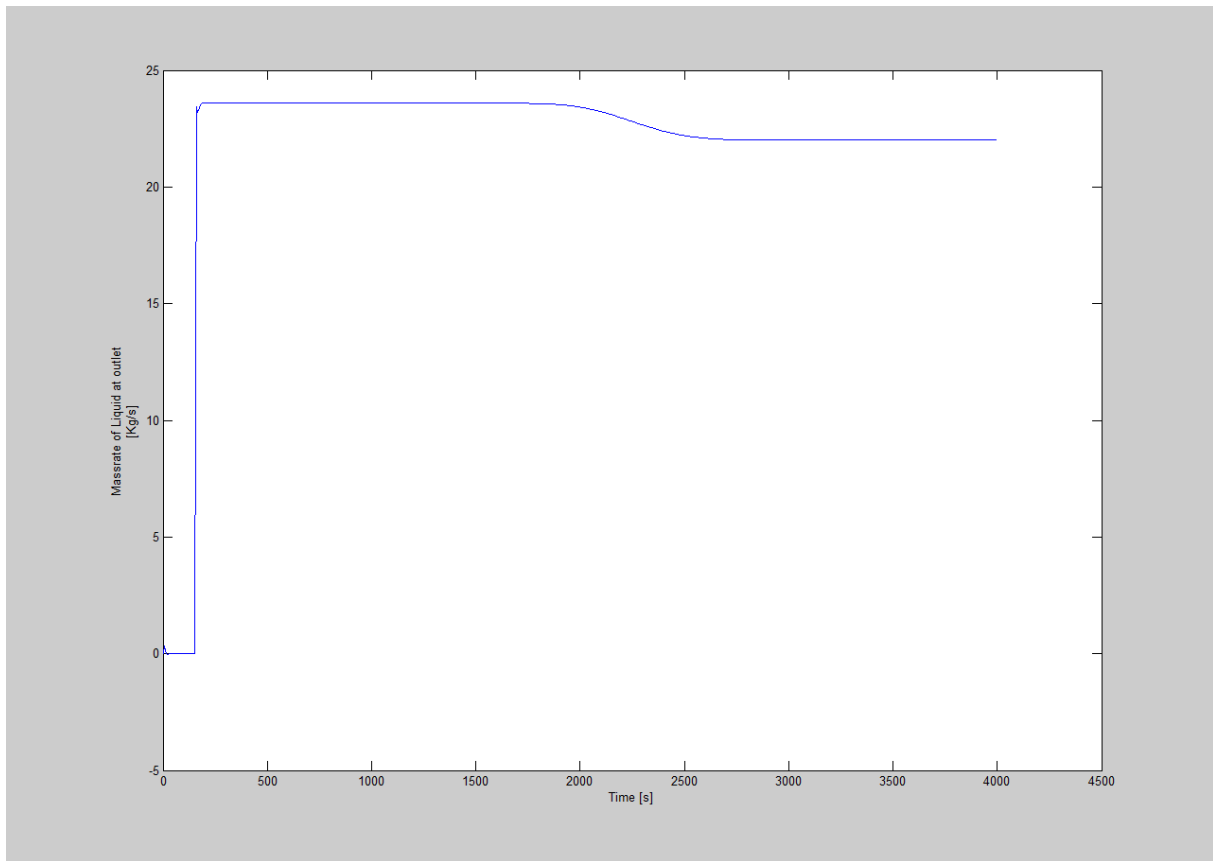
Figure 35: 4kg, 25 box, t=4000sec, Liquid massrate out against time plot.

It can be seen that the outlet rate is 24kg/s. This is due that we pump liquid and cuttings at the bottom of the well. However, when the cuttings reach the outlet, the liquid rate is reduced to a steady state value of 22kg/s.
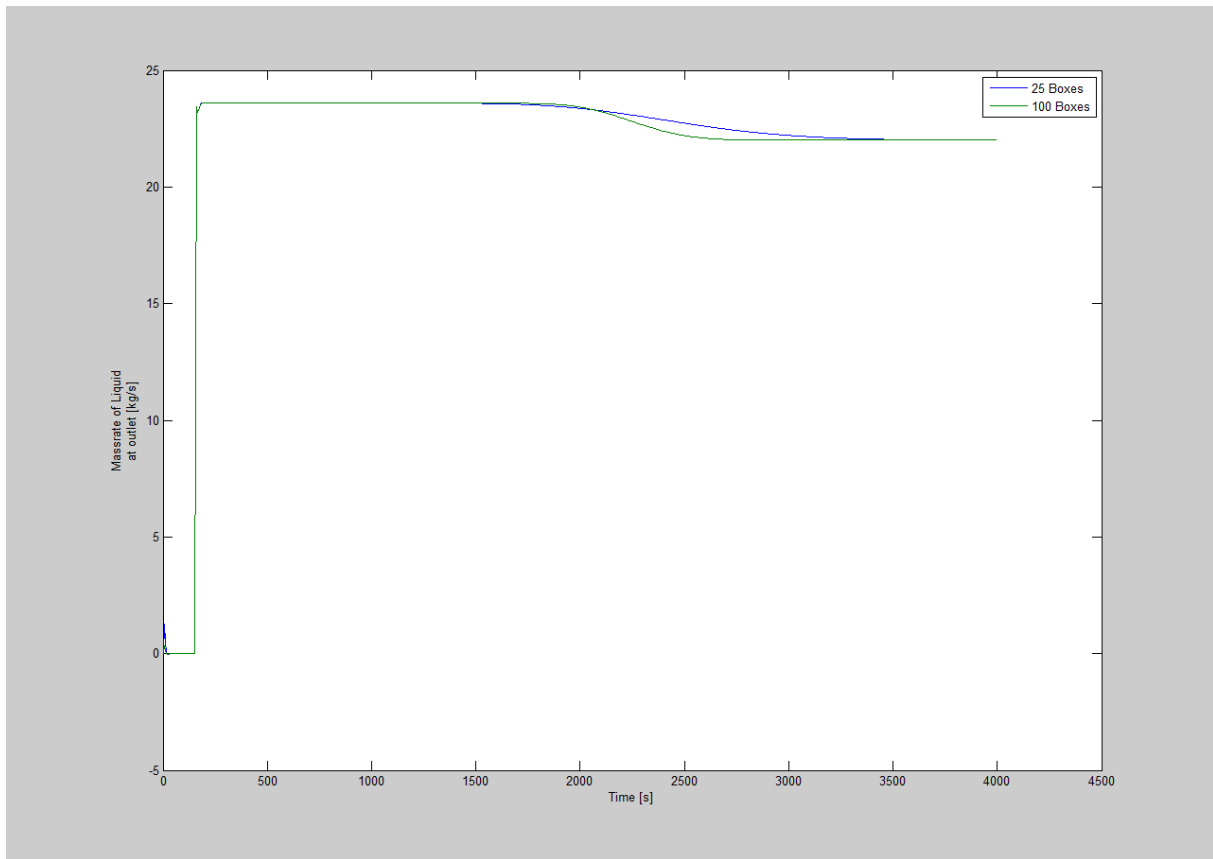
Figure 36: 4kg/s, 25 box, 100box, t=4000sec, Liquid massrate out against time plot.

Now as illustrated in Figure 36 the green curve represents the effect of numerical diffusion on the liquid massrate. In the beginning of this chapter it was shown that the transit time for cuttings in the well is 2172s. We started the simulation at 150s. This means that we should have a sharp transition to steady state conditions after 2322s. We observe that by using 100 boxes (green curve) compared to 25 boxes (blue curve), we get a sharper transition that is closer to the theoretical value.
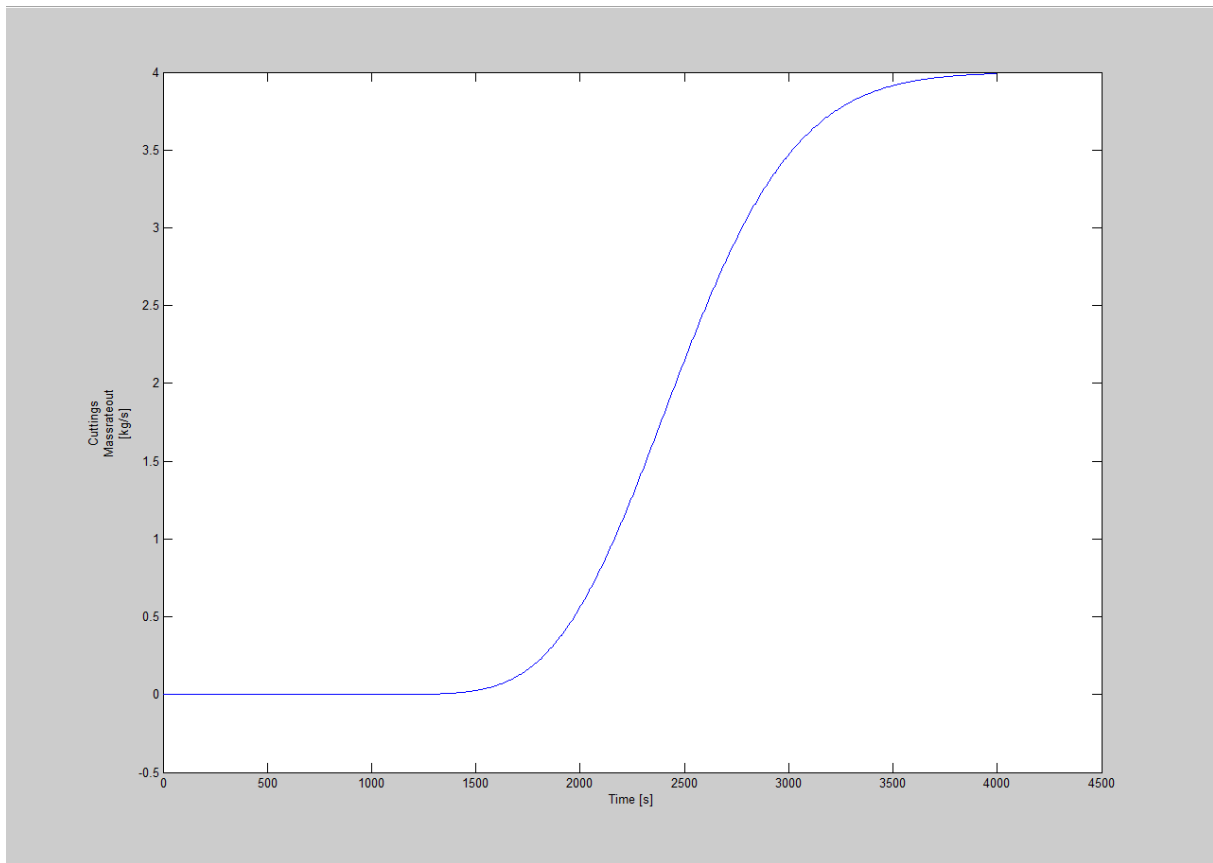
Figure 37: 4kg, 25 box, t=4000sec, Cuttings massrate out against time plot.

Figure 37 shows a very smooth curve with a linear increase in the cuttings massrate from 2000s to 2700s. Then finally a steady state is achieved at almost 4000 seconds. Here the cuttings massrate at the top of the well will be the same as the massrate at the bottom of the well (conservation of mass). Again, we see the effect of numerical diffusion. There should be a sharp transition from 0 to 4kg/s when the cuttings reach the outlet.
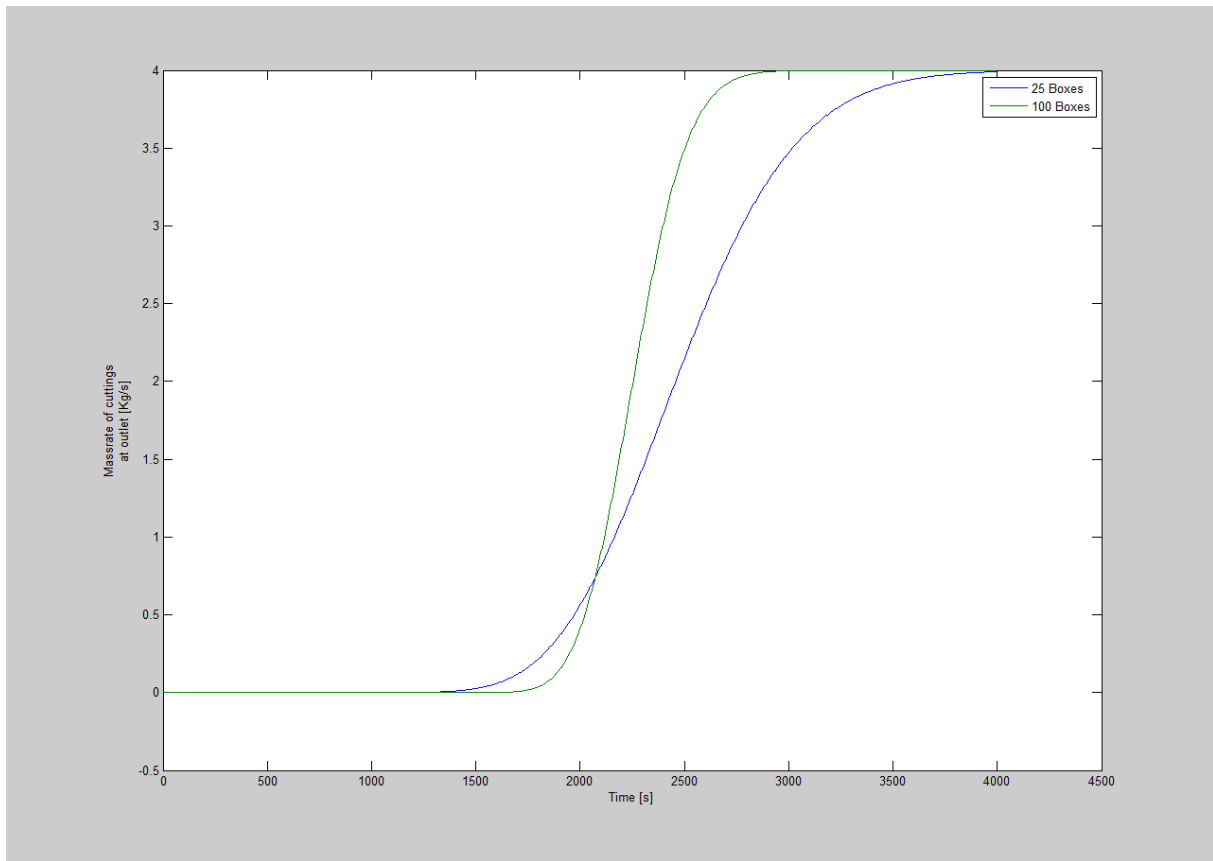
Figure 38: 4kg, 25 box, 100box, t=4000sec, Cuttings Massrate out against time plot.

Finally we can see the effect of numerical diffusion in figure 38 on the cuttings massrate. We can clearly see that the steady state is achieved earlier when the number of boxes was changed to 100 from 25. The massrate of cuttings corresponding to 4kg/s at 3000 seconds is 1000 seconds earlier than in the case of blue curve (25 boxes). Ideally, the curve should have been a complete sharp transition.
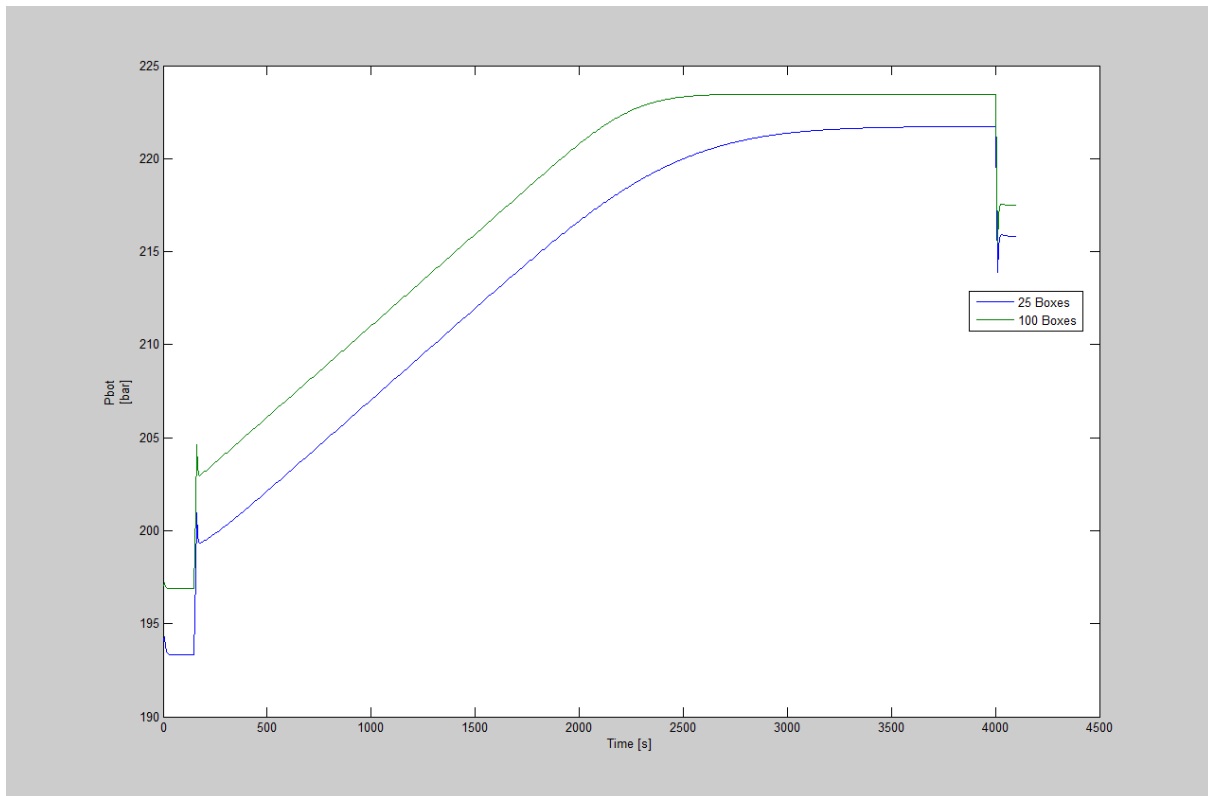
Figure 39: 4kg, 25 box, 100 box, t=4000sec, bottomhole pressure against time plot.

Finally we can see in Figure 39 the effect of numerical diffusion on the bottomhole pressure. There is an increase in the BHP (Bottomhole Pressure) of the well at 200 seconds from 201 bar to 205 bar. This is due to friction. Then we have a gradual build up as cuttings starts to be distributed in the well. The maximum bottomhole pressure for the green curve is 224 bar and for the blue curve is 222 bar. So a difference of 2 bar in the maximum value of BHP is observed by changing the number of boxes to 100. The reason is that with 100 boxes, we get a more accurate value for cuttings concentration.

Now finally some calculations will be shown to compare the theoretical results and the simulation results. The calculations made here are for 4kg/s case with 25 boxes which is used as an example to compare the simulation results with the theoretical results.

Calculations: We observed that when pumping 4kg/s, we saw that we got different concentration values for different discretizations.

Now let us calculate the cuttings concentration α_c theoretically by using two theoretical formulas. The calculations are shown below:

$w_1 = \rho_l(1 - \alpha_l)$ Known value
$w_2 = \rho_c \alpha_g$ Known value
$\alpha_g =$ Cuttings concentration

69

$\rho_c = 2500$ kg/m^3

$w_1 = \rho_l (1 - W_2/2500) = 0$

$(w_1 - \rho_{l0}) / (1 - \alpha_l) = (p - p_o)/ \alpha_l^2$

$w_1 = (\rho_{l0} + (p - p_o)/ \alpha_l^2) (1 - w_2/2500)$

$w_1 = (\rho_{l0} + (p - p_o)/ \alpha_l^2) c$

$w_1/C = (\rho_{l0} + (p - p_0)/ \alpha_l^2)$

$p = p_o + (w_1/C - \rho_{l0}) \alpha_l^2$

$V_c = K V_{mix} + S$ where $K = 1$ and $S = 0$

$V_c = V_l$ no slip condition

$V_c = V_{SG} + V_{Sl}$ where V_{SG} and V_{Sl} are superficial velocities

$V_{Sl} = M_l / A . \rho_l$ where $M_l = 22$ kg/s

$V_{SC} = M_c / A . \rho_c$ where $M_c = 4$ kg/s

$A = 0.0239$ m^2 and $\rho_l = 1000$ kg/m^3 and $\rho_c = 2500$ kg/m^3

$V_C \alpha_c = (V_{Sc} + V_{Sl})\alpha_c$

$V_{Sc} = (V_{Sc} + V_{Sl}) \alpha_c$

$\alpha_c = V_{Sc}/ (V_{Sc} + V_{Sl})$

$\alpha_c = V_{Sc}/ (V_{Sc} + V_{Sl} = M_c/A . \rho_c / (M_c/ A . \rho_c + M_l/ A . \rho_l)$

$\alpha_c = (M_C/A . \rho_c) \rho_c / (M_c/A . \rho_c + M_l/A . \rho_l) \rho_c = M_c/ (M_c + M_l \rho_c / \rho_l)$

$\alpha_c = 4 / (4 + 22(2500/1000)) = \mathbf{0.0678}$

Model gives 0.077

$V_{Sl} = 22$kg/s/0.0239m^2.1000 = 0.9205 m/s

$V_{Sc} = 4$kg/s/0.0239m^2.2500 = 0.06694 m/s

$\alpha_c = 0.06694/ 0.06694 + (0.9205) = \mathbf{0.0678}$

Now as it is shown that we achieve the same value for cuttings concentration $\boldsymbol{\alpha_c} = \mathbf{0.0678}$. 100 boxes simulation gave a value of $\boldsymbol{\alpha_c} = \mathbf{0.0707}$ which was closer to the value of $\boldsymbol{\alpha_c} = \mathbf{0.0678}$ as compared to the value obtained in simulation with 25 boxes, $\boldsymbol{\alpha_c} = \mathbf{0.078}$. However, we obtained a value of $\mathbf{0.078}$ as a result of the simulations performed with 25 boxes. This difference can be due to numerical inaccuracies and uncertainties.

Based on this, we will try to make some calculations and discuss these in relation to Figure 39.The first thing to observe in Figure 39 is that at time t = 0, the two simulations give different values to the hydrostatic pressure. The reason for this is that when we plot BHP, we plot the middle point in the cell. If we have a 2000 meter well and 25 boxes, each box will be 80m. In this case, we plot the pressure at a depth of 2000m – 80/2 = 1960m.

If we have a 2000 meter well and 25 boxes, each box will be 80m. In this case, we plot the pressure at a depth of 2000m – 20/2 = 1990m. The hydrostatic pressure difference between these points considering a 1.0 sg liquid gives $\Delta p = 1.0 \times 30 \times 0.0981 = 2.9$ bar and this explains the initial difference.

In the following, we will try to estimate the true hydrostatic pressure of the liquid and cuttings. The three cuttings concentration value was 0.0678.

We will assume 192 bar at bottom to estimate the average fluid density in the well.

$$\rho_l = \rho_{l0} + \frac{(p - p_0)}{a_l^2});$$

$$\rho_l = 1000 + \frac{(p - p_0)}{1500^2} = 1000 + \frac{19200000 - 100000}{1500^2} = 1008 \text{ kg/m}^3$$

The average of $\rho_l = \frac{1008 + 1000}{2} = 1004 \text{ kg/m}^3$.

$p = 19200000$ pascals and $p_0 = 100000$ pascals.

This gives an effective density in the well equal to $\rho_{\text{effective}} = (0.0678 \times 2.5) + (0.9322 \times 1.004) = 1.1054$ sg. The hydrostatic pressure will be $P_{\text{Hydrostatic}} = 1.1054 \times 2000 \times 0.0981 = 216.88$ bar. This is the true hydrostatic pressure.

However, in the numerical simulations, the hydrostatic pressures at final steady state conditions are calculated as follows:
$P_{25} = (0.078 \times 2.5 + 0.922 \times 1.004) \times 1960 \times 0.0981 = 215.5$ bar
$P_{100} = (0.0707 \times 2.5 + 0.9293 \times 1.004) \times 1990 \times 0.0981 = 216.64$ bar

These values are similar to the ones seen in Figure 34, when the pumps have been turned off and the friction in the system disappears. From above we observe that as we refine the grid, the simulated BHP approaches the true BHP.

So we can conclude that the difference in the results in Figure 39 is due to two factors:
- Cuttings concentration in the well is different for different number of boxes used.
- Discretization of the well and the fact that we plot middle point in the cell which is different in each case.

Finally, some comments will be given on the time step selection chosen in the different simulations using different grids.

The CFL condition is satisfied in the simulations. This is also shown below: When we changed the number of boxes from 25 to 100 in appendix A we had to divide dt by 4 (dt/4) in order to satisfy the CFL requirement. Hence the part of Matlab code in appendix A was changed to:

dt= 0.01/4= 0.0025; % Timestep
dtdx = dt/dx;
time = 0.0;
Number of boxes part in appendix A was changed to:
welldepth = 2000;
nobox = 100; %Number of boxes in the well
nofluxes = nobox+1;
dx = welldepth/nobox; % Boxlength

$\Delta t/\Delta x$ = constant
No. of boxes = 100
Then $\Delta t = 0.01$ seconds must be divided by 4
$\Delta t = 0.01/4 = 0.0025$
$\Delta t = CFL \times \Delta x/1500$
$\Delta t \leq 0.5 \times 80/1500 = 0.0533$
$\Delta t \leq 0.5 \times 20/1500 = 0.0133$
It is verified by calculations that the **CFL** requirement is fulfilled.

Time for circulation of the cuttings in the well:
Flowrate = 22 kg/s; also 1kg= 1l
Water = 22 l/s   → $(22 \times 60 = 1320 \ l/m)$
$T = V_{well}/V_{rate}$ = 47.8 m³/ 0.022 m³/s = 2172 seconds
$V_{well} = A_0 L = 0.0239 m^2 \times$ 2000m = 47.8 m³

As calculated above, it can be seen that the time it should take for cuttings to reach to the surface of the well = 2172 seconds = 2172/60 = 36.2 minutes. In the simulations, it was seen that the simulation with 100 boxes gave a better prediction of when the cuttings would be at surface.

$\rho_{\text{effective}}$= (0.078 × 2.5) + (0.922 ×1.004) = 1.1206 sg where 0.078 is the cuttings concentration read from the graph for 4kg/s cuttings rate and 0.922 is the concentration of the liquid found by subtracting 0.078 from 1 as follows:
Liquids concentration = 1− 0.078 = 0.922 = 92.2 %

Assuming that the friction is constant and increase in the pressure is due to increase and density is due to increase in the weight of the mud.
Liquid density= 1.0 sg, cuttings density = 2.5 sg
$P_{\text{Hydrostatic}}$ = 1.1206 × 1960 × 0.0981 = 215.5 bar

The pressure evens out in the well when the cuttings have distributed in the whole well. Here, we will discuss a discretization effect that explains the initial difference in the pressure in Figure 39.

dx = welldepth/nobox; % Boxlength
dx = 2000/25;
dx = 80m when the nobox = 25; %Number of boxes in the well

However, when we plot the BHP (Bottomhole Pressure) in the cell, we plot the middle point in the cell. Therefore, we subtract dx = 80/2 = 40m for number of boxes = 25. This means that in the simulation with 25 boxes, the bottomhole pressure is shown at 1960m.

For 100 boxes we get: dx = 2000/100 = 20m and taking the middle point in the cell we get 20/2 = 10m. This means that in the simulation with 100 boxes, the bottomhole pressure is plotted at 1990m.

ρ_m = Density of mud = 1000 kg/m^3; well depth = H = 2000m
$P = \rho_m \times g \times H = 2000 \times 0.0981 \times 1.0 = 196$ bar
$P_1 = (2000 - 40) \times 0.0981 \times 1.0 = 192$ bar
$P_2 = (2000 - 40) \times 0.0981 \times 1.004 = 193$ bar
The increase in the hydrostatic pressure which occurs due to increase in the mud weight caused by cuttings is approximately:

$\Delta P = 215.5$ bar $- 193 = 21$ bar

From the simulations done we can also observe that the pressure increased approximately 6 bar when we start pumping at time = 150 seconds. This is the friction in the system. It means that the pressure should be 215.5+6 = **221.6** bar which is in accordance with the simulation as can be read from the figure 39. The pressure read from the figure 39 is also approximately = **221.6** bar.

As calculated above, it can be seen that the time it should take for cuttings to reach to the surface of the well = 2172 seconds = 2172/60 = 36.2 minutes. In the simulations, it was seen that the simulation with 100 boxes gave a better prediction of when the cuttings would be at surface.

7. Conclusion

Finally we can conclude that the AUSMV scheme can be modified to simulate two phase flow considering liquid and particles. It was demonstrated that we could simulate the transient flow for no-slip conditions. In future work, one should also investigate no-slip conditions. The main changes in the Matlab code were done to modify the formulas for converting conservative variables into physical variables like pressure and density. The AUSMV scheme makes it easier to extract information about the dynamics of the particle (cuttings) flow, liquid flow and can be used to simulate the transient/dynamic transport of particles. It also makes it easy to make calculations of parameters like cuttings concentration α_c and the bottomhole pressure. Many different plots can be obtained of parameters such as liquid mass flowrate, cuttings flowrate and bottomhole pressure against time.

The scheme provides information about how different parameters affect the transport of the cuttings such as we saw in chapter 6 of the thesis. It also makes it very straightforward to compute the time it takes for the transport of cuttings and circulation of the liquid in the well. It also gives a clear indication of the various fluid dynamics going on in the well. It is very useful to solve complex transient models which consist of fluids in different phases. The scheme also gives information on how the bottomhole pressure changes with time as a function of cuttings concentration in the well.

It becomes very convenient to change the flowrates and observe the effect on the transport mechanism for different scenarios. The scheme makes it very easy to see the effect numerical diffusion [19] has on the cuttings transport as seen in chapter 6. ROP (Rate of Penetration) effects can also be observed by using the scheme. The information obtained from our simulations can be used to do a detailed analysis of the condition of the well and how different parameters affect the particle (cuttings in our case) transport in the well. So finally it can be concluded that the AUSMV scheme is very effective and beneficial in solving and evaluating different drilling fluid parameters involved in particle (transport) and also makes it feasible to perform detailed analysis of the conditions of the well during transport mechanism. It also handles the dynamics of the two phase flow very well.

As mentioned above, the effect of numerical diffusion and discretization errors related to having a rough grid were interesting to observe. It was seen that numerical diffusion smears out the sharp transition zone between pure liquid and liquid/cuttings. By increasing number of boxes, we saw that we could reduce the effect of numerical diffusion. Another interesting observation was that even for steady state conditions, we ended up with different concentration values for the

cuttings. This effect is probably caused by discretization errors and it was seen that the steady state concentration value approached the true value when the grid was refined.

In essence, the effect of numerical diffusion and discretization errors must be investigated further in future works. One should also keep in mind that the numerical values are defined in the midpoint of the cells and this must be taken into account if the pressure at a specific depth should be plotted.

References

1. A.A Pilehvari, SPE, Texas A & M U, at Kingsville and J.J Azar, SPE and S.A. Shirazi, SPE, U of Tulsa. "State-of-the-Art Cuttings Transport in Horizontal Wellbores." SPE-57716-PA.

2. T.I. Larsen, SPE, Unocal Corp., A.A. Pilehvari, SPE, Texas A & M U., and J.J. Azar, SPE, U. of Tulsa. "Development of a New Cuttings-Transport Model for High-Angle Wellbores Including Horizontal Wells." SPE-25872-PA.

3. J.Li, J. Misselbrook, M. Sach, BJ Services Company. "Sand Cleanouts with Coiled Tubing: Choice of Process, Tools and Fluids." SPE-113267-PA.

4. J. Li, T. Green, Baker Hughes. "Coiled Tubing Sand Clean Outs Utilizing BHA Technology and Simulation Software in Demanding Wellbore Geometries." SPE-149051-MS.

5. http://www.coiledtubingreels.com/wp-content/uploads/2011/05/1.png.

6. Udegbunam, J.E., Fjelde, K.K., Evje, S. and Nygaard, G. 2014. A Simple Transient Flow Model for MPD and UBD Applications. Paper SPE/IADC 168960 presented at the SPE /IADC Managed Pressure Drilling and Underbalanced Operations Conference and Exhibition held in Madrid, Spain, 8-9 April.

7. Evje, S. and Fjelde, K.K. 2002. Hybrid Flux-Splitting Schemes for a Two-Phase Flow Model. *J. Computational Physics*. **175** (2) 674-701.

8. J.T. Ford and M.B Oyeneyin, Heriot-Watt U. ; Erhu Gao, Anchor Drilling Fluids Ltd.; and R.S. Williamson and L.C. Peel, Mobil North Sea Ltd. "The Formulation of Milling Fluids for Efficient Hole Cleaning: An Experimental Investigation." SPE-28819-MS.

9. Donald P. Sparling Oryx Energy Co. Oklahoma city, Don Williamson International Drilling Fluids Inc. Houston. Oil & Gas Journal 06/10/1991 http://www.ogj.com/articles/print/volume-89/issue-23/in-this-issue/drilling/mixed-metal-hydroxide-mud-improves-drilling-in-unstable-shales.html. <05.05.2015>

10. Johnny Petersen, International Research Institute of Stavanger (IRIS). "Determining the Cuttings Critical Transport Fluid Velocity using Simple Geometric Approximations." SPE-173843-MS.

11. J. Li, S.Walker and B. Aitken, BJ Services Company. "How to Efficiently Remove Sand from Deviated Wellbores with a Solids Transport Simulator and a Coiled Tubing Cleanout Tool." SPE-77527-MS.

12. E. Cayeux (IRIS), Mesagan, T. Statoil, S. Tanripada Statoil, M. Zidan Statoil, Kjell Kåre Fjelde (University of Stavanger). "Real-Time Evaluation of Hole cleaning Conditions Using a Transient Cuttings Transport Model." SPE 163492-PA.

13. Standard Norway, Well integrity in drilling and well operations, Norsok Standard D-010 Rev. 3, 2013.

14. Modisette, Jerry L., Energy Solutions International Inc. Modisette, Jason P., Energy Solutions International Inc. "Transient and Succession-of-Steady-States Pipeline Flow Models." PSIG-0108-Conference Paper-2001.

15. John Emeka Udegbunam, Kjell Kåre Fjelde, Steinar Evje, Gerhard Nygaard, University of Stavanger. "A Simple Transient Flow Model for MPD and UBD Applications." SPE/IADC 168960.

16. Compendium Well Flow UiS/PET 510 Autumn 2015, Kjell Kåre Fjelde.

17. John Emeka Udegunam , Kjell Kåre Fjelde, Steinar Evje. "The Academic AUSMV Scheme – A Simple but Robust Model for Predicting Highly Dynamic Well Flow Phenomena" – Poster and Extended Abstract. Celle Drilling 2012 Conference. Celle, Germany.

18. Lage, A.C.V.M., 2000: "Two-phase Flow Models and Experiments for Low-head and underbalanced drilling", PhD thesis, University of Stavanger, ISBN 82-7644-126-2.

19. Kjell K. Fjelde, RF-Rogaland Research, Rolv Rommetveit, RF-Rogaland Research, Antonio Merlo, Eni-Agip Division and Antonio C.V.M Lage, Petrobras. "Improvements in Dynamic Modeling of Underbalanced Drilling." SPE/IADC 81636.

APPENDICES

APPENDIX A (12 PAGES)

APPENDIX B (1 PAGE)

APPENDIX C (2 PAGES)

APPENDIX D (1 PAGE)

APPENDIX E (1 PAGE)

APPENDIX F (1 PAGE)

APPENDIX G (1 PAGE)

APPENDIX H (1 PAGE)

APPENDIX A

```matlab
% Transient two-phase code based on AUSMV scheme: Gas and Water
% The code can handle area changes. The area changes are defined inside
% the cells such that the where the fluxes are calculated, the geometry is
% uniform.

clear;

% Geometry data/ Must be specified
welldepth = 2000;
nobox = 25; %Number of boxes in the well
nofluxes = nobox+1;
dx = welldepth/nobox; % Boxlength
%dt = 0.005;

% Welldepth array
x(1)= -1.0*welldepth+0.5*dx;
for i=1:nobox-1
 x(i+1)=x(i)+ dx;
end

dt= 0.01;  % Timestep
dtdx = dt/dx;
time = 0.0;
endtime = 4100; % Time for end of simulation
nosteps = endtime/dt;  %Number of total timesteps
timebetweensavingtimedata = 5;  % How often in s we save data vs time for
plotting.
nostepsbeforesavingtimedata = timebetweensavingtimedata/dt;

% Slip parameters used in the gas slip relation. vg =Kvmix+S
k = 1.0;
s = 0.0;

% Viscosities (Pa*s)/Used in the frictional pressure loss model.
viscl = 0.05; % Liquid phase
viscg = 0.05; % Cuttingsphase
```

```
% Density parameters. These parameters are used when finding the
% primitive variables pressure, densities in an analytical manner.
% Changing parameters here, you must also change parameters inside the
% density routines roliq and rogas.

% liquid density at stc and speed of sound in liquid
  dstc = 1000.0;   %Base density of liquid, See also roliq.
  pstc = 100000.0; % Pressure at standard conditions, 100000 Pascal
  al = 1500; % Speed of sound/compressibility of liquid phase.
  t1 = dstc-pstc/(al*al); % Help variable for calc primitive variables from
  % conservative variables
% Ideal gas law constant
  rt = 100000;

% Gravity constant

  grav = 9.81;

% Well opening. opening = 1, fully open well, opening = 0 (<0.01), the well
% is fully closed. This variable will control what boundary conditions that
% will apply at the outlet (both physical and numerical): We must change
% this further below in the code if we want to change status on this.

  wellopening = 1.0



% Specify if the primitive variables shall be found either by
% a numerical or analytical approach. If analytical = 1, analytical
% solution is used. If analytical = 0. The numerical approach is used.
% using the itsolver subroutine where the bisection numerical method
% is used.

  analytical = 1;



% Define and initilalize flow variables



%%IMPORTANT. HERE We specify the area changes. The indexes need to
% be changed if we change the grid size. Here we have assumed a
% 8.5 inch x 5 inch annulus space where diameters have been specified in
```

% meters. Box i = 1 starts at bottom. By dividing it into two loops one can
% possibly introduce flow area changes (then one must keep track on where
% we are

```matlab
  for i = 1:12
   do(i) = 0.2159;
   di(i) = 0.127;
   area(i) = 3.14/4*(do(i)*do(i)- di(i)*di(i));
   area(i) = 3.14/4*(do(i)*do(i)- di(i)*di(i));
%   area(i) = 3.14/4*(do(i)*do(i)- di(i)*di(i));
%   ang(i)=3.14/2;
  end

  for i = 14:nobox
   do(i) = 0.2159;
   di(i) = 0.127;
   areal(i) = 3.14/4*(do(i)*do(i)- di(i)*di(i));
   arear(i) = 3.14/4*(do(i)*do(i)- di(i)*di(i));
%   area(i) = 3.14/4*(do(i)*do(i)- di(i)*di(i));
%   ang(i)=3.14/2;
  end

  do(13)=(0.2159+0.2159)*0.5;
  di(13)=0.127;
  areal(13)=3.14/4*(0.2159^2-0.127^2);
  arear(13)=3.14/4*(0.2159^2-0.127^2);
```

% Now comes the initialization of the physical variables in the well.
% First primitive variables, then the conservative ones.
```matlab
   for i = 1:nobox
```
% Here the well is initialized. This code does not need change.
% The extension letter o refers to the table representing the
% values at the previous timestep (old values).

```matlab
    % Density of liquid and gas:
    dl(i) = 1000.0;
    dg(i)= 2500.0;
    %"Old" density is set equal to new density to calculate new values
    %based on the old ones:
    dlo(i)= dl(i);
```

```
        dgo(i)=dg(i);
        % Velocity of liquid and gas at new and previous timesteps:
        vl(i) = 0.0;
        vlo(i)= 0.0;
        vg(i)= 0.0;
        vgo(i)= 0.0;
        %The pressure in the horizontal pipe is the same
        %all over:
        p(i) = 100000.0;
        po(i) = p(i);
        %Phase volume fractions of gas and liquid:
        eg(i)= 0.0;    %Gas
        ego(i)=eg(i);
        ev(i)=1-eg(i); % Liquid
        evo(i)=ev(i);

        vg(i)=0.0;
        vgo(i)=0.0;
        vl(i)=0.0;
        vlo(i)=0.0;

        % Variables related to the velocity of the flux boundaries at old
        %and new times, and on the left and right side of the boxes
        % reflecting that area changes can take part inside cells (i.e :
        % (A x v)left = (A x v)right, continuity equation.
        vgr(i)=0.0;
        vgor(i)= 0.0;
        vgl(i)= 0.0;
        vgol(i)= 0.0;

        vlr(i)=0.0;
        vlor(i)=0.0;
        vll(i)=0.0;
        vlol(i)=0.0;

% Conservative variables:

        qv(i,1)=dl(i)*ev(i)*(areal(i)+arear(i))*0.5;
        qvo(i,1)=qv(i,1);

        qv(i,2)=dg(i)*eg(i)*(areal(i)+arear(i))*0.5;
        qvo(i,2)=qv(i,2);
```

```
      qv(i,3)=(qv(i,1)*vl(i)+qv(i,2)*vg(i))*(areal(i)+arear(i))*0.5;
      qvo(i,3)=qv(i,3);

   end
```

% Initialize fluxes between the cells/boxes

```
for i = 1:nofluxes
  for j =1:3
   flc(i,j)=0.0; % Flux of liquid over box boundary
   fgc(i,j)=0.0; % Flux of gas over box boundary
   fp(i,j)= 0.0; % Pressure flux over box boundary
  end
end
```

% CODE BELOW HAVE BEEN ADDED TO INITIALIZE
FLOWVARIABLES IN A
% VERTICAL WELL:

```
p(nobox)= 100000.0+0.5*dx*9.81*dstc;
dl(nobox)=rholiq(p(nobox));
dg(nobox)=rogas(p(nobox));

for i=nobox-1:-1:1
p(i)=p(i+1)+dx*9.81*dl(i+1);
dl(i)=rholiq(p(i));
dg(i)=rogas(p(i));
end

for i=nobox-1:-1:1
p(i)=p(i+1)+dx*9.81*(dl(i+1)+dl(i))*0.5;
dl(i)=rholiq(p(i));
dg(i)=rogas(p(i));

end

for i=1:nobox
  dlo(i)=dl(i);
  dgo(i)=dg(i);
  po(i)=p(i);
  qv(i,1)=dl(i)*ev(i)*(areal(i)+arear(i))*0.5;
```

```matlab
  qvo(i,1)=qv(i,1);

  qv(i,2)=dg(i)*eg(i)*(areal(i)+arear(i))*0.5;
  qvo(i,2)=qv(i,2);

  qv(i,3)=(qv(i,1)*vl(i)+qv(i,2)*vg(i))*(areal(i)+arear(i))*0.5;
  qvo(i,3)=qv(i,3);
end


% Main program. Here we will progress in time. First som intializations
% and definitions to take out results. The for loop below runs until the
% simulation is finished.

countsteps = 0;
counter=0;
printcounter = 1;
pbot(printcounter) = p(1);
pchoke(printcounter)= p(nobox);
liquidmassrateout(printcounter) = 0;
gasmassrateout(printcounter)=0;
timeplot(printcounter)=time;

for i = 1:nosteps
  countsteps=countsteps+1;
  counter=counter+1;
  time = time+dt;

  g = grav;

% Then a section where specify the boundary conditions.
% Here we specify the inlet rates of the different phases at the
% bottom of the pipe in kg/s. We interpolate to make things smooth.
% It is also possible to change the outlet boundary status of the well
% here. First we specify rates at the bottom and the pressure at the outlet
% in case we have an open well. This is a place where we can change the
% code.



%if (time < 150)

% inletliqmassrate=0.0;
```

```matlab
%    inletgasmassrate=0.0;
%
% elseif ((time>=150) & (time < 160))
%    inletliqmassrate = 22*(time-150)/10;
%    inletgasmassrate = 4.0*(time-150)/10;
%
% elseif (time>=160)
%    inletliqmassrate = 22;
%    inletgasmassrate = 4.0;
%
%     inletliqmassrate=0.0;
%    inletgasmassrate=0.0;

if (time < 150)

  inletliqmassrate=0.0;
  inletgasmassrate=0.0;

elseif ((time>=150) & (time < 160))
  inletliqmassrate = 22*(time-150)/10;
  inletgasmassrate = 4.0*(time-150)/10;

elseif ((time>=160)&(time<4000))
  inletliqmassrate = 22;
  inletgasmassrate = 4.0;
elseif((time>4000)&(time<4010))
  inletliqmassrate = 22-22*(time-4000)/10;
  inletgasmassrate = 4.0-4.0*(time-4000)/10;
elseif((time>4010))
  inletliqmassrate=0;
  inletgasmassrate=0;
end


% elseif ((time >=160) & (time<1700))
%    inletliqmassrate = 22;
%    inletgasmassrate = 2.0;
%
% elseif ((time>=1700)& (time<1710))
%    inletliqmassrate = 22-22*(time-1700)/10;
%    inletgasmassrate = 2.0-2.0*(time-1700)/10;
% elseif ((time>=1710)&(time<2000))
%    inletliqmassrate =0;
```

```
%   inletgasmassrate =0;
% elseif ((time>=2000)& (time<2010))
%   inletliqmassrate= 22*(time-2000)/10;
%   inletgasmassrate= 2.0*(time-2000)/10;
% elseif (time>2010)
%   inletliqmassrate= 22;
%   inletgasmassrate= 2.0;
%end
```

```
% specify the outlet pressure /Physical. Here we have given the pressure as
% constant. It would be possible to adjust it during open well conditions
% either by giving the wanted pressure directly (in the command lines
% above) or by finding it indirectly through a choke model where the well
opening
% would be an input parameter. The well opening variable would equally had
% to be adjusted inside the command line structure given right above.

 pressureoutlet = 100000.0;
```

```
% Based on these boundary values combined with use of extrapolations
techniques
% for the remaining unknowns at the boundaries, we will define the mass and
% momentum fluxes at the boundaries (inlet and outlet of pipe).

% inlet fluxes first.

    flc(1,1)= inletligmassrate/areal(1);
    flc(1,2)= 0.0;
    flc(1,3)= flc(1,1)*vlo(1);

    fgc(1,1)= 0.0;
    fgc(1,2)= inletgasmassrate/areal(1);
    fgc(1,3)= fgc(1,2)*vgo(1);

    fp(1,1)= 0.0;
    fp(1,2)= 0.0;
```

```matlab
    fp(1,3)= po(1)+0.5*(po(1)-po(2)); %Interpolation used to find the
% pressure at the inlet/bottom of the well.




% Outlet fluxes (open & closed conditions)

   if (wellopening>0.01)

% Here open end condtions are given
      flc(nofluxes,1)= dlo(nobox)*evo(nobox)*vlo(nobox);

      flc(nofluxes,2)= 0.0;
      flc(nofluxes,3)= flc(nofluxes,1)*vlo(nobox);

      fgc(nofluxes,1)= 0.0;
      fgc(nofluxes,2)= dgo(nobox)*ego(nobox)*vgo(nobox);
      fgc(nofluxes,3)= fgc(nofluxes,2)*vgo(nobox);

      fp(nofluxes,1)= 0.0;
      fp(nofluxes,2)= 0.0;
      fp(nofluxes,3)= pressureoutlet;
   else

% Here closed end conditions are given

      flc(nofluxes,1)= 0.0;
      flc(nofluxes,2)= 0.0;
      flc(nofluxes,3)= 0.0;

      fgc(nofluxes,1)= 0.0;
      fgc(nofluxes,2)= 0.0;
      fgc(nofluxes,3)= 0.0;

      fp(nofluxes,1)=0.0;
      fp(nofluxes,2)=0.0;
      fp(nofluxes,3)= po(nobox)-0.5*(po(nobox-1)-po(nobox));

   end
```

% Now we will find the fluxes between the different cells.
% NB - IMPORTANE - Note that if we change the compressibilities/sound velocities of
% the fluids involved, we need to do changes inside the csound function.

```
    for j = 2:nofluxes-1
     cl = csound(ego(j-1),po(j-1),dlo(j-1),k);
     cr = csound(ego(j),po(j),dlo(j),k);
     c = max(cl,cr);
     pll = psip(vlor(j-1),c,evo(j));
     plr = psim(vlol(j),c,evo(j-1));
     pgl = psip(vgor(j-1),c,ego(j));
     pgr = psim(vgol(j),c,ego(j-1));
     vmixr = vlol(j)*evo(j)+vgol(j)*ego(j);
     vmixl = vlor(j-1)*evo(j-1)+vgor(j-1)*ego(j-1);

     pl = pp(vmixl,c);
     pr = pm(vmixr,c);
     mll= evo(j-1)*dlo(j-1);
     mlr= evo(j)*dlo(j);
     mgl= ego(j-1)*dgo(j-1);
     mgr= ego(j)*dgo(j);

     flc(j,1)= mll*pll+mlr*plr;
     flc(j,2)= 0.0;
     flc(j,3)= mll*pll*vlor(j-1)+mlr*plr*vlol(j);

     fgc(j,1)=0.0;
     fgc(j,2)= mgl*pgl+mgr*pgr;
     fgc(j,3)= mgl*pgl*vgor(j-1)+mgr*pgr*vgol(j);

     fp(j,1)= 0.0;
     fp(j,2)= 0.0;
     fp(j,3)= pl*po(j-1)+pr*po(j);
    end
```

% Fluxes have now been calculated. We will now update the conservative
% variables in each of the numerical cells.

```
    for j=1:nobox
```

```matlab
    densmix = dlo(j)*evo(j)+dgo(j)*ego(j);

    a2 = arear(j);
    a1 = areal(j);
    avg = (a2+a1)*0.5;

    pressure=p(j);

%    We calculate the frictional gradient by calling upon the dpfric function.
    friclossgrad =
dpfric(vlo(j),vgo(j),evo(j),ego(j),dlo(j),dgo(j),pressure,do(j),di(j),viscl,viscg);




    qv(j,1)=qvo(j,1)-dtdx*((a2*flc(j+1,1)-a1*flc(j,1))...
            +(a2*fgc(j+1,1)-a1*fgc(j,1))...
            +(avg*fp(j+1,1)-avg*fp(j,1)));

    qv(j,2)=qvo(j,2)-dtdx*((a2*flc(j+1,2)-a1*flc(j,2))...
            +(a2*fgc(j+1,2)-a1*fgc(j,2))...
            +(avg*fp(j+1,2)-avg*fp(j,2)));

    qv(j,3)=qvo(j,3)-dtdx*((a2*flc(j+1,3)-a1*flc(j,3))...
            +(a2*fgc(j+1,3)-a1*fgc(j,3))...
            +(avg*fp(j+1,3)-avg*fp(j,3))...
        -dt*avg*((friclossgrad)+g*densmix);

    end



% Section where we find the physical variables (pressures, densities etc)
% from the conservative variables. Some trickes to ensure stability. These
% are induced to avoid negative masses.


    for j=1:nobox
```

```matlab
% Remove the area from the conservative variables to find the
% the primitive variables from the conservative ones.

    qv(j,1)= qv(j,1)/(areal(j)+arear(j))*2.0;
    qv(j,2)= qv(j,2)/(areal(j)+arear(j))*2.0;

    if (qv(j,1)<0.00000001)
      qv(j,1)=0.0000001;
    end

    if (qv(j,2)< 0.00000001)
      qv(j,2)=0.0000001;
    end




% Below, we find the primitive variables pressure and densities based on
% the conservative variables q1,q2. One can choose between getting them by
% analytical or numerical solution approach specified in the beginning of
% the program.

    if (analytical == 1)
      % Coefficients:
%       a = 1/(al*al);
%       b = t1-qv(j,1)-rt*qv(j,2)/(al*al);
%       c = -1.0*t1*rt*qv(j,2);

      % Analytical solution:
%       p(j)=(-b+sqrt(b*b-4*a*c))/(2*a);  % Pressure

      c =1-qv(j,2)/2500;
      p(j)=pstc+(qv(j,1)/c-dstc)*al*al;

      dl(j)= dstc + (p(j)-pstc)/(al*al); % Density of liquid
      dg(j) = p(j)/rt;
      dg(j)= 2500;% Density of cuttings
    else
      %Numerical Solution:
      [p(j),error]=itsolver(po(j),qv(j,1),qv(j,2)); % Pressure
      dl(j)=rholiq(p(j)); % Density of liquid
      dg(j)=rogas(p(j)); % Density of gas
```

```matlab
    % Incase a numerical solution is not found, the program will write out
"error":
    if error > 0
      error
    end
  end



% Find the phase volume fractions based on new conservative variables and
% updated densities.

    eg(j)= qv(j,2)/dg(j);
    ev(j)=1-eg(j);



%    Reset average conservative varibles in cells with area changes inside.

    qv(j,1)=qv(j,1)*(areal(j)+arear(j))/2.0;
    qv(j,2)=qv(j,2)*(areal(j)+arear(j))/2.0;



%    The section below is used to find the primitive variables vg,vl
%    (phase velocities) based on the updated conservative variable q3 and
%    the slip relation.



% Part where we interpolate in the slip parameters to avoid a
% singularities when approaching one phase gas flow.
% In the transition to one-phase gas flow, we need to
% have a smooth transition to no-slip conditions.

    xint = (eg(j)-0.75)/0.25;
    k0 = k;
    s0 = s;
    if ((eg(j)>=0.75) & (eg(j)<=1.0))
      k0 =1.0*xint+k*(1-xint);
      s0 = 0.0*xint+s*(1-xint);
    end

    if (eg(j)>=0.999999)
      k1 = 1.0;
      s1 = 0.0;
```

```matlab
   else
     k1 = (1-k0*eg(j))/(1-eg(j));
     s1 = -1.0*s0*eg(j)/(1-eg(j));
   end
```

```matlab
%    Below we operate with gas vg and liquid vl velocoities specified
%    both in the right part and left part inside a box. (since we have
%    area changes inside a box these can be different. vgl is gas velocity
%    to the left of the discontinuity. vgr is gas velocity to the right of
%    the discontinuity.
%

   help1 = dl(j)*ev(j)*k1+dg(j)*eg(j)*k0;
   help2 = dl(j)*ev(j)*s1+dg(j)*eg(j)*s0;

   vmixhelpl = (qv(j,3)/areal(j)-help2)/help1;
   vgl(j)=k0*vmixhelpl+s0;
   vll(j)=k1*vmixhelpl+s1;

   vmixhelpr = (qv(j,3)/arear(j)-help2)/help1;
   vgr(j)=k0*vmixhelpr+s0;
   vlr(j)=k1*vmixhelpr+s1;

%  Averaging velocities.

   vl(j)= 0.5*(vll(j)+vlr(j));
   vg(j)= 0.5*(vgl(j)+vgr(j));

  end
```

```matlab
% Old values are now set equal to new values in order to prepare
% computation of next time level.
   for j = 1:nobox
    po(j)=p(j);
    dlo(j)=dl(j);  %Liquid density
    dgo(j)=dg(j);  %Gas density
    vlo(j)=vl(j);  %Liquid velocity
    vgo(j)=vg(j);  %Gas velocity
    ego(j)=eg(j);  %Gas fration
```

```matlab
    evo(j)=ev(j);  %Liquid fraction.

    vlor(j)=vlr(j);
    vlol(j)=vll(j);
    vgor(j)=vgr(j);
    vgol(j)=vgl(j);

     for m =1:3
      qvo(j,m)=qv(j,m);
     end
   end
```

```matlab
% Section where we save some time dependent variables in arrays.
% e.g. the bottomhole pressure. They will be saved for certain
% timeintervalls defined in the start of the program in order to ensure
% that the arrays do not get to long!

  if (counter>=nostepsbeforesavingtimedata)
    printcounter=printcounter+1;
    time
    pbot(printcounter)= p(1);
    pchoke(printcounter)=p(nobox);
    pcasingshoe(printcounter)=p(25); %NB THIS MUST BE DEFINED IN
CORRECT BOX

liquidmassrateout(printcounter)=dl(nobox)*ev(nobox)*vl(nobox)*arear(nobox);

gasmassrateout(printcounter)=dg(nobox)*eg(nobox)*vg(nobox)*arear(nobox);
    timeplot(printcounter)=time;
    counter = 0;


  end
end

% end of stepping forward in time.




% Printing of results section
```

countsteps % Marks number of simulation steps.

% Plot commands for variables vs time. The commands can also
% be copied to command screen where program is run for plotting other
% variables.

plot(timeplot,pbot/100000)
%plot(timeplot,pchoke/100000)
%plot(timeplot,liquidmassrateout)
%plot(timeplot,gasmassrateout)
%plot(vg)

%Plot commands for variables vs depth/Only the last simulated
%values/endtime is visualised

%plot(vl,x);
%plot(vg,x);
%plot(eg,x);
%plot(p,x);
%plot(dl,x);
%plot(dg,x);

APPENDIX B

```
function mixsoundvelocity = csound(gvo,po,dlo,k)
% Note that at this time k is set to 1.0 (should maybe be
% included below

temp= gvo*dlo*(1.0-gvo);
a=1;
if (temp < 0.01)
  temp = 0.01;
end

cexpr = sqrt(po/temp);

% if (gvo <= 0.5)
%   mixsoundvelocity = min(cexpr,1000);
% else
%   mixsoundvelocity = min(cexpr,316);
% end

mixsoundvelocity = 1500;
```

APPENDIX C

```matlab
function [press,error] = itsolver(p,qv1,qv2)

% The numerical solver implementeted here for solving the equation f(x)= 0
% "wellpressure(p)= 0" is called the
% Method of Halving the Interval (Bisection Method)

% You will not find exact match for f(x)= 0. Maybe f(x) = 0.0001. By using
% ftol we say that if f(x)<ftol, we are satisfied. Since our function
% gives results in Pascal, we say that ftol = 1000 Pa gives us a quite good
% answer.

 ftol = 0.00001;
 ftol = 0.001;

% Specify the search interval". xguess is the pressure you guess for the
% pressure. (Remember x is in Pa). 1 Bar = 100 000 Pa.

% Set number of iterations to zero

 noit = 0;
 error = 1.0; % Error is set to zero because we havent any input information yet.

 i = 0;
 while (error > 0)
    i = i+1;
    xguess = p;
    xint = 150000*i;
    x1 = xguess-xint/2.0;
    x2 = xguess+xint/2.0;

f1 = qv1-rholiq(x1)*(1.0-qv2/rogas(x1));
f2 = qv1-rholiq(x2)*(1.0-qv2/rogas(x2));

% First include a check on whether f1xf2<0. If not you must adjust your
% initial search intervall. If error is 1 and zero pbot, then you must
% adjust the intervall here.


if (f1*f2)>=0
```

```matlab
      error = 0;
      if (f1<ftol)
         press=x1;
      elseif (f2<ftol)
         press=x2;
      else
          error=1
      end

else
% start iterating, we are now on the track.
   x3 = (x1+x2)/2.0;
   f3 = qv1-rholiq(x3)*(1.0-qv2/rogas(x3));

   while (f3>ftol | f3 < -ftol)
     noit = noit +1 ;

     if (f3*f1) < 0
       x2 = x3;
     else
       x1 = x3;
     end

     x3 = (x1+x2)/2.0;
     f3 = qv1-rholiq(x3)*(1.0-qv2/rogas(x3));
     f1 = qv1-rholiq(x1)*(1.0-qv2/rogas(x1));

   end
   error = 0;
   press = x3;
   noit;
end
 end
```

APPENDIX D

```
function pmvalue = pm(v,c)


  if (abs(v)<=c)
    pmvalue = -1.0*(v-c)*(v-c)/(4*c)*(-2.0-v/c)/c;
  else
    pmvalue = 0.5*(v-abs(v))/v;
  end
end
```

APPENDIX E

```
function pmvalue = pp(v,c)

 if (abs(v)<=c)
   pmvalue = (v+c)*(v+c)/(4*c)*(2.0-v/c)/c;
 else
   pmvalue = 0.5*(v+abs(v))/v;
 end
end
```

APPENDIX E

```
function pmvalue = psim(v,c,alpha)

  if (abs(v)<=c)
    pmvalue = -1.0*alpha*(v-c)*(v-c)/(4*c)+(1-alpha)*(v-abs(v))/2;
  else
    pmvalue = 0.5*(v-abs(v));
  end
end
```

APPENDIX F

```
function pmvalue = psip(v,c,alpha)


  if (abs(v)<=c)
    pmvalue = alpha*(v+c)*(v+c)/(4*c)+(1-alpha)*(v+abs(v))/2;
  else
    pmvalue = 0.5*(v+abs(v));
  end
end
```

APPENDIX G

```matlab
function [rhol] = rholiq(pressure)
%Simple model for liquid density
p0 = 100000.0; % Assumed

rhol = 1000.0 + (pressure-p0)/(1500.0*1500.0);
end
```

APPENDIX H

```matlab
function rhog = rogas(pressure)

%Simple gas density model. Temperature is neglected.
% rhogas = pressure / (velocity of sound in the gas phase)^2 = pressure /
% rT --> gas sound velcoity = SQRT(rT)

rhog = pressure/100000.0;
rhog = 2500;
```